Models, Verification, Validation, Identification and Stochastic Eigenvalue Problems

Udine, June 13 - 17, 2005

Sondipon Adhikari
Department of Aerospace Engineering
Queens Building
University of Bristol
Bristol BS8 1TR

This lecture note is a part of the CISM Lecture course entitled *Mechanical Vibration: Where Do We Stand?* held in Udine, Italy between June 13 - 17, 2005 and coordinated by Professor I. Elishakoff.

Contents

1 What is a Model? Why do We Need a Model? How We Use a Model? 4

1.1 Introduction 4

1.2 Equation of Motion of Linear Mechanical Systems 7

1.3 Classical Modal Analysis 9

1.4 Models of Damping 12

1.4.1 Viscous Damping: 13

1.4.2 Non-viscous Damping Models: 14

1.5 The Assumption of Proportional Damping: Classical Normal Modes and Complex Modes 17

1.5.1 Generalized proportional damping 22

1.6 Forced Dynamic Response of Generally Damped Linear Systems 27

1.6.1 Eigenvalues and Eigenvectors 28

1.6.2 Elastic Modes 30

1.6.3 Non-viscous Modes 33

1.6.4 Transfer Function of the System 35

1.6.5 Dynamic Response 38

1.6.6 Numerical Example 41

1.7 Conclusions 45

2 What is Model Validation and Model Verification? How it is Done? 46

2.1 Introduction 46
2.2 Experimental Modal Analysis (EMA 50
2.3 Measures of Model Correlations 52
2.4 Conclusions 58

3 Identification of Damping 59
3.1 Introduction 59
3.2 Damping Identification Using Generalized Proportional Damping Model 60
3.2.1 Comparison with the existing methods 64
3.3 Conclusions 74

4 Model Uncertainty: Quantification and Propagation 75
4.1 Why and How a Model Turns Uncertain? 75
4.2 Parametric Uncertainty in Structural Dynamics 80
4.3 Uncertainty Propagation Using Stochastic Finite Element Method 81

5 Random Eigenvalue Problems in Structural Dynamics 84
5.1 Introduction 84
5.2 Classical Perturbation Methods 86
5.2.1 Perturbation Expansion 86
5.2.2 Eigenvalue Statistics Using the Theory of Quadratic Forms 88
5.3 Perturbation Method Based on an Optimal Point 90
5.3.1 Perturbation Expansion 90
5.3.2 Eigenvalue Statistics Using the Theory of Quadratic Forms 92

5.4 Method Based on the Asymptotic Integral 95
5.4.1 Multidimensional Integrals in Unbounded Domains . . 95
5.4.2 Calculation of Arbitrary Moments of The Eigenvalues . 97
5.5 Probability Density Function of the Eigenvalues 100
5.5.1 Maximum Entropy Probability Density Function 100
5.5.2 Approximation by χ^2 Probability Density Function . . 102
5.6 Numerical Examples 104
5.6.1 A two DOF system 104
5.6.2 A Three Dof System with Closely Spaced Eigenvalues . 111
5.7 Conclusions 120

A Derivation of the Residues in the Transfer Function of Non-viscously Damped Dynamic Systems 130

B Gradient vector and Hessian matrix of the eigenvalues 134

1 What is a Model? Why do We Need a Model? How We Use a Model?

1.1 Introduction

- Proper understanding of the vibration phenomena is needed to cater 21st century design needs.

- Broadly speaking, there are two ways to understand the dynamics of complex structures:

  - The first is the experimental approach. A carefully conducted experiment can yield high quality data which can provide crucial information regarding the dynamics of a system. However, the experimental process is time consuming, expensive and it may be not be possible to dynamically test a complex structure under various loading conditions which the structure might experience during its service period.

  - The alternative is to 'replace' the actual structure by a *mathematical model* and perform numerical experiments in a computer.

- A model is a mathematical representation of the true structure. Figure 1.1 shows different types of models of dynamic systems used by today's engineers.

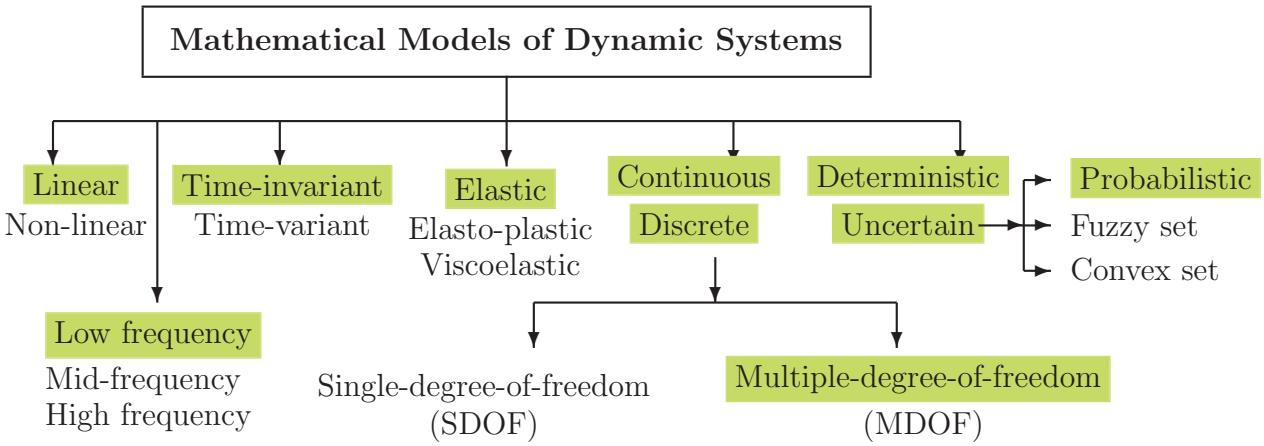

Figure 1.1: Different types of mathematical models for dynamic systems

A model can be created with various levels of sophistication. The choice of a particular model depends on the physics of the system, accuracy required for the problem and also on the nature of the forces the structure is expected to withstand in practice. The quality of a model of a dynamic system depends on the following there factors (the Good, Bad and Ugly!):

- *Fidelity to (experimental) data:* (The Good)

  The results obtained from a numerical or mathematical model undergoing a given excitation force should be close to the results obtained from the vibration testing of the same structure undergoing the same excitation.

- *Robustness with respect to (random) errors:* (The Bad)

  Errors in estimating the system parameters, boundary conditions and dynamic loads are unavoidable in practice. The output of the model should not be very sensitive to such errors.

- *Predictive capability* (The Ugly)

  In general it is not possible to experimentally validate a model over the entire domain of its scope of application. The model should predict the response well beyond its validation domain.

1.2 Equation of Motion of Linear Mechanical Systems

- Lord Rayleigh (1877) in his classic monograph 'Theory of Sound' outlined the fundamental concepts of modeling and analysis of linear dynamic systems. Current methods for modeling and analysis of complex engineering systems are largely based on Rayleigh's approach.

- From a mathematical point of view, models of vibrating systems are commonly divided into two broad classes – discrete, or lumped-parameter models, and continuous, or distributed-parameter models.

- Distributed-parameter modeling of vibrating systems leads to *partial-differential equations* as the equation of motion. Exact solutions of such equations are limited.

- For general complex engineering structures, such as an aircraft, normally we need some kind of approximate methods for dynamic analysis. Such approaches are generally based on spatial discretization of the displacement field (for example, the Finite Element Method), which amounts to approximating distributed-parameter systems by lumped-parameter systems. Equations of motion of lumped-parameter systems can be shown to be expressed by a set of coupled *ordinary-differential equations*.

Suppose that a system with N degrees of freedom is executing small oscillations around equilibrium points. Considering the vector of *generalized coordinates*

$$\mathbf{q} = \{q_1(t), q_2(t), \cdots, q_N(t)\}^T \in \mathbb{R}^N \tag{1.1}$$

the potential energy could be expanded in the form of a Taylor series in the neighborhood of the equilibrium position as

$$\mathcal{V}(\mathbf{q}) = \mathcal{V}(\mathbf{0}) + \sum_{j=1}^{N} \left(\frac{\partial \mathcal{V}}{\partial q_j}\right)_{\mathbf{q}=\mathbf{0}} q_j + \frac{1}{2}\sum_{j=1}^{N}\sum_{k=1}^{N} \left(\frac{\partial^2 \mathcal{V}}{\partial q_j \partial q_k}\right)_{\mathbf{q}=\mathbf{0}} q_j q_k + \mathcal{O}(\mathbf{q}^3). \tag{1.2}$$

Since the potential energy is defined only to a constant, it may be assumed that $\mathcal{V}(\mathbf{0}) = 0$, and consequently the second order approximation yields

$$\mathcal{V}(\mathbf{q}) = \frac{1}{2}\sum_{j=1}^{N}\sum_{k=1}^{N} K_{jk} q_j q_k \tag{1.3}$$

because second term is zero at equilibrium. Here the *elastic coefficients*

$$K_{jk} = \left(\frac{\partial^2 \mathcal{V}}{\partial q_j \partial q_k}\right)_{\mathbf{q}=\mathbf{0}}. \tag{1.4}$$

Equation (1.3) can also be put in the matrix positive definite quadratic form as

$$\mathcal{V}(\mathbf{q}) = \frac{1}{2}\mathbf{q}^T \mathbf{K} \mathbf{q} \tag{1.5}$$

where $\mathbf{K} \in \mathbb{R}^{N\times N}$, the (linear) *stiffness matrix* of the system, is symmetric and non-negative definite. In a similar way, in the absence of any centripetal and Coriolis forces, the kinetic energy of a system can be expressed as

$$\mathcal{T}(\mathbf{q}) = \frac{1}{2}\sum_{j=1}^{N}\sum_{k=1}^{N} M_{jk}\dot{q}_j \dot{q}_k = \frac{1}{2}\dot{\mathbf{q}}^T \mathbf{M} \dot{\mathbf{q}}. \tag{1.6}$$

In the above expression $\dot{\mathbf{q}}$ is the vector of the generalized velocities and $\mathbf{M} \in \mathbb{R}^{N\times N}$, the *mass matrix* of the system, is a symmetric and positive definite matrix. The equation of motion of free vibration can now be obtained by the application of Lagrange's equation

$$\frac{\mathrm{d}}{\mathrm{d}t}\left(\frac{\partial \mathcal{L}}{\partial \dot{q}_k}\right) - \frac{\partial \mathcal{L}}{\partial q_k} = Q_{\mathrm{nc}_k} + f_k, \quad \forall k = 1, \cdots, N \tag{1.7}$$

where $\mathcal{L} = \mathcal{T} - \mathcal{V}$ is the Lagrangian, Q_{nc_k} are the non-conservative forces and f_k are the applied forces acting on the system. For undamped systems $Q_{\mathrm{nc}_k} = 0, \forall k$. Using the expressions of $\mathcal{V}$ and $\mathcal{T}$ from equation (1.5) and (1.6) and substituting $\mathcal{L}$, from equation (1.7), the equation of motion of an undamped non-gyroscopic system can be obtained as

$$\mathbf{M}\ddot{\mathbf{q}}(t) + \mathbf{K}\mathbf{q}(t) = \mathfrak{f}(t) \tag{1.8}$$

where $\mathfrak{f}(t) \in \mathbb{R}^N$ is the forcing vector. Equation (1.8) represents a set of coupled second-order ordinary-differential equations. The solution of this equation also requires knowledge of the initial conditions in terms of the displacements and velocities of all the coordinates.

1.3 Classical Modal Analysis

Rayleigh (1877) has shown that undamped linear systems, equation of motion of which is given by (1.8), are capable of so-called *natural motions*. This essentially implies that all the system coordinates execute harmonic oscillation at a given frequency and form a certain displacement pattern. The oscillation frequency and displacement pattern are called *natural frequencies* and *normal modes*, respectively. The natural frequencies (ω_j) and the mode shapes ($\mathbf{x}_j$)

are intrinsic characteristic of a system and can be obtained by solving the associated matrix eigenvalue problem

$$\mathbf{K}\mathbf{x}_j = \omega_j^2 \mathbf{M}\mathbf{x}_j, \quad \forall\, j = 1, \cdots, N. \tag{1.9}$$

Since the above eigenvalue problem is in terms of real symmetric matrices $\mathbf{M}$ and $\mathbf{K}$, the eigenvalues and consequently the eigenvectors are real, that is $\omega_j \in \mathbb{R}$ and $\mathbf{x}_j \in \mathbb{R}^N$. The undamped eigenvectors satisfy an orthogonality relationship over the mass and stiffness matrices

$$\mathbf{x}_l^T \mathbf{M}\mathbf{x}_j = \delta_{lj} \tag{1.10}$$

$$\text{and} \quad \mathbf{x}_l^T \mathbf{K}\mathbf{x}_j = \omega_j^2 \delta_{lj}, \quad \forall\, l, j = 1, \cdots, N \tag{1.11}$$

where δ_{lj} is the Kroneker delta function. Construct the matrices

$$\mathbf{\Omega} = \text{diag}\,[\omega_1, \omega_2, \cdots, \omega_N] \in \mathbb{R}^{N\times N} \tag{1.12}$$

$$\text{and} \quad \mathbf{X} = [\mathbf{x}_1, \mathbf{x}_2, \cdots, \mathbf{x}_N] \in \mathbb{R}^{N\times N} \tag{1.13}$$

where the eigenvalues are arranged such that $\omega_1 < \omega_2$, $\omega_2 < \omega_3, \cdots, \omega_k < \omega_{k+1}$. Use a coordinate transformation

$$\mathbf{q}(t) = \mathbf{X}\mathbf{y}(t). \tag{1.14}$$

Substituting $\mathbf{q}(t)$ in equation (1.8), premultiplying by $\mathbf{X}^T$ and using the orthogonality relationships in (1.12) and (1.13), the equation of motion in the modal coordinates:

$$\ddot{\mathbf{y}}(t) + \mathbf{\Omega}^2 \mathbf{y}(t) = \tilde{\mathbf{f}}(t) \tag{1.15}$$

where $\tilde{\mathbf{f}}(t) = \mathbf{X}^T \mathbf{f}(t)$ is the forcing function in modal coordinates. Clearly, this method significantly simplifies the dynamic analysis because complex multiple

degrees of freedom systems can be treated as collections of single-degree-of-freedom oscillators. This approach of analyzing linear undamped systems is known as *modal analysis*, possibly the most efficient tool for vibration analysis of complex engineering structures.

1.4 Models of Damping

- Damping is the dissipation of energy from a vibrating structure. In this context, the term dissipate is used to mean the transformation of energy into the other form of energy and, therefore, a removal of energy from the vibrating system. The type of energy into which the mechanical energy is transformed is dependent on the system and the physical mechanism that cause the dissipation. For most vibrating system, a significant part of the energy is converted into heat.

- The specific ways in which energy is dissipated in vibration are dependent upon the physical mechanisms active in the structure. These physical mechanisms are complicated physical process that are not totally understood. The types of damping that are present in the structure will depend on which mechanisms predominate in the given situation. Thus, any mathematical representation of the physical damping mechanisms in the equations of motion of a vibrating system will have to be a generalization and approximation of the true physical situation. Any mathematical damping model is really only a crutch which does not give a detailed explanation of the underlying physics.

1.4.1 Viscous Damping:

The most popular approach to model damping in the context of multiple degrees-of-freedom (MDOF) systems – first introduced by Rayleigh (1877). By analogy with the potential energy and the kinetic energy, Rayleigh assumed the *dissipation function*:

$$\mathcal{F}(\mathbf{q}) = \frac{1}{2}\sum_{j=1}^{N}\sum_{k=1}^{N} C_{jk}\dot{q}_j\dot{q}_k = \frac{1}{2}\dot{\mathbf{q}}^T\mathbf{C}\dot{\mathbf{q}}. \tag{1.16}$$

$\mathbf{C} \in \mathbb{R}^n$ is a non-negative definite symmetric matrix – the viscous damping matrix. Viscous damping matrices can be further divided into classical and non-classical damping.

1.4.2 Non-viscous Damping Models:

- It is important to avoid the widespread misconception that viscous damping is the *only* linear model of vibration damping in the context of MDOF systems. Any causal model which makes the energy dissipation functional non-negative is a possible candidate for a damping model.

- Fractional Derivative Model:

  One popular approach is to model damping in terms of fractional derivatives of the displacements. The damping force:

$$\mathbf{F}_d = \sum_{j=1}^{l} \mathbf{g}_j D^{\nu_j}[\mathbf{q}(t)]. \tag{1.17}$$

  $\mathbf{g}_j$ are complex constant matrices and the fractional derivative operator

$$D^{\nu_j}[\mathbf{q}(t)] = \frac{\mathrm{d}^{\nu_j}\mathbf{q}(t)}{\mathrm{d}t^{\nu_j}} = \frac{1}{\Gamma(1-\nu_j)}\frac{\mathrm{d}}{\mathrm{d}t}\int_0^t \frac{\mathbf{q}(t)}{(t-\tau)^{\nu_j}}\mathrm{d}\tau \tag{1.18}$$

  where ν_j is a fraction and $\Gamma(\bullet)$ is the Gamma function.

  - The familiar viscous damping appears as a special case when $\nu_j = 1$.
  - Although this model might fit experimental data quite well, the physical justification for such models, however, is far from clear at the present time.

- Convolution Integration Model:

Here damping forces depend on the past history of motion via convolution integrals over some kernel functions. A *modified dissipation function* for such damping model can be defined as

$$\mathcal{F}(\mathbf{q}) = \frac{1}{2}\sum_{j=1}^{N}\sum_{k=1}^{N}\dot{q}_k \int_0^t \mathcal{G}_{jk}(t-\tau)\dot{q}_j(\tau)\mathrm{d}\tau = \frac{1}{2}\dot{\mathbf{q}}^T \int_0^t \boldsymbol{\mathcal{G}}(t-\tau)\dot{\mathbf{q}}(\tau)\mathrm{d}\tau. \tag{1.19}$$

Here $\boldsymbol{\mathcal{G}}(t) \in \mathbb{R}^n$ is a symmetric matrix of the damping kernel functions, $\mathcal{G}_{jk}(t)$.

- The familiar viscous damping appears as a special case when $\boldsymbol{\mathcal{G}}(t-\tau) = \mathbf{C}\,\delta(t-\tau)$, where $\delta(t)$ is the Dirac-delta function.
- By choosing suitable kernel functions, it can also be shown that the fractional derivative model discussed before is also a special case of this damping model. It is therefore, possibly the most general way to model damping.
- For further discussions see Adhikari (2002, 2000), Woodhouse (1998)

The damping kernel functions are commonly defined in the frequency/Laplace domain. Several authors have proposed several damping models and they are summarized below:

Table 1.1: Summary of damping functions in the Laplace domain

Damping functions	Author, Year
$G(s) = \sum_{k=1}^{n} \frac{a_k s}{s + b_k}$	Biot (1955, 1958)
$G(s) = as \int_0^\infty \frac{\gamma(\rho)}{s+\rho} \mathrm{d}\rho$	Buhariwala (1982)
$\gamma(\rho) = \begin{cases} \frac{1}{\beta - \alpha} & \alpha \leq \gamma \leq \beta \\ 0 & \text{otherwise} \end{cases}$	
$G(s) = \frac{E_1 s^\alpha - E_0 b s^\beta}{1 + b s^\beta}$	Bagley and Torvik (1983)
$0 < \alpha < 1, \quad 0 < \beta < 1$	
$sG(s) = G^\infty \left[1 + \sum_k \alpha_k \frac{s^2 + 2\xi_k \omega_k s}{s^2 + 2\xi_k \omega_k s + \omega_k^2}\right]$	Golla and Hughes (1985) and McTavish and Hughes (1993)
$G(s) = 1 + \sum_{k=1}^{n} \frac{\Delta_k s}{s + \beta_k}$	Lesieutre and Mingori (1990)
$G(s) = c \frac{1 - e^{-st_0}}{st_0}$	Adhikari (1998)
$G(s) = c \frac{1 + 2(st_0/\pi)^2 - e^{-st_0}}{1 + 2(st_0/\pi)^2}$	Adhikari (1998)

1.5 The Assumption of Proportional Damping: Classical Normal Modes and Complex Modes

- The non-conservative forces in Lagrange's equation

$$Q_{\mathrm{nc}_k} = -\frac{\partial \mathcal{F}}{\partial \dot{q}_k}, \quad k = 1, \cdots, N \tag{1.20}$$

The equations of motion

$$\mathbf{M}\ddot{\mathbf{q}}(t) + \mathbf{C}\dot{\mathbf{q}}(t) + \mathbf{K}\mathbf{q}(t) = \mathbf{f}(t). \tag{1.21}$$

The aim is to solve this equation (together with the initial conditions) by modal analysis as described in Section 1.3.

- Equations of motion of a damped system in the modal coordinates

$$\ddot{\mathbf{y}}(t) + \mathbf{X}^T\mathbf{C}\mathbf{X}\dot{\mathbf{y}}(t) + \mathbf{\Omega}^2\mathbf{y}(t) = \tilde{\mathbf{f}}(t). \tag{1.22}$$

Unless $\mathbf{X}^T\mathbf{C}\mathbf{X}$ is a diagonal matrix, no advantage can be gained by employing modal analysis because the equations of motion will still be coupled.

- Proportional damping assumptions is required.

With proportional damping assumption:

- The damping matrix $\mathbf{C}$ is simultaneously diagonalizable with $\mathbf{M}$ and $\mathbf{K}$ *i.e.*, the damping matrix in the modal coordinate

$$\mathbf{C}' = \mathbf{X}^T \mathbf{C} \mathbf{X} \tag{1.23}$$

  is a diagonal matrix.

- The damping ratios ζ_j are defined from the diagonal elements of the modal damping matrix as

$$C'_{jj} = 2\zeta_j \omega_j \quad \forall j = 1, \cdots, N. \tag{1.24}$$

- It allows to analyze damped systems in very much the same manner as undamped systems since the equations of motion in the modal coordinate can be decoupled as

$$\ddot{y}_j(t) + 2\zeta_j \omega_j \dot{y}_j(t) + \omega_j^2 y_j(t) = \tilde{f}_j(t) \quad \forall\, j = 1, \cdots, N. \tag{1.25}$$

- The classical proportional damping model expresses the damping matrix as a linear combination of the mass and stiffness matrices:

$$\mathbf{C} = \alpha_1 \mathbf{M} + \alpha_2 \mathbf{K} \tag{1.26}$$

  where α_1, α_2 are real scalars. This damping model is also known as 'Rayleigh damping' or 'classical damping'.

The Conditions for Proportional Damping

Classical damping can exist in more general situation. Modifying the original theorem by Caughey and O'Kelly (1965) for a non-negative definite system we have the following theorem:

Theorem 1.1. *A viscously damped linear system can possess classical normal modes if and only if at least one of the following conditions is satisfied: (a)* $\boldsymbol{KM^{-1}C = CM^{-1}K}$*, (b)* $\boldsymbol{MK^{-1}C = CK^{-1}M}$*, (c)* $\boldsymbol{MC^{-1}K = KC^{-1}M}$*.*

This can be easily proved by following Caughey and O'Kelly's approach and interchanging **M**, **K** and **C** successively. If a system is $(\bullet)$-singular then the condition(s) involving $(\bullet)^{-1}$ have to be disregarded and remaining condition(s) have to be used. Thus, for a positive definite system, along with Caughey and O'Kelly's result (condition (a) of the theorem), there exist two other equivalent criterion to judge whether a damped system can possess classical normal modes. It is important to note that these three conditions are equivalent and simultaneously valid but in general *not* the same.

Example 1.1.

Assume that a system's mass, stiffness and damping matrices are given by

$$\mathbf{M} = \begin{bmatrix} 1.0 & 1.0 & 1.0 \\ 1.0 & 2.0 & 2.0 \\ 1.0 & 2.0 & 3.0 \end{bmatrix}, \quad \mathbf{K} = \begin{bmatrix} 2 & -1 & 0.5 \\ -1 & 1.2 & 0.4 \\ 0.5 & 0.4 & 1.8 \end{bmatrix} \text{ and } \mathbf{C} = \begin{bmatrix} 15.25 & -9.8 & 3.4 \\ -9.8 & 6.48 & -1.84 \\ 3.4 & -1.84 & 2.22 \end{bmatrix}. \tag{1.27}$$

It may be verified that all the system matrices are positive definite. The mass-normalized undamped modal matrix is obtained as

$$\mathbf{\Phi} = \begin{bmatrix} 0.4027 & -0.5221 & -1.2511 \\ 0.5845 & -0.4888 & 1.1914 \\ -0.1127 & 0.9036 & -0.4134 \end{bmatrix}. \tag{1.28}$$

Since Caughey and O'Kelly's condition

$$\mathbf{K}\mathbf{M}^{-1}\mathbf{C} = \mathbf{C}\mathbf{M}^{-1}\mathbf{K} = \begin{bmatrix} 125.45 & -80.92 & 28.61 \\ -80.92 & 52.272 & -18.176 \\ 28.61 & -18.176 & 7.908 \end{bmatrix}$$

is satisfied, the system possess classical normal modes and that $\mathbf{\Phi}$ given in equation (1.28) is the modal matrix. Because the system is positive definite the other two conditions,

$$\mathbf{M}\mathbf{K}^{-1}\mathbf{C} = \mathbf{C}\mathbf{K}^{-1}\mathbf{M} = \begin{bmatrix} 2.0 & -1.0 & 0.5 \\ -1.0 & 1.2 & 0.4 \\ 0.5 & 0.4 & 1.8 \end{bmatrix}$$

and

$$\mathbf{M}\mathbf{C}^{-1}\mathbf{K} = \mathbf{K}\mathbf{C}^{-1}\mathbf{M} = \begin{bmatrix} 4.1 & 6.2 & 5.6 \\ 6.2 & 9.73 & 9.2 \\ 5.6 & 9.2 & 9.6 \end{bmatrix}$$

are also satisfied. Thus all three conditions described in Theorem 1.1 are simultaneously valid although none of them are the same. So, if any one of the three conditions proposed in Theorem 1.1 is satisfied, a viscously damped positive definite system will possess classical normal modes.

1.5.1 Generalized proportional damping

- We want to find $\mathbf{C}$ in terms of $\mathbf{M}$ and $\mathbf{K}$ such that the system still possesses classical normal modes. Caughey and O'Kelly (1965) proved that the series ('Caughey series') representation of damping

$$\mathbf{C} = \mathbf{M} \sum_{j=0}^{N-1} \alpha_j \left[\mathbf{M}^{-1}\mathbf{K}\right]^j \tag{1.29}$$

  is the *necessary and sufficient* condition for existence of classical normal modes. This generalized Rayleigh's proportional damping, which turns out to be the first two terms of the series.

- A further generalized and useful form of proportional damping can be obtained. Assuming that the system is positive definite, a further generalized and useful form of proportional damping will be derived in this note. Consider the conditions (a) and (b) of Theorem 1.1; premultiplying (a) by $\mathbf{M}^{-1}$ and (b) by $\mathbf{K}^{-1}$ one has

$$\begin{aligned} \left(\mathbf{M}^{-1}\mathbf{K}\right)\left(\mathbf{M}^{-1}\mathbf{C}\right) &= \left(\mathbf{M}^{-1}\mathbf{C}\right)\left(\mathbf{M}^{-1}\mathbf{K}\right) \quad \text{or} \quad \mathbf{AB} = \mathbf{BA} \\ \left(\mathbf{K}^{-1}\mathbf{M}\right)\left(\mathbf{K}^{-1}\mathbf{C}\right) &= \left(\mathbf{K}^{-1}\mathbf{C}\right)\left(\mathbf{K}^{-1}\mathbf{M}\right) \quad \text{or} \quad \mathbf{A}^{-1}\mathbf{D} = \mathbf{D}\mathbf{A}^{-1}, \end{aligned} \tag{1.30}$$

  where $\mathbf{A} = \mathbf{M}^{-1}\mathbf{K}$, $\mathbf{B} = \mathbf{M}^{-1}\mathbf{C}$ and $\mathbf{D} = \mathbf{K}^{-1}\mathbf{C}$.

- For any two matrices $\mathbf{A}$ and $\mathbf{B}$, if $\mathbf{A}$ commutes with $\mathbf{B}$, $\beta(\mathbf{A})$ also commutes with $\mathbf{B}$ where the real function $\beta(x)$ is smooth, continuous and has a Taylor series expansion about $x = 0$.

- From the commutative relationships in equation (1.30), one can use many well known functions to represent $\mathbf{M}^{-1}\mathbf{C}$ in terms of $\mathbf{M}^{-1}\mathbf{K}$ and also

$\mathbf{K}^{-1}\mathbf{C}$ in terms of $\mathbf{K}^{-1}\mathbf{M}$. So representations like $\mathbf{C} = \mathbf{M}\,\beta(\mathbf{M}^{-1}\mathbf{K})$ and $\mathbf{C} = \mathbf{K}\,\beta(\mathbf{K}^{-1}\mathbf{M})$ are valid.

- The damping matrix can be expressed by adding these two quantities as

$$\mathbf{C} = \mathbf{M}\,\beta_1\left(\mathbf{M}^{-1}\mathbf{K}\right) + \mathbf{K}\,\beta_2\left(\mathbf{K}^{-1}\mathbf{M}\right) \tag{1.31}$$

such that the system possesses classical normal modes. Postmultiplying condition (a) of Theorem 1.1 by $\mathbf{M}^{-1}$ and (b) by $\mathbf{K}^{-1}$ one has

$$\begin{aligned}\left(\mathbf{K}\mathbf{M}^{-1}\right)\left(\mathbf{C}\mathbf{M}^{-1}\right) &= \left(\mathbf{C}\mathbf{M}^{-1}\right)\left(\mathbf{K}\mathbf{M}^{-1}\right)\\ \left(\mathbf{M}\mathbf{K}^{-1}\right)\left(\mathbf{C}\mathbf{K}^{-1}\right) &= \left(\mathbf{C}\mathbf{K}^{-1}\right)\left(\mathbf{M}\mathbf{K}^{-1}\right).\end{aligned} \tag{1.32}$$

- Following a similar procedure we can express the damping matrix in the form

$$\mathbf{C} = \beta_3\left(\mathbf{K}\mathbf{M}^{-1}\right)\mathbf{M} + \beta_4\left(\mathbf{M}\mathbf{K}^{-1}\right)\mathbf{K} \tag{1.33}$$

such that system (1.21) possesses classical normal modes.

- Although the functions $\beta_i(\bullet)$, $i = 1, \cdots, 4$ can have very general forms, the expressions of $\mathbf{C}$ in equations (1.31) and (1.33) get restricted because of the special nature of the *arguments* in the functions. As a consequence, $\mathbf{C}$ represented in (1.31) or (1.33) does not cover the whole $\mathbb{R}^{N\times N}$, which is well known that many damped systems do not possess classical normal modes.

- Rayleigh's proportional damping is a special case:

$$\beta_i(\bullet) = \alpha_i\mathbf{I}. \tag{1.34}$$

The functions $\beta_i(\bullet)$ are called *proportional damping functions*.

From this discussion we have the following general result for damped linear systems:

Theorem 1.2. *Viscously damped positive definite linear systems will have classical normal modes if and only if the damping matrix can be represented as*

(a) $\boldsymbol{C} = \boldsymbol{M}\,\beta_1\left(\boldsymbol{M}^{-1}\boldsymbol{K}\right) + \boldsymbol{K}\,\beta_2\left(\boldsymbol{K}^{-1}\boldsymbol{M}\right)$, *or*

(b) $\boldsymbol{C} = \beta_3\left(\boldsymbol{K}\boldsymbol{M}^{-1}\right)\boldsymbol{M} + \beta_4\left(\boldsymbol{M}\boldsymbol{K}^{-1}\right)\boldsymbol{K}$

for any smooth continuous functions $\beta_i(\bullet), i = 1, \cdots, 4$.

Example 1.2.

This example is chosen to show the general nature of the proportional damping functions which can be used within the scope of conventional modal analysis. It will be shown that the linear dynamic system satisfying the following equation of free vibration

$$\begin{aligned}\mathbf{M}\ddot{\mathbf{q}}+ \Big[&\mathbf{M}e^{-\left(\mathbf{M}^{-1}\mathbf{K}\right)^2/2}\sinh(\mathbf{K}^{-1}\mathbf{M}\ln(\mathbf{M}^{-1}\mathbf{K})^{2/3}) \\ &+ \mathbf{K}\cos^2(\mathbf{K}^{-1}\mathbf{M})\sqrt[4]{\mathbf{K}^{-1}\mathbf{M}}\,\tan^{-1}\frac{\sqrt{\mathbf{M}^{-1}\mathbf{K}}}{\pi}\Big]\dot{\mathbf{q}}+\mathbf{K}\mathbf{q}=\mathbf{0}\end{aligned} \tag{1.35}$$

possesses classical normal modes. Numerical values of $\mathbf{M}$ and $\mathbf{K}$ matrices are assumed to be the same as in example 1.1.

Direct calculation shows

$$\mathbf{C}=-\begin{bmatrix}67.9188 & 104.8208 & 95.9566\\ 104.8208 & 161.1897 & 147.7378\\ 95.9566 & 147.7378 & 135.2643\end{bmatrix}. \tag{1.36}$$

Using the modal matrix calculated before in equation (1.28), we obtain

$$\mathbf{\Phi}^T\mathbf{C}\mathbf{\Phi}=\begin{bmatrix}-88.9682 & 0.0 & 0.0\\ 0.0 & 0.0748 & 0.0\\ 0.0 & 0.0 & 0.5293\end{bmatrix},$$

a diagonal matrix. Analytically the modal damping factors can be obtained as

$$2\xi_j\omega_j=e^{-\omega_j^4/2}\sinh\left(\frac{1}{\omega_j^2}\ln\frac{4}{3}\omega_j\right)+\omega_j^2\cos^2\left(\frac{1}{\omega_j^2}\right)\frac{1}{\sqrt{\omega_j}}\tan^{-1}\frac{\omega_j}{\pi}. \tag{1.37}$$

This example shows that using the generalized proportional damping it is possible to model any variation of the damping factors with respect to the frequency. This is the basis of the damping identification method to be proposed later in section 3.2. With Rayleigh's proportional damping in equation (1.26), the modal damping factors have a special form

$$\zeta_j = \frac{1}{2}\left(\frac{\alpha_1}{\omega_j} + \alpha_2\omega_j\right). \tag{1.38}$$

Clearly, not all form of variations of ζ_j with respect to ω_j can be captured using equation (1.38). The damping identification method proposed in the next section removes this restriction.

1.6 Forced Dynamic Response of Generally Damped Linear Systems

- The conditions for existence of proportional damping are purely mathematical in nature and there is no reason why a general system should obey such conditions.

- In general a linear system will have non-proportional as well as non-viscous damping.

- The equation of motion of forced vibration of an N-degrees-of-freedom linear system with non-viscous damping of the form (1.19) is given by

$$\mathbf{M}\ddot{\mathbf{q}}(t) + \int_0^t \boldsymbol{\mathcal{G}}(t-\tau)\dot{\mathbf{q}}(\tau)\mathrm{d}\tau + \mathbf{K}\mathbf{q}(t) = \mathbf{f}(t). \tag{1.39}$$

  together with the *initial conditions*

$$\mathbf{q}(0) = \mathbf{q}_0 \in \mathbb{R}^N \text{and} \quad \dot{\mathbf{q}}(0) = \dot{\mathbf{q}}_0 \in \mathbb{R}^N. \tag{1.40}$$

- **Question:** Is classical modal analysis valid for such systems?

  - The **answer** is **yes**, but not in a straightforward manner (Adhikari, 2002).

1.6.1 Eigenvalues and Eigenvectors

- Considering the free vibration, that is $\mathbf{f}(t) = \mathbf{q}_0 = \dot{\mathbf{q}}_0 = \mathbf{0}$, and taking the Laplace transform of the equation of motion (1.39) one has

$$s^2\mathbf{M}\bar{\mathbf{q}} + s\mathbf{G}(s)\bar{\mathbf{q}} + \mathbf{K}\bar{\mathbf{q}} = \mathbf{0}. \tag{1.41}$$

  Here $\bar{\mathbf{q}}(s) = \mathcal{L}[\mathbf{q}(t)] \in \mathbb{C}^N$, $\mathbf{G}(s) = \mathcal{L}[\boldsymbol{\mathcal{G}}(t)] \in \mathbb{C}^{N\times N}$ and $\mathcal{L}[\bullet]$ denotes the Laplace transform.

- Assumptions: (a) $\mathbf{M}^{-1}$ exists, and (b) *all* the eigenvalues of $\mathbf{M}^{-1}\mathbf{K}$ are distinct and positive, and (c) $\mathbf{G}(s)$ is such that the motion is dissipative.

- The elements of $\mathbf{G}(s)$ can be represented as

$$G_{jk}(s) = \frac{p_{jk}(s)}{q_{jk}(s)}; \quad \lim_{|s|\to s_j} |G_{jk}(s)| < \infty \tag{1.42}$$

- The eigenvalues associated with equation (1.41) are the roots of the characteristic equation

$$\det\left[s^2\mathbf{M} + s\mathbf{G}(s) + \mathbf{K}\right] = 0. \tag{1.43}$$

  The roots of this equation are either real, or if complex, then must appear in conjugate pairs.

- Suppose the order of the characteristic polynomial $m = 2N + p$; $p \geq 0$.

- For an underdamped systems, among the m eigenvalues, $2N$ woll appear in complex conjugate pairs and the remaining p will be purely real. Arrange the eigenvalues as

$$s_1, s_2, \cdots, s_N, s_1^*, s_2^*, \cdots, s_N^*, s_{2N+1}, \cdots, s_m \tag{1.44}$$

- The eigenvalue problem associated with equation (1.39) can be defined from (1.41) as

$$\mathbf{D}(s_j)\mathbf{z}_j = \mathbf{0}, \quad \text{for } j = 1, \cdots, m \tag{1.45}$$

$$\text{where} \quad \mathbf{D}(s_j) = s_j^2\mathbf{M} + s_j\,\mathbf{G}(s_j) + \mathbf{K} \in \mathbb{C}^{N\times N} \tag{1.46}$$

- Corresponding to the $2N$ complex conjugate pairs of eigenvalues, the N eigenvectors together with their complex conjugates will be called *elastic modes*. These modes are related to the N modes of vibration of the structural system. Physically, the '$2N$ complex conjugate pairs of eigenvalues' means that all the elastic modes are oscillatory in nature, that is, they are sub-critically damped.

- The modes corresponding to the 'additional' p eigenvalues will be called *non-viscous modes*. These modes are induced by the non-viscous effect of the damping mechanism. For stable passive systems the non-viscous modes are over-critically damped (i.e., negative real eigenvalues) and not oscillatory in nature.

1.6.2 Elastic Modes

- Once the eigenvalues are known, all modes can be obtained from equation (1.45) by fixing any one element and inverting the associated $(N-1) \times (N-1)$ complex matrix-partition of $\mathbf{D}(s_j)$.

- An approximate solution will be given to enhance the understanding of non-viscously damped systems.

- Sine for distinct undamped eigenvalues (ω_l^2), the undamped mode shapes $\mathbf{x}_l$, $\forall\, l = 1, \cdots, N$, form a complete set of vectors, $\mathbf{z}_j$ can be expanded as a complex linear combination of $\mathbf{x}_l$:

$$\mathbf{z}_j = \sum_{l=1}^{N} \alpha_l^{(j)} \mathbf{x}_l; \quad \alpha_j^{(j)} = 1 \quad \text{(the normalization)} \tag{1.47}$$

- Substituting the expansion of $\mathbf{z}_j$, from equation (1.45)

$$\sum_{l=1}^{N} s_j^2 \alpha_l^{(j)} \mathbf{M}\mathbf{x}_l + s_j \alpha_l^{(j)} \mathbf{G}(s_j)\mathbf{x}_l + \alpha_l^{(j)} \mathbf{K}\mathbf{x}_l = \mathbf{0}. \tag{1.48}$$

- Premultiplying by $\mathbf{x}_k^T$ and using the orthogonality property of the undamped eigenvectors

$$s_j^2 \alpha_k^{(j)} + s_j \sum_{l=1}^{N} \alpha_l^{(j)} G'_{kl}(s_j) + \omega_k^2 \alpha_k^{(j)} = 0, \quad \forall k = 1, \cdots, N \tag{1.49}$$

where $G'_{kl}(s_j) = \mathbf{x}_k^T \mathbf{G}(s_j)\mathbf{x}_l$.

- For light non-proportionally damped systems, $G'_{kl}(s_j) \leq G'_{kk}(s_j)$, $\forall k \neq l, s_j$. Considering the j-th set of equation (1.49) and neglecting the

second-order terms involving $\alpha_k^{(j)}$ and $G'_{kl}(s_j)$, $\forall k \neq l$:

$$\begin{aligned} & s_j^2 + s_j G'_{jj}(s_j) + \omega_j^2 \approx 0 \\ \text{or} \quad & s_j \approx \pm \mathrm{i}\omega_j - G'_{jj}(\pm \mathrm{i}\omega_j)/2 \end{aligned} \tag{1.50}$$

that is $s_j \approx \mathrm{i}\omega_j - G'_{jj}(\mathrm{i}\omega_j)/2$ or $s_j \approx -\mathrm{i}\omega_j - G'_{jj}(-\mathrm{i}\omega_j)/2$.

This is the first-order approximate expression of the eigenvalues of the non-viscously damped system (1.39) corresponding to the elastic modes.

- Because $\boldsymbol{\mathcal{G}}(t)$ is a real function, $G'_{jj}(\bullet)$ satisfies the property

$$G'_{jj}(-\mathrm{i}\omega_j) = G'^{*}_{jj}(\mathrm{i}\omega_j). \tag{1.51}$$

Using this it can be confirmed that approximate eigenvalues in (1.50) appear in complex conjugate pairs.

- To obtain an approximate expression of the eigenvectors, rewrite equation (1.49) as

$$s_j^2 \alpha_k^{(j)} + s_j \left(G'_{kj}(s_j) + \alpha_k^{(j)} G'_{kk}(s_j) + \sum_{l \neq k \neq j}^{N} \alpha_l^{(j)} G'_{kl}(s_j) \right) + \omega_k^2 \alpha_k^{(j)} = 0, \quad \forall k = 1, \cdots, N; \neq j. \tag{1.52}$$

- Neglecting the second-order terms involving $\alpha_k^{(j)}$ and $G'_{kl}(s_j)$, $\forall k \neq l$

$$\begin{aligned} & s_j^2 \alpha_k^{(j)} + s_j G'_{kk}(s_j) \alpha_k^{(j)} \omega_k^2 \alpha_k^{(j)} \approx -s_j G'_{kj}(s_j), \\ \text{or} \quad & \alpha_k^{(j)} \approx \frac{s_j G'_{kj}(s_j)}{\omega_k^2 + s_j^2 + s_j G'_{kk}(s_j)} \quad \forall k = 1, \cdots, N; \neq j. \end{aligned} \tag{1.53}$$

- Substituting $\alpha_k^{(j)}$ in equation (1.47)

$$\mathbf{z}_j \approx \mathbf{x}_j - \sum_{\substack{k=1 \\ k \neq j}}^{N} \frac{s_j G'_{kj}(s_j)\mathbf{x}_k}{\omega_k^2 + s_j^2 + s_j G'_{kk}(s_j)}. \tag{1.54}$$

This is the approximate first-order expression of the complex modes.

1.6.3 Non-viscous Modes

- When $2N < j \leq m$, the eigenvalues and eigenvectors become real Partition $\mathbf{z}_j$ as

$$\mathbf{z}_j = \begin{Bmatrix} \mathbf{z}_{1j} \\ \mathbf{z}_{2j} \end{Bmatrix}. \tag{1.55}$$

and $\mathbf{D}(s_j)$ as

$$\mathbf{D}(s_j) = \begin{bmatrix} \mathbf{D}_{11}(s_j) & \mathbf{D}_{12}(s_j) \\ \mathbf{D}_{21}(s_j) & \mathbf{D}_{22}(s_j) \end{bmatrix} \tag{1.56}$$

where $\mathbf{D}_{11}(s_j) \in \mathbb{R}$, $\mathbf{D}_{12}(s_j) \in \mathbb{R}^{1\times(N-1)}$, $\mathbf{D}_{21}(s_j) \in \mathbb{R}^{(N-1)\times 1}$ and $\mathbf{D}_{22}{}^{(j)} \in \mathbb{R}^{(N-1)\times(N-1)}$.

- Select $\mathbf{z}_{1j} = 1$ so that $\mathbf{z}_{2j} \in \mathbb{R}^{(N-1)}$ can be determined from equations (1.45)

$$\mathbf{D}_{22}(s_j)\mathbf{z}_{2j} = -\mathbf{D}_{21}(s_j) \text{ or } \mathbf{z}_{2j} = -\left[\mathbf{D}_{22}(s_j)\right]^{-1}\mathbf{D}_{21}(s_j). \tag{1.57}$$

The Special Case: Viscously Damped Systems With Light Non-proportional Damping

- The eigensolutions of viscously damped systems consist of only the elastic modes. The results derived for elastic modes can be applied to viscously damped systems by considering the fact that the matrix of the damping functions, $\mathbf{G}(s)$, is a constant matrix, say $\mathbf{G}(s) = \mathbf{C}$, $\forall s$, where $\mathbf{C}$ is the viscous damping matrix.

- Using this simplification, from equation (1.50), the approximate eigenvalues (appear in complex conjugate pairs) are obtained as

$$s_j \approx \pm \mathrm{i}\omega_j - C'_{jj}/2 = -C'_{jj}/2 + \mathrm{i}\omega_j, \quad -C'_{jj}/2 - \mathrm{i}\omega_j. \tag{1.58}$$

- From equation (1.54), the first-order approximate expressions of eigenvectors are obtained as

$$\mathbf{z}_j \approx \mathbf{x}_j - \sum_{\substack{k=1 \\ k \neq j}}^{N} \frac{s_j C'_{kj} \mathbf{x}_k}{\omega_k^2 + s_j^2 + s_j C'_{kk}}. \tag{1.59}$$

1.6.4 Transfer Function of the System

- The transfer function (matrix) of a system completely defines its input-output relationship in the *steady-state*.

- Taking the Laplace transform of equation (1.39) gives

$$s^2\mathbf{M}\bar{\mathbf{q}} + s\,\mathbf{G}(s)\bar{\mathbf{q}} + \mathbf{K}\bar{\mathbf{q}} = \bar{\mathbf{f}} \quad \text{or} \quad \mathbf{D}(s)\bar{\mathbf{q}} = \bar{\mathbf{f}} \tag{1.60}$$

  where the *dynamic stiffness matrix*

$$\mathbf{D}(s) = s^2\mathbf{M} + s\,\mathbf{G}(s) + \mathbf{K} \ \in \mathbb{C}^{N\times N}. \tag{1.61}$$

- From equation (1.60) the response vector $\bar{\mathbf{q}}$ can be obtained as

$$\bar{\mathbf{q}} = \mathbf{D}^{-1}(s)\bar{\mathbf{f}} = \mathbf{H}(s)\bar{\mathbf{f}} \tag{1.62}$$

  where

$$\mathbf{H}(s) = \mathbf{D}^{-1}(s) \in \mathbb{C}^{N\times N} \tag{1.63}$$

  is the transfer function matrix.

- Clearly

$$\mathbf{H}(s) = \frac{\text{adj}\,[\mathbf{D}(s)]}{\det\,[\mathbf{D}(s)]}. \tag{1.64}$$

- The *poles* of $\mathbf{H}(s)$, denoted by s_j, are the eigenvalues of the system. Because it is assumed that *all* the m eigenvalues are distinct, each pole is a *simple pole*.

- From the residue theorem it is known that any analytic complex function can be expressed in terms of the poles and *residues*, that is, the transfer

function has the form

$$\mathbf{H}(s) = \sum_{j=1}^{m} \frac{\mathbf{R}_j}{s - s_j}. \tag{1.65}$$

Where

$$\mathbf{R}_j = \underset{s=s_j}{\text{res}} \left[\mathbf{H}(s)\right] \stackrel{\text{def}}{=} \lim_{s \to s_j} (s - s_j) \left[\mathbf{H}(s)\right] \tag{1.66}$$

is the residue of the transfer function matrix at the pole s_j.

- The residues can be obtained exactly (see Appendix A for details) in terms of the system eigenvectors as

$$\mathbf{R}_j = \frac{\mathbf{z}_j \mathbf{z}_j^T}{\mathbf{z}_j^T \frac{\partial \mathbf{D}(s_j)}{\partial s_j} \mathbf{z}_j}. \tag{1.67}$$

- Recalling that, among the m eigenvalues $2N$ appear in complex conjugate pairs, from equation (1.65) the transfer function matrix is obtained as

$$\mathbf{H}(\mathrm{i}\omega) = \sum_{j=1}^{N} \left[\frac{\gamma_j \mathbf{z}_j \mathbf{z}_j^T}{\mathrm{i}\omega - s_j} + \frac{\gamma_j^* \mathbf{z}_j^* \mathbf{z}_j^{*T}}{\mathrm{i}\omega - s_j^*} \right] + \sum_{j=2N+1}^{m} \frac{\gamma_j \mathbf{z}_j \mathbf{z}_j^T}{\mathrm{i}\omega - s_j}, \tag{1.68}$$

where

$$\gamma_j = \frac{1}{\mathbf{z}_j^T \frac{\partial \mathbf{D}(s_j)}{\partial s_j} \mathbf{z}_j}. \tag{1.69}$$

The transfer function matrix has two parts, the first part is due to the elastic modes, and the second part is due to the non-viscous modes.

- This expression is a natural generalization of the familiar transfer function matrices of undamped or viscously damped systems:

1. *Undamped systems*: In this case $\mathbf{G}(s) = 0$ results the order of the characteristic polynomial $m = 2N$; s_j is purely imaginary so that

$s_j = \mathrm{i}\omega_j$ where $\omega_j \in \mathbb{R}$ are the undamped natural frequencies and $\mathbf{z}_j = \mathbf{x}_j \in \mathbb{R}^N$. In view of the mass normalization relationship in (1.10), $\gamma_j = \frac{1}{2\mathrm{i}\omega_j}$ and equation (1.68) leads to

$$\mathbf{H}(\mathrm{i}\omega) = \sum_{j=1}^{N} \frac{1}{2\mathrm{i}\omega_j} \left[\frac{1}{\mathrm{i}\omega - \mathrm{i}\omega_j} - \frac{1}{\mathrm{i}\omega + \mathrm{i}\omega_j} \right] \mathbf{x}_j \mathbf{x}_j^T = \sum_{j=1}^{N} \frac{\mathbf{x}_j \mathbf{x}_j^T}{\omega_j^2 - \omega^2}. \tag{1.70}$$

2. *Viscously-damped systems with non-proportional damping* (see for example, Géradin and Rixen, 1997): In this case $m = 2N$ and $\gamma_j = \frac{1}{\mathbf{z}_j^T [2s_j \mathbf{M} + \mathbf{C}] \mathbf{z}_j}$. These reduce expression (1.68) to

$$\mathbf{H}(\mathrm{i}\omega) = \sum_{j=1}^{N} \left[\frac{\gamma_j \mathbf{z}_j \mathbf{z}_j^T}{\mathrm{i}\omega - s_j} + \frac{\gamma_j^* \mathbf{z}_j^* \mathbf{z}_j^{*T}}{\mathrm{i}\omega - s_j^*} \right]. \tag{1.71}$$

1.6.5 Dynamic Response

Frequency Domain Analysis

- Taking the Laplace transform of equation (1.39) and considering the initial conditions in (1.40)

$$\begin{aligned} & s^2\mathbf{M}\bar{\mathbf{q}} - s\mathbf{M}\mathbf{q}_0 - \mathbf{M}\dot{\mathbf{q}}_0 + s\,\mathbf{G}(s)\bar{\mathbf{q}} - \mathbf{G}(s)\mathbf{q}_0 + \mathbf{K}\bar{\mathbf{q}} = \bar{\mathbf{f}}(s) \\ \text{or} \quad & \left[s^2\mathbf{M} + s\,\mathbf{G}(s) + \mathbf{K}\right]\bar{\mathbf{q}} = \bar{\mathbf{f}}(s) + \mathbf{M}\dot{\mathbf{q}}_0 + \left[s\mathbf{M} + \mathbf{G}(s)\right]\mathbf{q}_0. \end{aligned} \tag{1.72}$$

- Using the expression for the transfer function derived before, the response vector $\bar{\mathbf{q}}$ may be obtained as

$$\bar{\mathbf{q}} = \sum_{j=1}^{m} \frac{\gamma_j \mathbf{z}_j \mathbf{z}_j^T}{s - s_j} \left\{\bar{\mathbf{f}}(s) + \mathbf{M}\dot{\mathbf{q}}_0 + \left[s\mathbf{M} + \mathbf{G}(s)\right]\mathbf{q}_0\right\}. \tag{1.73}$$

- This can be simplified further to

$$\begin{aligned} \bar{\mathbf{q}}(\mathrm{i}\omega) &= \sum_{j=1}^{m} \frac{\gamma_j A_j(\mathrm{i}\omega)}{\mathrm{i}\omega - s_j}\mathbf{z}_j \\ &= \sum_{j=1}^{N} \left\{ \frac{\gamma_j A_j(\mathrm{i}\omega)}{\mathrm{i}\omega - s_j}\mathbf{z}_j + \frac{\gamma_j^* A_j^*(\mathrm{i}\omega)}{\mathrm{i}\omega - s_j^*}\mathbf{z}_j^* \right\} + \sum_{j=2N+1}^{m} \frac{\gamma_j A_j(\mathrm{i}\omega)}{\mathrm{i}\omega - s_j}\mathbf{z}_j \end{aligned} \tag{1.74}$$

where the frequency-dependent complex scalar

$$A_j(\mathrm{i}\omega) = \mathbf{z}_j^T\bar{\mathbf{f}}(\mathrm{i}\omega) + \mathbf{z}_j^T\mathbf{M}\dot{\mathbf{q}}_0 + \mathrm{i}\omega\mathbf{z}_j^T\mathbf{M}\mathbf{q}_0 + \mathbf{z}_j^T\mathbf{G}(\mathrm{i}\omega)\mathbf{q}_0. \tag{1.75}$$

The first part of the summation in equation (1.74) corresponds to the $2N$ complex conjugate pairs of elastic modes and the second part corresponds to the contribution of the non-viscous modes.

Time Domain Analysis

- From the expression of the transfer function in equation (1.68), the impulse response function matrix $\mathbf{h}(t) \in \mathbb{R}^{N\times N}$ may be obtained as

$$\mathbf{h}(t) = \sum_{j=1}^{N} \left[\gamma_j \mathbf{z}_j \mathbf{z}_j^T e^{s_j t} + \gamma_j^* \mathbf{z}_j^* \mathbf{z}_j^{*^T} e^{s_j^* t}\right] + \sum_{j=2N+1}^{m} \gamma_j \mathbf{z}_j \mathbf{z}_j^T e^{s_j t}. \tag{1.76}$$

- The response due to the initial conditions may also be obtained by taking the inverse transform of equation (1.73). First, simplify equation (1.73)

$$\bar{\mathbf{q}}(s) = \sum_{j=1}^{m} \gamma_j \left[\frac{\mathbf{z}_j^T \bar{\mathbf{f}}(s) + \mathbf{z}_j^T \mathbf{G}(s)\mathbf{q}_0}{s - s_j} + \frac{\mathbf{z}_j^T \mathbf{M}\dot{\mathbf{q}}_0}{s - s_j} + \left(1 + \frac{s_j}{s - s_j}\right) \mathbf{z}_j^T \mathbf{M}\mathbf{q}_0\right] \mathbf{z}_j. \tag{1.77}$$

- From the above

$$\mathbf{q}(t) = \mathcal{L}^{-1}[\bar{\mathbf{q}}(s)] = \sum_{j=1}^{N} \left[\gamma_j a_j(t)\mathbf{z}_j + \gamma_j^* a_j^*(t)\mathbf{z}_j^*\right] + \sum_{j=2N+1}^{m} \gamma_j a_j(t)\mathbf{z}_j \tag{1.78}$$

where the time-dependent scalar coefficients

$$a_j(t) = \int_0^t e^{s_j(t-\tau)} \left\{\mathbf{z}_j^T \mathbf{f}(\tau) + \mathbf{z}_j^T \boldsymbol{\mathcal{G}}(\tau)\mathbf{q}_0\right\} \mathrm{d}\tau + e^{s_j t} \left\{\mathbf{z}_j^T \mathbf{M}\dot{\mathbf{q}}_0 + s_j \mathbf{z}_j^T \mathbf{M}\mathbf{q}_0\right\}; \quad \forall t > 0. \tag{1.79}$$

- Summary of the response analysis

  - The expression of the system response, either the frequency-domain description in equation (1.74) or the time-domain description in equation (1.78), is similar to the classical modal superposition result for undamped or proportionally damped systems usually obtained using the mode-orthogonality relationships.
  - It is a generalization of the classical result where the real normal modes are appropriately 'replaced' by the elastic modes and the non-viscous modes.
  - We have not used any orthogonality relationship – the expression of the transfer function residue in equation (1.67) allows us to express the response in terms of superposition of individual modes even when the equation of motion cannot be decoupled.

1.6.6 Numerical Example

Consider a three degree-of-freedom system in figure 1.2. Damping is associated

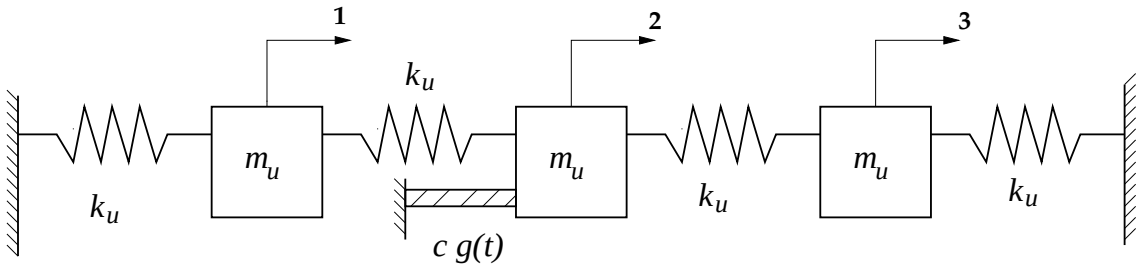

Figure 1.2: Three degree-of-freedom non-viscously damped system, $m_u = 1$ kg, $k_u = 1$ N/m, $c = 0.3$ Ns/m

only with the middle mass, and the kernel function corresponding to this damper

$$\mathcal{G}_{22}(t) = c\,g(t), \text{ where } g(t) = \mu e^{-\mu t}; \quad \mu, t \geq 0. \tag{1.80}$$

- For a viscously damped system $g(t) = \delta(t)$. The value of μ give a notion of *non-viscousness* – if it is large the damping behavior will be near-viscous, and vice versa.

- The mass and stiffness matrices and the damping matrix in the Laplace domain for the problem can be obtained as:

$$\mathbf{M} = \begin{bmatrix} m_u & 0 & 0 \\ 0 & m_u & 0 \\ 0 & 0 & m_u \end{bmatrix}, \quad \mathbf{K} = \begin{bmatrix} 2k_u & -k_u & 0 \\ -k_u & 2k_u & -k_u \\ 0 & -k_u & 2k_u \end{bmatrix}, \quad \mathbf{G}(s) = \begin{bmatrix} 0 & 0 & 0 \\ 0 & cG(s) & 0 \\ 0 & 0 & 0 \end{bmatrix}. \tag{1.81}$$

  where $G(s) = \frac{\mu}{s+\mu}$.

- Using these expressions, the characteristic equation can be simplified as

$$m_u^3 s^7 + m_u^3 \mu\, s^6 + \left(2\, m_u^2 k_u + m_u\left(\mu\, c m_u + 4\, m_u k_u\right)\right) s^5 + 6\, k_u m_u^2 \mu\, s^4 + \left(2\, k_u\left(\mu\, c m_u + 4\, m_u k_u\right) + m_u\left(2\,\mu\, c k_u + 2\, {k_u}^2\right)\right) s^3 + 10\, {k_u}^2 m_u \mu\, s^2 + 2\, k_u\left(2\,\mu\, c k_u + 2\, {k_u}^2\right) s + 4\, {k_u}^3 \mu = 0. \quad (1.82)$$

The order of the above polynomial, $m = 7$. Since the system has three degrees of freedom there are three elastic modes corresponding to the three modes of vibration. The number of the non-viscous modes, $p = m - 2N = 1$.

Behaviour of the Eigenvalues

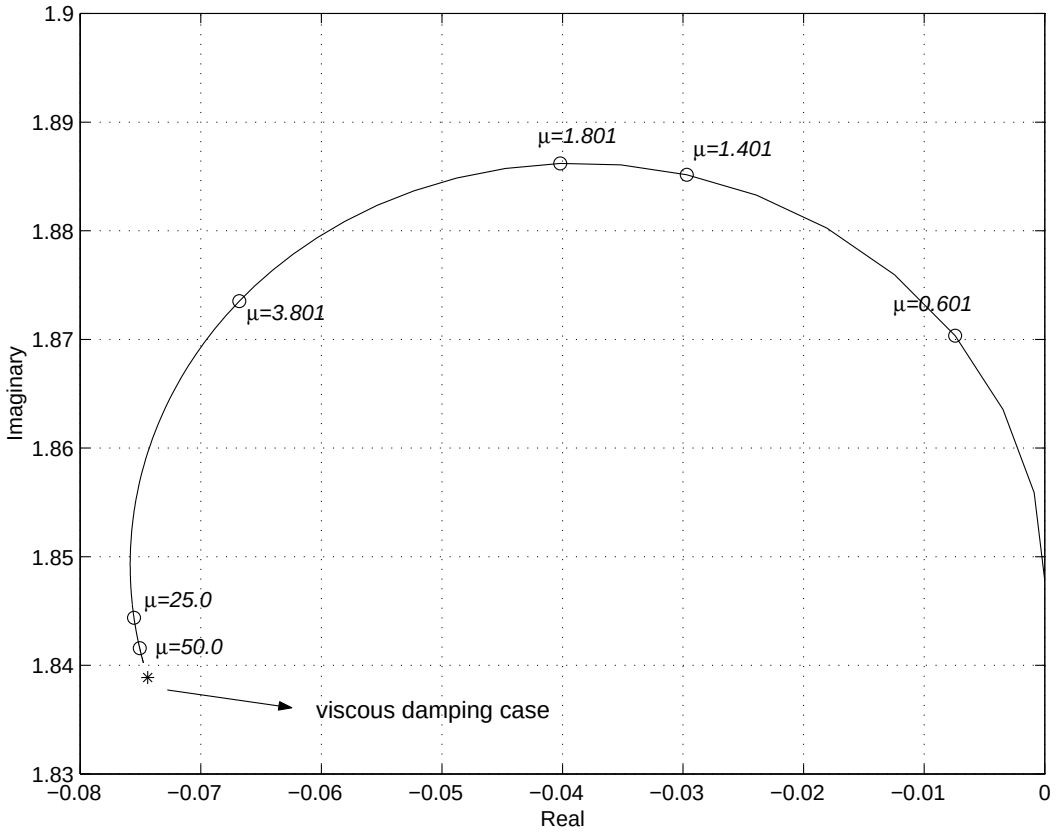

Figure 1.3: Root-locus plot of the third eigenvalue (s_3) as a function of μ.

- The locus is much more sensitive in the region of lower values of μ (*i.e.*, when damping is significantly non-viscous) compared to that in the region of higher values.
- The eigenvalue of the corresponding viscously damped system is also plotted (marked by *) in the same diagram. The non-viscous damping model approaches the viscous damping model when $\mu \gtrsim 50.0$.

Dynamic Response Analysis

The stationary random vibration of the system is considered. Suppose the system is subjected to a band-limited Gaussian *white noise* at the third DOF. We are interested in the resulting displacement at the third DOF (i.e., $\mathbf{z}_3$). The power spectral density (PSD) of the response

$$S_{uu}(\mathrm{i}\omega) = |H_{33}(\mathrm{i}\omega)|^2 S_{ff}(\mathrm{i}\omega) \tag{1.83}$$

where $S_{ff}(\mathrm{i}\omega) = 1$ if $0 < \omega \leq 2.5$ and $S_{ff}(\mathrm{i}\omega) = 0$ elsewhere.

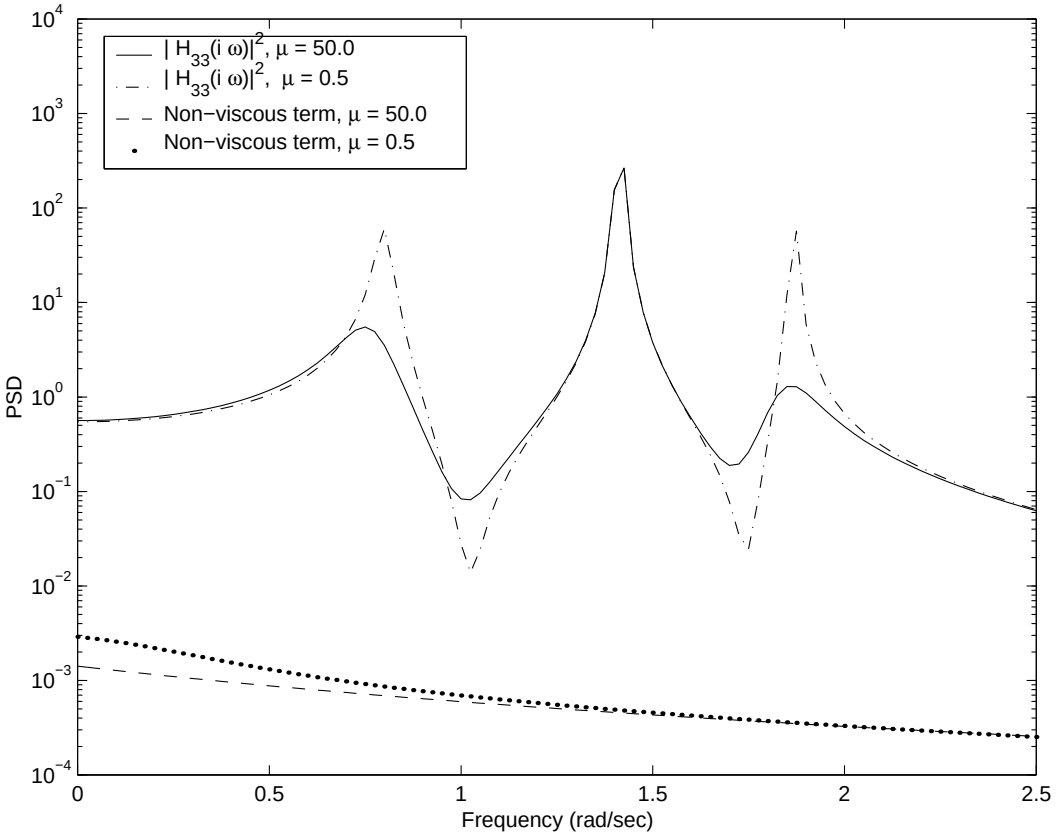

Figure 1.4: Power spectral density function of the displacement at the third DOF ($\mathbf{z}_3$) together with the non-viscous term (the second term) appearing in equation (1.68)

1.7 Conclusions

- In this lecture different mathematical models used for dynamic analysis of engineering structures have been introduced.
- Different models of damping used in the literature have been briefly reviewed.
- The proportional damping assumption has been critically examined and the concept of generalized proportional damping has been introduced. The generalized proportional damping extend the Rayleigh's classical damping model by expressing the damping matrix in terms of *any* non-linear function involving specially arranged mass and stiffness matrices.
- The problem of dynamic analysis of general non-viscously damped multiple-degrees-of-freedom linear systems has been considered. The non-viscous damping model is such that the damping forces depend on the past history of motion via convolution integrals over some kernel functions.
- The dynamics of non-viscously damped system is governed by elastic modes and non-viscous modes.
- Exact closed-form expressions of the dynamic response due to arbitrary forcing functions and initial conditions were obtained.
- It was shown that, like classically damped systems, the dynamic response can be expressed in terms of modal superposition even when the equation of motion cannot be decoupled in the modal coordinate.

2 What is Model Validation and Model Verification? How it is Done?

2.1 Introduction

Once the modeling and the simulation have been performed, it is required to 'judge' the model and simulation against the three criteria mentioned before, namely, fidelity to experimental data, robustness with respect to random errors and predictive capability. This process broadly falls under model validation and verification (V&V).

- ***Model Verification:*** Model verification is defined as ensuring that the computer program of the computerized model and its implementation are correct.

- ***Model Validation:*** Model validation is defined to mean substantiation that a computerized model within its domain of applicability possesses a satisfactory range of accuracy consistent with the intended application of the model.

- With the development of the finite-element method together with easily available computational hardware, within the past three decades the models have become more complex and simulations have become more computationally intensive.
- These, combined with the development of powerful computing languages, software packages, realistic pre and post processing visualization software and hardware, development of sophisticated information technology (IT) systems and easily available trained software professionals have pushed the engineering community to rely more on their models than ever before.
- This fact is also fuelled by increasing cost of conducting full-scale experiments compared to simulations due to tough environmental regulations, stringent health and safety conditions and various social factors.
- As a direct result of all these factors, the developers and users of the models, the decision makers using information derived from the results of the models, and people affected by decisions based on such models are highly concerned with the accuracy, predictive capability and credibility of the modeling and simulation process as a whole.
- The objective of V&V activities is to provide measures by which these qualities can be judged in a scientific, methodical, rigorous, consistent, generalized and possibly simple manner.

The scope of V&V activities

- Why should we believe that the predictions of our numerical simulations are any better than crystal-ball reading?
- What is the prediction accuracy of the model, especially away from those settings that can be measured experimentally?
- What is the validation domain for a given application?
- Is the computer code free of programming mistakes?
- Does the computational mesh (or grid) provide converged solutions?
- Which feature of the response best provides physical insight about the phenomenon?
- Where is an observed variability coming from?
- Which parameters of the numerical simulation control the spread of output results?
- What is the effect of modeling uncertainty on the predictions?
- Can the physics-based simulation be replaced by a fast-running surrogate?
- How to meaningfully compare physical measurements to numerical predictions?
- Where is the modeling error coming from, and how can it be reduced?

- Which numerical modeling technique is better for a particular application?
- How robust are predictions to the modeling error?
- How to study the trade-offs between prediction accuracy and modeling lack-of-knowledge?

2.2 Experimental Modal Analysis (EMA

- An essential step of V&V in structural dynamics is the experimental modal analysis (EMA).

- References: See the books by Ewins (2000), Maia and Silva (1997) and Silva and Maia (1998). Another important source of information is the Proceedings of the International Modal Analysis Conference (IMAC). This conference, organized by the Society of Experimental Mechanics (SEM, see http://www.sem.org), is running since 1982 and has produced great amount useful infirmation.

Outline of EMA

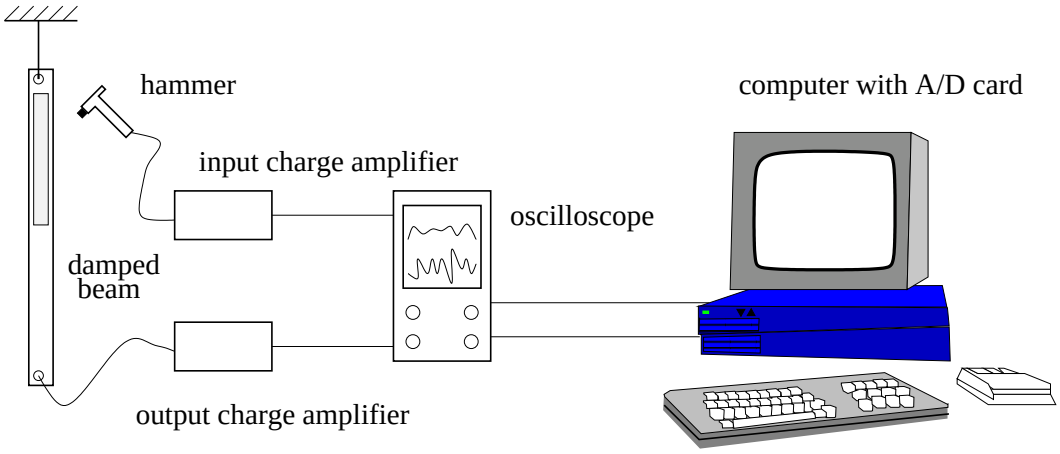

Figure 2.1: Schematic representation of a typical modal testing setup

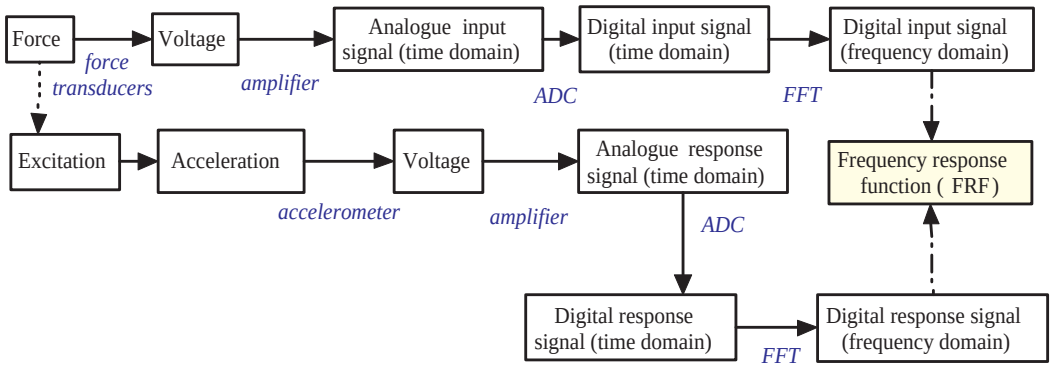

Figure 2.2: Data flow in a typical experimental modal analysis procedure

2.3 Measures of Model Correlations

A crucial step for dynamic model validation is to compare experimental results from the test structure with predicted results from the corresponding finite element model. The basic questions surrounding this process are

1. What quantities shall we compare?
2. How do we actually compare them?
3. How many modes shall we (or can we) compare?
4. The FE model has more degrees-of-freedom compared to the number of transducers in the experimental set up. How can we take account of this fact?
5. The FE model is normally undamped. How to deal with damping?
6. What about the (random) errors introduced by experimental hardware which have not been modeled in FE?
7. Finally, does a good comparison result always means a good analytical model?

The comparison between the test results and analytical results can be performed in the following three levels:

(a) Comparison of the modal properties

(b) Comparison of the spatial properties (the mass and stiffness matrices)

(c) Comparison of response (transfer functions)

Comparison of the modal properties

- This process consist of comparing the mode shapes and natural frequencies. Suppose $\mathbf{X}_e \in \mathbb{R}^{N_e \times m}$ is the matrix of modes shapes and $\mathbf{\Omega}_e \in \mathbb{R}^{m \times m}$ is the diagonal matrix of the natural frequencies obtained from the experiment.

- Comparing the natural frequencies obtained from the experiment with that from the FE model is the easiest task. Once can simply plot them together in a single graph or tabulate them to see their differences.

- For systems with well separated modes it is also possible to compare the mode shapes graphically. A typical case is shown in figure 2.3 where first four experimental and analytical mode shapes of a free-free beam in compared.

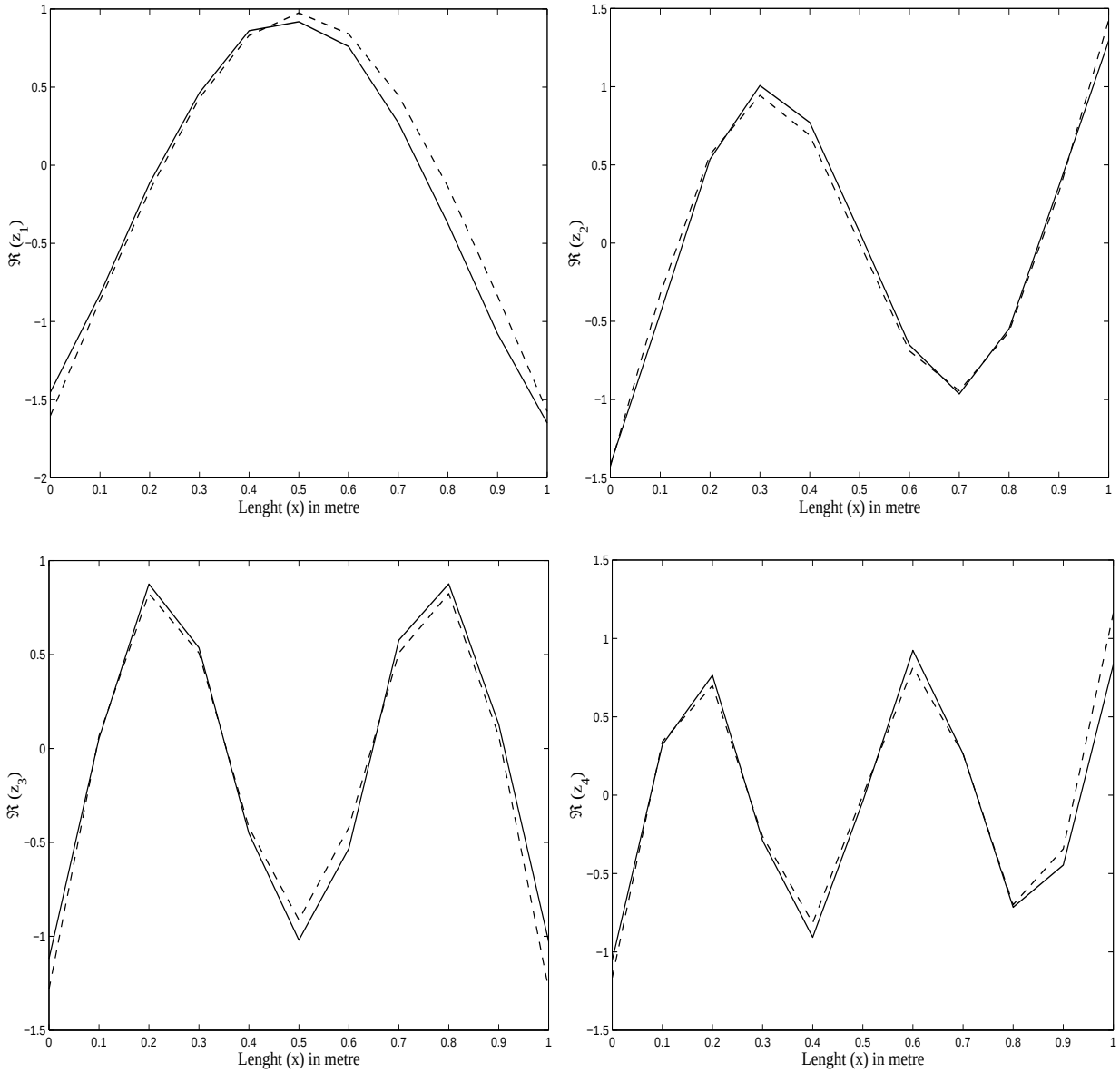

Figure 2.3: Comparison of the first four mode shapes of a free-free beam,'—' experiment, '– –' theory

- For structures with closely spaced modes or structures with complex geometry (such as an automobile body) this type of comparison is less simple to do. The main challenge there is to identify an experimental mode which correlates to an FE mode or vice versa.

- Several researchers have developed different methods to quantify the correlation between experimental and FE mode shapes. Among all, most popular is the Modal Assurance Criterion (MAC) (Allemang and Brown, 1982). The MAC between an experimentally obtained mode $\mathbf{x}_{e_j}$ and an analytical mode $\mathbf{x}_{a_k}$ is defined as

$$\mathrm{MAC}_{jk} = \frac{\left|\mathbf{x}_{e_j}^T \mathbf{x}_{a_k}\right|^2}{\left|\mathbf{x}_{a_k}^T \mathbf{x}_{a_k}\right| \left|\mathbf{x}_{e_j}^T \mathbf{x}_{e_j}\right|}. \tag{2.1}$$

  The value of MAC is between 0 and 1. A value of 1 indicates one mode shape is fully correlated to the other.

- Usually the values of MAC are placed in a matrix. For a well correlated model one expects the diagonal of the MAC matrix close to one and zero elsewhere.

Comparison of the spatial properties (the mass and stiffness matrices)

Using the orthogonality properties of the mode shapes it can be shown that the mass and stiffness matrices of the experimental system are given by

$$\mathbf{M}_e^{-1} = \mathbf{X}_e \mathbf{X}_e^T \in \mathbb{R}^{N_e \times N_e} \tag{2.2}$$

$$\text{and} \quad \mathbf{K}_e^{-1} = \mathbf{X}_e \mathbf{\Omega}_e^{-2} \mathbf{X}_e^T \in \mathbb{R}^{N_e \times N_e} \tag{2.3}$$

- N_e, the number of degrees-of-freedom of the experimental system (i.e., the number of response measurement points), is much smaller compared to the number of degrees-of-freedom of the FE model N. Since $N \gg N_e$, the comparison of $\mathbf{M}_e$ and $\mathbf{K}_e$ with $\mathbf{M}$ and $\mathbf{K}$ is not very meaningful.

- There are two approaches one could adopt at this stage. The first is to perform a *model reduction* of the FE system matrices so that they comparable to that of the experimental matrices. The second is to perform a *model expansion* of the experimental matrices using FE mode shapes. See the book by Friswell and Mottershead (1995) for further discussions on model reduction and model expansion methods.

Comparison of response (transfer functions))

- It is difficult to compare the experimentally obtained time histories with the time histories obtained from the analytical model. The main reason behind this is the damping. The time histories are very sensitive to damping and since the initial numerical model normally do not have any damping it hardly meaningful to compare them directly.

- The usual way to compare the response is to look at the frequency domain response. Individual FRFs can be compared graphically by simply plotting the test and analytical results together.

- There are four issues to be kept in mind while comparing the frequency response functions: (a) the amount and nature of damping, (b) range of frequency (c) number of modes and (d) separation between the modes.

- In some applications it is required to compare the complete set of transfer functions. This is a difficult task simply due to overwhelming volume of data that one has to deal with. Extending the analogy of MAC, in this case a frequency response assurance criteria (FRAC) can be defined in a similar way

$$\text{FRAC}_{jk} = \frac{\left|\mathbf{H}_e(\omega_j)^T \mathbf{H}_a(\omega_k)\right|^2}{\left|\mathbf{H}_a(\omega_k)^T \mathbf{H}_a(\omega_k)\right| \left|\mathbf{H}_e(\omega_j)^T \mathbf{H}_e(\omega_j)\right|}. \tag{2.4}$$

A diagram similar to MAC can be used to represent FRAC. The only difference will be that a FRAC diagram will be very dense since there are thousands of frequency points in each FRFs.

2.4 Conclusions

- The scope of validation and verification (V&V) of numerical models of dynamic systems have been explained.
- The experimental modal analysis (EMA) plays a central role in the V&V of structural dynamic models.
- Some approaches to measure the correlation between experimental results and output of numerical models in dynamics, such as MAC and FRAC have been discussed.

After an initial validation exercise one usually finds that there are discrepancies between the results from the FE models and that from the experiments. Once such differences are quantified using the methods outlined here, the next step is to update the FE model so that these differences can be reduced. Model updating is an essential step for building a credible numerical model. It is an active area of research, see the book by Friswell and Mottershead (1995) for details.

3 Identification of Damping

3.1 Introduction

The Aim is to obtain the viscous damping matrix $\mathbf{C}$ from EMA.

- The validation of FE models hinges crucially on damping.
- In general obtaining a damping matrix from the first-principle is difficult. Normally the damping matrix is constructed from modal testing data.
- The methods of damping identification can be divided into two basic categories:
  - damping identification from modal data (Alvin et al., 1997, Hasselsman, 1972, Ibrahim, 1983, Minas and Inman, 1991)
  - direct damping identification from the forced response measurements (Baruch, 1997, Chen et al., 1996, Mottershead, 1990).

3.2 Damping Identification Using Generalized Proportional Damping Model

- This method assumes that the system is effectively proportionally damped so that the complex modes can be neglected.
- The damping matrix will be identified using the expressions of the proportional damping matrix given in Theorem 1.2.

Considering expression (a) in Theorem 1.2 it can be shown that

$$\begin{aligned} \mathbf{\Phi}^T\mathbf{C}\mathbf{\Phi} &= \beta_1\left(\mathbf{\Omega}^2\right) + \mathbf{\Omega}^2\beta_2\left(\mathbf{\Omega}^{-2}\right) \\ \text{or} \quad 2\boldsymbol{\zeta}\,\mathbf{\Omega} &= \beta_1\left(\mathbf{\Omega}^2\right) + \mathbf{\Omega}^2\beta_2\left(\mathbf{\Omega}^{-2}\right). \end{aligned} \tag{3.1}$$

The modal damping factors can be expressed from equation (3.1) as

$$\zeta_j = \frac{1}{2}\frac{\beta_1(\omega_j^2)}{\omega_j} + \frac{1}{2}\omega_j\beta_2\left(1/\omega_j^2\right). \tag{3.2}$$

For the purpose of damping identification the function β_2 can be omitted without any loss of generality. To simplify the identification procedure, the damping matrix is expressed by

$$\mathbf{C} = \mathbf{M}f\left(\mathbf{M}^{-1}\mathbf{K}\right). \tag{3.3}$$

Using this simplified expression, the modal damping factors

$$2\zeta_j\omega_j = f\left(\omega_j^2\right) \tag{3.4}$$

$$\text{or} \quad \zeta_j = \frac{1}{2\omega_j}f\left(\omega_j^2\right) = \widehat{f}(\omega_j) \quad \text{(say)}. \tag{3.5}$$

The function $\widehat{f}(\bullet)$ can be obtained by fitting a continuous function representing the variation of the measured modal damping factors with respect to the

natural frequencies. From equations (3.3) and (3.4) note that in the argument of $f(\bullet)$, the term ω_j can be replaced by $\sqrt{\mathbf{M}^{-1}\mathbf{K}}$ while obtaining the damping matrix. With the fitted function $\widehat{f}(\bullet)$, the damping matrix can be identified using equation (3.5) as

$$2\zeta_j\omega_j = 2\omega_j\widehat{f}(\omega_j) \tag{3.6}$$

$$\text{or} \quad \widehat{\mathbf{C}} = 2\mathbf{M}\sqrt{\mathbf{M}^{-1}\mathbf{K}}\,\widehat{f}\left(\sqrt{\mathbf{M}^{-1}\mathbf{K}}\right). \tag{3.7}$$

Example 3.1.

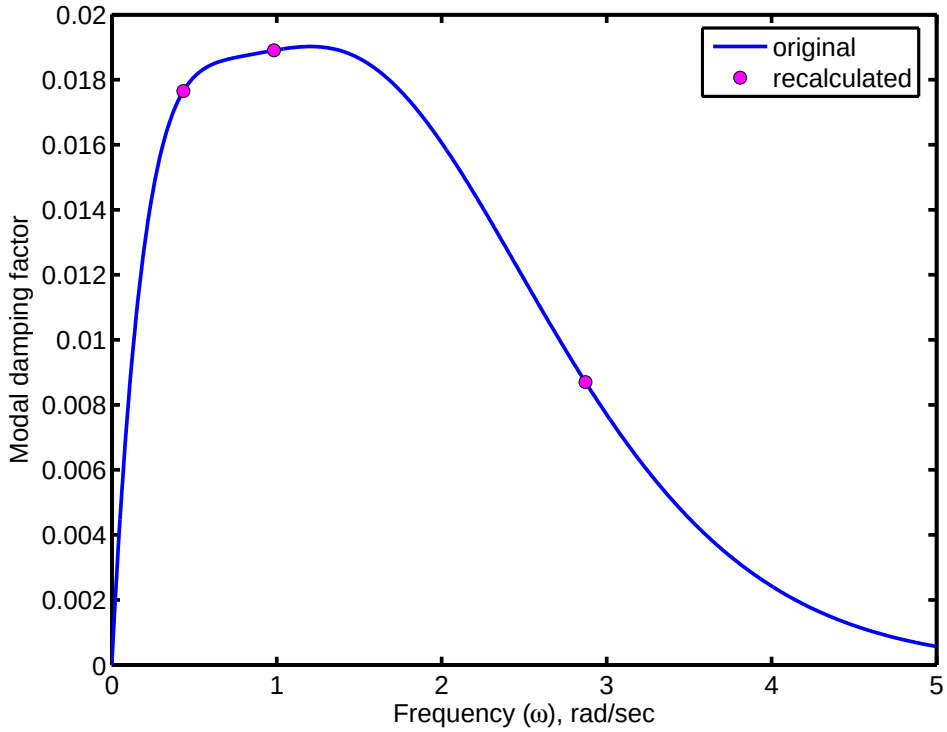

Figure 3.1: Variation of modal damping factors.

Suppose figure 3.1 shows modal damping factors as a function of frequency obtained by conducting simple vibration testing on a structure. We want to identify a damping matrix which shows this kind of behavior.

The first step is to fit a function which passes through these points:

$$\widehat{f}(\omega) = \frac{1}{15}\left(e^{-2.0\omega} - e^{-3.5\omega}\right)\left(1 + 1.25\sin\frac{\omega}{7\pi}\right)\left(1 + 0.75\omega^3\right). \tag{3.8}$$

From the above equation, the modal damping factors in terms of the discrete natural frequencies, can be obtained by

$$2\xi_j\omega_j = \frac{2\omega_j}{15}\left(e^{-2.0\omega_j} - e^{-3.5\omega_j}\right)\left(1 + 1.25\sin\frac{\omega_j}{7\pi}\right)\left(1 + 0.75\omega_j^3\right). \tag{3.9}$$

To obtain the damping matrix, consider equation (3.9) as a function of ω_j^2 and replace ω_j^2 by $\mathbf{M}^{-1}\mathbf{K}$ (that is ω_j by $\sqrt{\mathbf{M}^{-1}\mathbf{K}}$) and any constant terms by that constant times $\mathbf{I}$. Therefore, from equation (3.9) we have

$$\begin{aligned}\mathbf{C} =& \mathbf{M}\,\frac{2}{15}\sqrt{\mathbf{M}^{-1}\mathbf{K}}\left[e^{-2.0\sqrt{\mathbf{M}^{-1}\mathbf{K}}} - e^{-3.5\sqrt{\mathbf{M}^{-1}\mathbf{K}}}\right] \\ &\times \left[\mathbf{I} + 1.25\sin\left(\frac{1}{7\pi}\sqrt{\mathbf{M}^{-1}\mathbf{K}}\right)\right]\left[\mathbf{I} + 0.75(\mathbf{M}^{-1}\mathbf{K})^{3/2}\right]\end{aligned} \tag{3.10}$$

as the identified damping matrix. Using the numerical values of $\mathbf{M}$ and $\mathbf{K}$ from example 1.1 we obtain

$$\mathbf{C} = \begin{bmatrix} 2.3323 & 0.9597 & 1.4255 \\ 0.9597 & 3.5926 & 3.7624 \\ 1.4255 & 3.7624 & 7.8394 \end{bmatrix} \times 10^{-2}. \tag{3.11}$$

If we recalculate the damping factors from the above constructed damping matrix, it will produce three points corresponding to the three natural frequencies which will exactly match with our initial data.

The damping identification procedure itself does not introduce errors as long as the modes are not highly complex. From equation (3.7) it is obvious that the accuracy of the fitted damping matrix depends on the accuracy the mass and stiffness matrix models.

3.2.1 Comparison with the existing methods

Two existing methods are considered:

- Method 1: Caughey Series Method

  Géradin and Rixen (1997) have outlined a systematic method to obtain the damping matrix using Caughey series (1.29). The coefficients α_j in series (1.29) can be obtained by solving the linear system of equations

$$\mathbf{W}\boldsymbol{\alpha} = \boldsymbol{\zeta}_e \tag{3.12}$$

  where

$$\mathbf{W} = \frac{1}{2}\begin{bmatrix} \frac{1}{\omega_1} & \omega_1 & \omega_1^3 & \cdots \omega_1^{2N-3} \\ \frac{1}{\omega_2} & \omega_2 & \omega_2^3 & \cdots \omega_2^{2N-3} \\ \vdots & \vdots & \vdots & \vdots \\ \frac{1}{\omega_N} & \omega_N & \omega_N^3 & \cdots \omega_N^{2N-3} \end{bmatrix}, \quad \boldsymbol{\alpha} = \begin{Bmatrix} \alpha_1 \\ \alpha_2 \\ \vdots \\ \alpha_N \end{Bmatrix} \quad \text{and} \quad \boldsymbol{\zeta}_e = \begin{Bmatrix} \zeta_1 \\ \zeta_2 \\ \vdots \\ \zeta_N \end{Bmatrix}. \tag{3.13}$$

  The mass and stiffness matrices and the constants α_j calculated from the preceding equation can be substituted in equation (1.29) to obtain the damping matrix. Géradin and Rixen (1997) have mentioned that the coefficient matrix $\mathbf{W}$ in (3.13) becomes ill-conditioned for systems with well separated natural frequencies.

- Method 2: Inverse Modal Transformation Method

  Another simple, yet very general, method to obtain the proportional damping matrix is by using the inverse modal transformation method.

From experimentally obtained modal damping factors and natural frequencies one can construct the diagonal modal damping matrix $\mathbf{C}' = \mathbf{\Phi}^T \mathbf{C} \mathbf{\Phi}$ as

$$\mathbf{C}' = 2\boldsymbol{\zeta}_e \mathbf{\Omega}. \tag{3.14}$$

From this, the damping matrix in the original coordinate can be obtained using the inverse transformation as

$$\mathbf{C} = \mathbf{\Phi}^{-T} \mathbf{C}' \mathbf{\Phi}^{-1}. \tag{3.15}$$

Example 3.2.

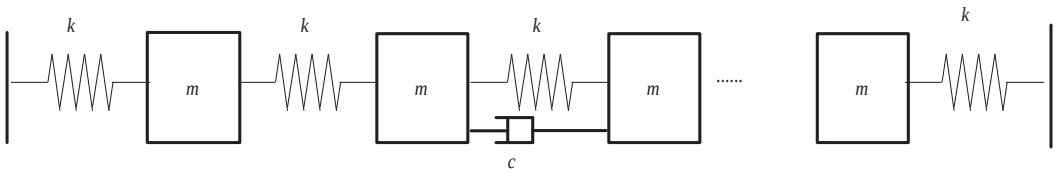

Figure 3.2: Linear array of N spring-mass oscillators, $N = 30$, $m = 1\,Kg$, $k = 3.95 \times 10^5 N/m$. Dampers are attached between 8th and 23rd masses with $c = 40$ Ns/m.

The mass matrix of the system has the form $\mathbf{M} = m\mathbf{I}$ where $\mathbf{I}$ is the $N \times N$ identity matrix. The stiffness matrix of the system is given by

$$\mathbf{K} = k \begin{bmatrix} 2 & -1 & & & & & \\ -1 & 2 & -1 & & & & \\ & \ddots & \ddots & \ddots & & & \\ & & -1 & 2 & -1 & & \\ & & & \ddots & \ddots & -1 & \\ & & & & -1 & 2 & \end{bmatrix}. \tag{3.16}$$

Some of the masses of the system shown in figure 3.2 have viscous dampers connecting them to each other. The damping matrix $\mathbf{C}$ has similar form to the stiffness matrix except that it has non-zero entries corresponding to the masses attached with the dampers only. With such a damping matrix it is easy to verify that the system is actually non-proportionally damped.

Consider a situation where the modal parameters of only first ten modes are known. Numerical values of ω_j and ζ_j for the first ten modes are shown in table 3.1.

Table 3.1: Natural frequencies (Hz) and modal damping factors for first ten modes

ω_j	ζ_j
10.1326	0.0005
20.2392	0.0032
30.2938	0.0057
40.2707	0.0060
50.1442	0.0067
59.8890	0.0095
69.4800	0.0117
78.8927	0.0117
88.1029	0.0125
97.0869	0.0155

Using this data, the following three methods are used to fit a proportional damping model:

(a) method using Caughey series

(b) inverse modal transformation method

(c) the method using generalized proportional damping

The modal damping factors corresponding to the higher modes, that is from mode number 11 to 30, are available from simulation results. The aim of this example is to see how the modal damping factors obtained using the identified damping matrices from the above three methods compare with the 'true' modal

damping factors corresponding to the higher modes.

- For the method using Caughey series, it has not been possible to obtain the constants α_j from equation (3.12) since the associated $\mathbf{W}$ matrix become highly ill-conditioned. Numerical calculation shows that the 10×10 matrix $\mathbf{W}$ has a condition number of 1.08×10^{51}.

- To apply the inverse modal transformation method, only the first ten columns of the analytical modal matrix $\mathbf{\Phi}$ are retained in the truncated modal matrix $\widehat{\mathbf{\Phi}} \in \mathbb{R}^{30\times 10}$. Using the pseudo inverse, the damping matrix in the original coordinate has been obtained from equation (3.15) as

$$\mathbf{C} = \left[\left(\widehat{\mathbf{\Phi}}^T\widehat{\mathbf{\Phi}}\right)^{-1}\widehat{\mathbf{\Phi}}^T\right]^T [2\boldsymbol{\zeta}_e\mathbf{\Omega}]\left[\left(\widehat{\mathbf{\Phi}}^T\widehat{\mathbf{\Phi}}\right)^{-1}\widehat{\mathbf{\Phi}}^T\right] \in \mathbb{R}^{30\times 30}. \tag{3.17}$$

From the identified $\mathbf{C}$ matrix, the modal damping factors are recalculated using

$$\boldsymbol{\zeta}_2 = \frac{1}{2}[\mathbf{\Phi}^T\mathbf{C}\mathbf{\Phi}]\mathbf{\Omega}^{-1} \in \mathbb{R}^{30\times 30} \tag{3.18}$$

where $\mathbf{\Phi}$ is the full 30×30 modal matrix.

Now consider the method using generalized proportional damping. Using the data in table 3.1, figure 3.3 shows the variation of modal damping factors for first the ten modes. Looking at the pattern of the curve in figure 3.3 we have

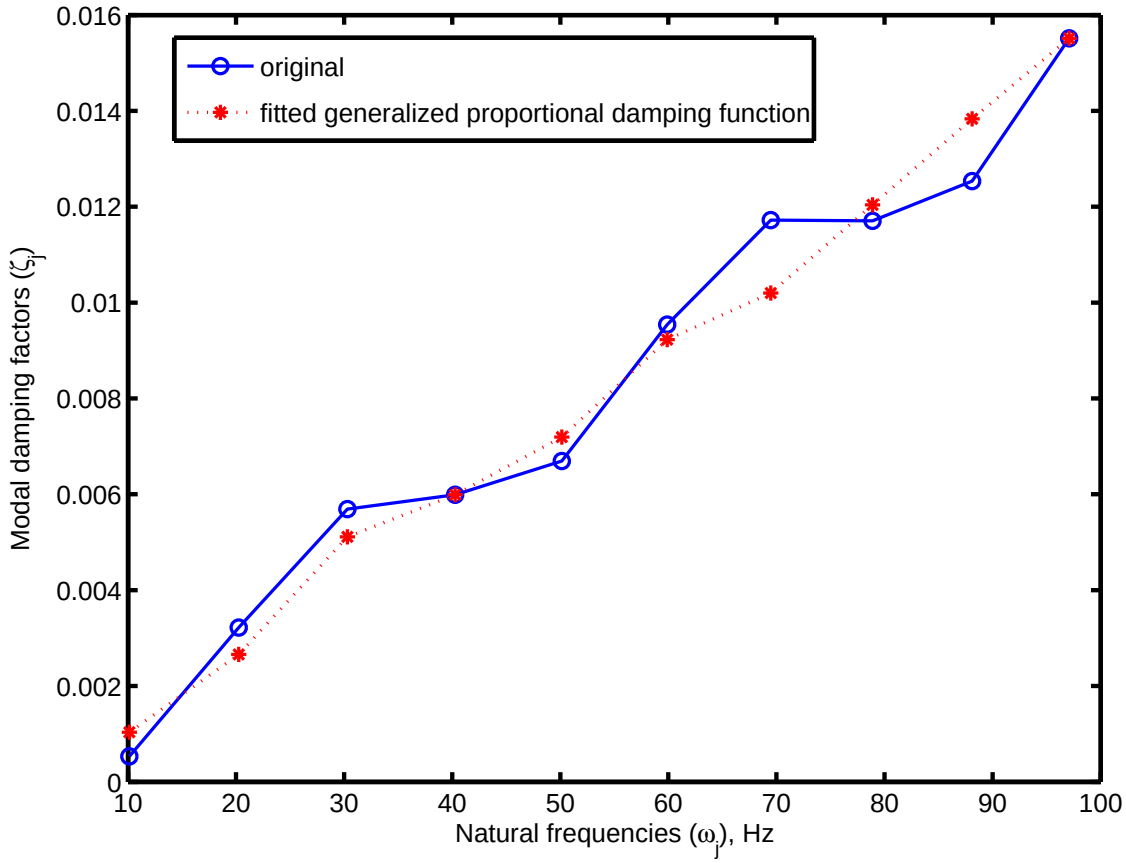

Figure 3.3: Variation of modal damping factors for first ten modes.

selected the function $\widehat{f}(\bullet)$ as

$$\zeta = \widehat{f}(\omega) = \theta_1 \omega + \theta_2 \sin(\theta_3 \omega) \tag{3.19}$$

where $\theta_i, i = 1, 2, 3$ are undetermined constants. Using the data in table 3.1, together with a least-square error minimization approach results

$$\theta_1 = 0.0245 \times 10^{-3} \quad \text{and} \quad \theta_2 = -0.5622 \times 10^{-3} \quad \text{and} \quad \theta_3 = 9.0. \tag{3.20}$$

- Recalculated values of ζ_j using this fitted function is compared with the original function in figure 3.3.
- This simple function matches well with the original modal data.
- Neither the function in equation (3.19), nor the parameter values in equation (3.20) are unique. One can use more complex functions and sophisticated parameter fitting procedures to obtain more accurate results.

The damping matrix corresponding to the fitted function in equation (3.19) can be obtained using equation (3.7) as

$$\begin{aligned}\mathbf{C} &= 2\mathbf{M}\sqrt{\mathbf{M}^{-1}\mathbf{K}}\,\widehat{f}\left(\sqrt{\mathbf{M}^{-1}\mathbf{K}}\right)\\ &= 2\mathbf{M}\sqrt{\mathbf{M}^{-1}\mathbf{K}}\left[\theta_1\sqrt{\mathbf{M}^{-1}\mathbf{K}}+\theta_2\sin\left(\theta_3\sqrt{\mathbf{M}^{-1}\mathbf{K}}\right)\right]\\ &= 2\theta_1\,\mathbf{K}+2\theta_2\,\mathbf{M}\sqrt{\mathbf{M}^{-1}\mathbf{K}}\,\sin\left(\theta_3\sqrt{\mathbf{M}^{-1}\mathbf{K}}\right)\end{aligned} \tag{3.21}$$

The first part of the $\mathbf{C}$ matrix in equation (3.21) is stiffness proportional and the second part is mass proportional in the sense of generalized proportional damping.

The aim of this study is to see how the different methods work when modal damping factors are compared against full set of 30 modes.

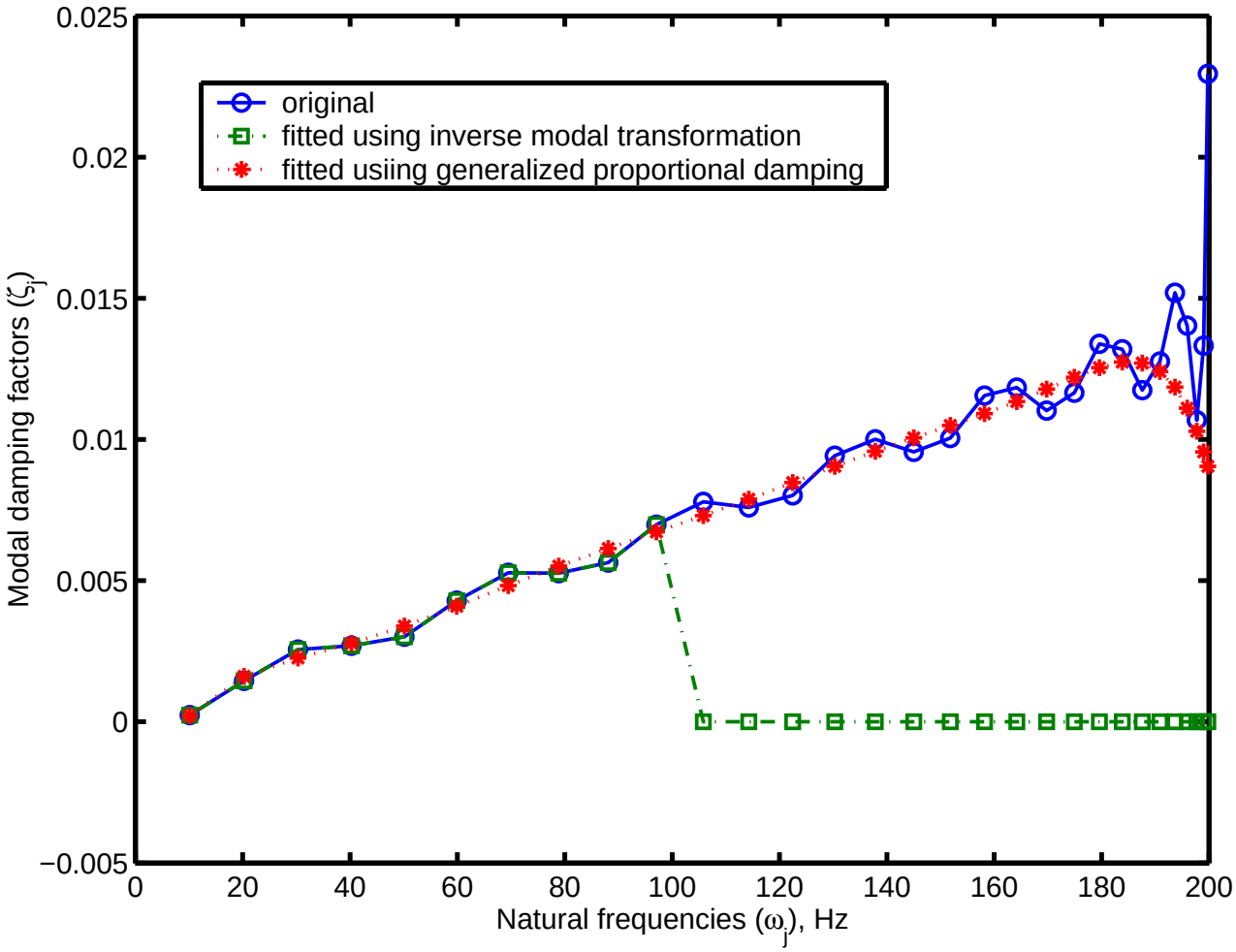

Figure 3.4: Variation of modal damping factors for all 30 modes.

In figure 3.4, the values of ζ_j obtained by the inverse modal transformation method in equation (3.18) is compared with the original damping factors for all the 30 modes calculated using complex modal analysis. As expected, there is a perfect match with the original damping factors for the first ten modes. However, beyond the first ten modes the damping factors obtained using the

inverse modal transformation method do not match with the true damping factors. This is also expected since this information has not been used in equations (3.17) and (3.18) and the method itself is not capable of extrapolating the available modal information. Modal damping factors using the fitted function in equation (3.19) are also shown in figure 3.4 for all 30 modes. The 'predicted' damping factors for modes 11 to 30 matched well with the original modal damping factors. This is due to the fact that the pattern of the variation of modal damping factors with natural frequencies does not change significantly beyond the first ten modes and hence the fitted function provides a good description of the variation. This study demonstrates the advantage of using generalized proportional damping over the conventional proportional damping models.

In summary, this identification procedure can be described by the following steps:

1. Measure a suitable transfer function $H_{ij}(\omega)$ by conducting vibration testing.
2. Obtain the undamped natural frequencies ω_j and modal damping factors ζ_j, for example, using the circle-fitting method.
3. Fit a function $\zeta = \widehat{f}(\omega)$ which represents the variation of ζ_j with respect to ω_j for the range of frequency considered in the study.
4. Calculate the matrix $\mathbf{T} = \sqrt{\mathbf{M}^{-1}\mathbf{K}}$
5. Obtain the damping matrix using $\widehat{\mathbf{C}} = 2\,\mathbf{M}\,\mathbf{T}\,\widehat{f}\,(\mathbf{T})$

Most of the currently available finite element based modal analysis packages usually offer Rayleigh's proportional damping model or a constant damping factor model. A generalized proportional damping model together with the proposed damping identification technique can be easily incorporated within the existing tools to enhance their damping modelling capabilities without using significant additional resources.

3.3 Conclusions

- The identification of the damping matrix from experimental measurements is a key component in model validation and verification.
- A damping identification method based on generalized proportional damping model has been described. The generalized proportional damping expresses the damping matrix in terms of smooth continuous functions involving specially arranged mass and stiffness matrices so that the system still posses classical normal modes.
- This enables one to model variations in the modal damping factors with respect to the frequency in a simplified manner.
- Once a scalar function is fitted to model such variations, the damping matrix can be identified very easily using the proposed method. This implies that the problem of damping identification is effectively reduced to the problem of a scalar function fitting.
- The method requires the measurement of damping factors and natural frequencies only and it is applicable to any linear structures provided accurate mass and stiffness matrices are available and the modes are not significantly complex.

4 Model Uncertainty: Quantification and Propagation

4.1 Why and How a Model Turns Uncertain?

The Classification of Uncertainty

Uncertainties can be broadly divided into following three categories.

- The first type of uncertainty is due to the inherent variability in the system parameters, for example, different cars manufactured from a single production line are not exactly the same. This type of uncertainty is often referred to as *aleatoric uncertainty*. If enough samples are present, it is possible to characterize the variability using well established statistical methods and the probably density functions of the parameters can be obtained.

- The second type is uncertainty due to lack of knowledge regarding a system. This type of uncertainty is often referred to as *epistemic uncertainty* and generally arise in the modelling of complex systems, for example the problem of predicting cabin noise in helicopters. Due its very nature, it is difficult to quantify or model this type uncertainties. Unlike aleatoric uncertainties, it is recognized that probabilistic models are not quite suitable for epistemic uncertainties. Several possibilistic approaches based on interval algebra, convex sets, Fuzzy sets and generalized Dempster-Schafer theory have been proposed to characterize this type of uncertainties.

- The third type of uncertainty is similar to the first type except that the corresponding variability characterization is not available, in which case work can be directed to gain better knowledge. This type uncertainty often termed as *prejudicial uncertainty*, may consist of systematic and/or random errors, bias or other prejudices. An example of this type of uncertainty is the use of viscous damping model in spite of knowing that the true damping model is not viscous.

The total uncertainty of a system is the combination of these three types of uncertainties.

Anatomy of Uncertainty in Structural Dynamics

Different sources of uncertainties in the modeling and simulation of dynamic systems may be attributed, but not limited, to the following factors:

- Mathematical models
  - Equations (linear, non-linear)
  - Geometry
  - Damping model (viscous, non-viscous, fractional derivative, $\cdots$)
  - Boundary conditions (fixed, free, clamped, $\cdots$)
  - Joints
  - Initial conditions
  - Input forces
  - Unmodeled dynamics
- Model parameters
  - Young's modulus
  - Mass density
  - Poisson's ratio
  - Damping model parameters (damping coefficient, relaxation modulus, fractional derivative order)
  - Initial stresses
  - Temperature

- Numerical algorithms
  - Weak formulations
  - Discretisation of displacement fields (in finite element method)
  - Choice of elements (beam, shell, 3D brick element, $\cdots$)
  - Discretisation of stochastic fields (in stochastic finite element method)
  - Approximate solution algorithms
  - Truncation and roundoff errors
  - Tolerances in the optimization and iterative methods
  - Artificial intelligent (AI) method (choice of neural network types)
- Surrogate models
  - Choice of model
  - Approximation error
  - Interpolation error
  - Extrapolation error

- Measurements
  - Noise
  - Resolution (number of sensors and actuators)
  - Experimental hardware
  - Excitation method (nature of shakers and hammers)
  - Excitation and measurement point
  - Data processing (amplification, number of data points, FFT, filtering)
  - Calibration

We will focus our attention to the modeling and propagation of parametric uncertainties using probabilistic models.

4.2 Parametric Uncertainty in Structural Dynamics

The governing equation of motion of a linear structural system with stochastic parameter uncertainties, subjected to external excitations is most often a set of linear differential equation with random coefficients. The problem can be stated as finding the solution of the equation

$$\mathbf{L}(\Omega, \mathbf{r}, t)\mathbf{u}(\Omega, \mathbf{r}, t) = \mathbf{f}(\Omega, \mathbf{r}, t) \tag{4.1}$$

with prescribed boundary conditions and initial conditions. In the above equation $\mathbf{L}$ is a linear stochastic differential operator, $\mathbf{u}$ is the random system response to be determined, $\mathbf{f}$ is the dynamic excitation which can be random, $\mathbf{r}$ is the special coordinate vector, t is the time and Ω is the sample space denoting the stochastic nature of the problem.

- Equation (4.1) with $\mathbf{L}$ as a deterministic operator and $\mathbf{f}$ as a random forcing function, has been studied extensively within the scope of random vibration theory.
- Our interest is when the operator $\mathbf{L}$ itself is random.
- There are mainly two methods to model parametric uncertainty using the probabilistic approach: (a) uncertainty modeling using random variables, and (b) uncertainty modeling using random processes.

The methods for solving structural dynamic problems with statistical uncertainties can be broadly grouped under Stochastic Finite Element Method (SFEM) and Statistical Energy Analysis (SEA). SEA was developed during

1960s (Lyon and Dejong, 1995) to analyze high frequency vibration problems where non-parametric uncertainties plays a key role. The stochastic finite element method is ideally suitable for low-frequency vibration problems where parametric uncertainties plays a key role.

4.3 Uncertainty Propagation Using Stochastic Finite Element Method

Stochastic finite element method (SFEM) is a generalization of the deterministic finite element method (FEM) to incorporate the random field models for the elastic, mass and damping properties (see the monographs by Ghanem and Spanos, 1991, Kleiber and Hien, 1992). Application of the stochastic finite element method to linear structural dynamics problems typically consists of the following steps:

1. Selection of appropriate probabilistic models for parameter uncertainties and boundary conditions (such as Gaussian/non-Gaussian models).

2. Discretization of random fields, i. e., replacement of the element property random fields by an equivalent finite set of random variables.

3. Formulation of the system equations of motion of the form (1.20), using stochastic generalization of standard methods such as variational method, energy method, virtual work method or weighted residual method. As a result of this process, the elements of $\mathbf{M}, \mathbf{C}$ and $\mathbf{K}$ will be random variables.

4. At this point one can take two routes. The first, and the most common approach, is to solve the free vibration problem, which in this case turns

out to be a random matrix eigenvalue problem. The aim is to obtain the joint statistics of the mode shapes and natural frequencies. Once they are obtained, the next step is the characterization of response variability for the forced vibration problem.

5. The second route to solve the problem is using the dynamic stiffness method. The main challenge here is to invert the global dynamic stiffness matrix, which in general is a random complex symmetric matrix.

Extensive research works have been done in all of the above mentioned areas during the last few decades. In this course we will discuss the random eigenvalue problems.

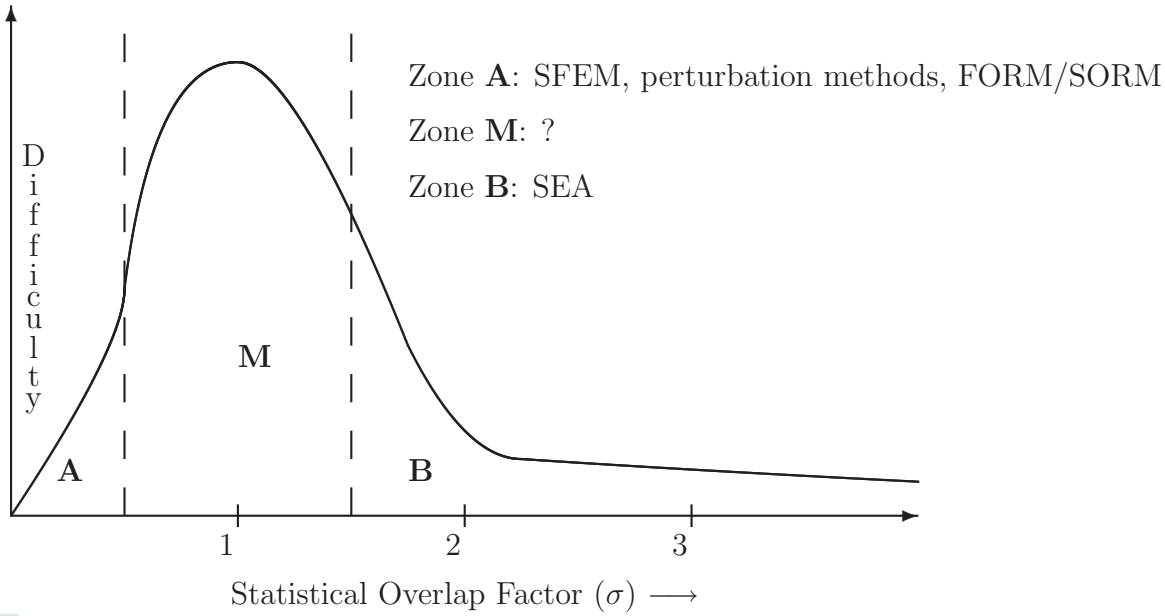

Figure 4.1: 'Difficulty' in structural analysis as an approximate function of the 'amount of uncertainty' (statistical overlap factor)

The *statistical overlap factor* (σ), as defined by Manohar and Keane (1994), is the ratio of standard deviation of the natural frequencies to the average spacing of the natural frequencies.

5 Random Eigenvalue Problems in Structural Dynamics

5.1 Introduction

- Random eigenvalue problem is a fundamental problem in the dynamics of linear stochastic systems.

- This problem could either be a differential eigenvalue problem or a matrix eigenvalue problem, depending on whether a continuous model or a discrete model is used to describe the given vibrating system. We will discuss stochastic matrix eigenvalue problems.

- Several studies have been conducted on this topic since the mid-sixties. The paper by Boyce (1968) and the book by Scheidt and Purkert (1983) are useful sources of information on early work in this area of research and also provide a systematic account of different approaches to random eigenvalue problems. Several review papers, for example, by Benaroya (1992), Benaroya and Rehak (1988), Ibrahim (1987), Manohar and Ibrahim (1999) and Manohar and Gupta (2003) have appeared in this field which summarize the current as well as the earlier works.

In this note discrete linear systems or discretized continuous systems are considered. The random eigenvalue problem of undamped or proportionally damped systems can be expressed by

$$\mathbf{K}(\mathbf{x})\boldsymbol{\phi}_j = \lambda_j \mathbf{M}(\mathbf{x})\boldsymbol{\phi}_j \tag{5.1}$$

Here λ_j and $\boldsymbol{\phi}_j$ are the eigenvalues and the eigenvectors of the dynamic system. $\mathbf{M}(\mathbf{x}) : \mathbb{R}^m \mapsto \mathbb{R}^{N\times N}$ and $\mathbf{K}(\mathbf{x}) : \mathbb{R}^m \mapsto \mathbb{R}^{N\times N}$, the mass and stiffness matrices, are assumed to be smooth, continuous and at least twice differentiable functions of a random parameter vector $\mathbf{x} \in \mathbb{R}^m$. The vector $\mathbf{x}$ may consist of material properties, *eg.*, mass density, Poisson's ratio, Young's modulus; geometric properties, *eg.*, length, thickness, and boundary conditions. The matrices $\mathbf{K}(\mathbf{x})$ and $\mathbf{M}(\mathbf{x})$ can be obtained using the stochastic finite element method (Kleiber and Hien, 1992). The statistical properties of the system are completely described by the joint probability density function $p_{\mathbf{X}}(\mathbf{x}) : \mathbb{R}^m \mapsto \mathbb{R}$. For mathematical convenience we express

$$p_{\mathbf{X}}(\mathbf{x}) = \exp\{-L(\mathbf{x})\} \tag{5.2}$$

where $-L(\mathbf{x})$ is often known as the log-likelihood function. For example, if $\mathbf{x}$ is a m-dimensional multivariate Gaussian random vector with mean $\boldsymbol{\mu} \in \mathbb{R}^m$ and covariance matrix $\boldsymbol{\Sigma} \in \mathbb{R}^{m\times m}$ then

$$L(\mathbf{x}) = \frac{m}{2}\ln(2\pi) + \frac{1}{2}\ln\|\boldsymbol{\Sigma}\| + \frac{1}{2}(\mathbf{x}-\boldsymbol{\mu})^T\boldsymbol{\Sigma}^{-1}(\mathbf{x}-\boldsymbol{\mu}) \tag{5.3}$$

It is assumed that in general the random parameters are non-Gaussian and correlated, *i.e.*, $L(\mathbf{x})$ can have any general form provided it is a smooth, continuous and at least twice differentiable function. It is further assumed that $\mathbf{M}$ and $\mathbf{K}$ are symmetric and positive definite random matrices so that all the eigenvalues are real and positive.

The central aim of studying random eigenvalue problems is to obtain the joint probability density function of the eigenvalues and the eigenvectors. The cur-

rent literature on random eigenvalue problems arising in engineering systems is dominated by the perturbation methods.

5.2 Classical Perturbation Methods

5.2.1 Perturbation Expansion

The mass and the stiffness matrices are in general non-linear functions of the random vector $\mathbf{x}$. Denote the mean of $\mathbf{x}$ as $\boldsymbol{\mu} \in \mathbb{R}$, and consider that

$$\mathbf{M}(\boldsymbol{\mu}) = \overline{\mathbf{M}}, \quad \text{and} \quad \mathbf{K}(\boldsymbol{\mu}) = \overline{\mathbf{K}} \tag{5.4}$$

are the 'deterministic parts' of the mass and stiffness matrices respectively. In general $\overline{\mathbf{M}}$ and $\overline{\mathbf{K}}$ are different from the mean matrices. The deterministic part of the eigenvalues:

$$\overline{\lambda}_j = \lambda_j(\boldsymbol{\mu}) \tag{5.5}$$

is obtained from the deterministic eigenvalue problem:

$$\overline{\mathbf{K}}\,\overline{\boldsymbol{\phi}}_j = \overline{\lambda}_j\,\overline{\mathbf{M}}\,\overline{\boldsymbol{\phi}}_j \tag{5.6}$$

The eigenvalues, $\lambda_j(\mathbf{x}) : \mathbb{R}^m \mapsto \mathbb{R}$ are non-linear functions of the parameter vector $\mathbf{x}$. If the eigenvalues are not repeated, then each $\lambda_j(\mathbf{x})$ is expected to be a smooth and twice differentiable function since the mass and stiffness matrices are smooth and twice differentiable functions of the random parameter vector. In the mean-centered perturbation approach the function $\lambda_j(\mathbf{x})$ is expanded by its Taylor series about the point $\mathbf{x} = \boldsymbol{\mu}$ as

$$\lambda_j(\mathbf{x}) \approx \lambda_j(\boldsymbol{\mu}) + \mathbf{d}_{\lambda_j}^T(\boldsymbol{\mu})\,(\mathbf{x} - \boldsymbol{\mu}) + \frac{1}{2}\,(\mathbf{x} - \boldsymbol{\mu})^T\,\mathbf{D}_{\lambda_j}(\boldsymbol{\mu})\,(\mathbf{x} - \boldsymbol{\mu}) \tag{5.7}$$

Here $\mathbf{d}_{\lambda_j}(\boldsymbol{\mu}) \in \mathbb{R}^m$ and $\mathbf{D}_{\lambda_j}(\boldsymbol{\mu}) \in \mathbb{R}^{m \times m}$ are respectively the gradient vector and the Hessian matrix of $\lambda_j(\mathbf{x})$ evaluated at $\mathbf{x} = \boldsymbol{\mu}$, that is

$$\left\{\mathbf{d}_{\lambda_j}(\boldsymbol{\mu})\right\}_k = \frac{\partial \lambda_j(\mathbf{x})}{\partial x_k}|_{\mathbf{x}=\boldsymbol{\mu}} \tag{5.8}$$

$$\text{and} \quad \left\{\mathbf{D}_{\lambda_j}(\boldsymbol{\mu})\right\}_{kl} = \frac{\partial^2 \lambda_j(\mathbf{x})}{\partial x_k \, \partial x_l}|_{\mathbf{x}=\boldsymbol{\mu}} \tag{5.9}$$

Expressions of the elements of the gradient vector and the Hessian matrix are given in Section B. Due to equation (5.5), equation (5.7) implies that the eigenvalues are effectively expanded about their corresponding deterministic value $\overline{\lambda}_j$.

Equation (5.7) represents a quadratic form in the basic non-Gaussian random variables. The first-order perturbation, which is often used in practice, is obtained from equation (5.7) by neglecting the Hessian matrix. In this case the eigenvalues are simple linear functions of the basic random variables. This formulation is expected to produce acceptable results when the random variation in $\mathbf{x}$ is small. If the basic random variables are Gaussian then first-order perturbation results in a Gaussian distribution of the eigenvalues. In this case a closed-form expression for their joint probability density function can be obtained easily, see for example, Collins and Thomson (1969), Hart (1973), Hasselman and Hart (1972), Ramu and Ganesan (1993) and Sankar et al. (1993). However, if the elements of $\mathbf{x}$ are non-Gaussian then even the first-order perturbation method is not helpful because there is no general method to obtain the resulting pdf in a simple manner.

5.2.2 Eigenvalue Statistics Using the Theory of Quadratic Forms

Considering $\mathbf{x}$ as a multivariate Gaussian random vector, the moment generating function of $\lambda_j(\mathbf{x})$, for any $s \in \mathbb{C}$, can be obtained from (5.7) as

$$\begin{aligned} M_{\lambda_j}(s) &= \mathrm{E}\left[\exp\left\{s\lambda_j(\mathbf{x})\right\}\right] \\ &= \int_{\mathbb{R}^m} \exp\left\{s\lambda_j(\boldsymbol{\mu}) + s\mathbf{d}_{\lambda_j}^T(\boldsymbol{\mu})\left(\mathbf{x}-\boldsymbol{\mu}\right) + \frac{s}{2}\left(\mathbf{x}-\boldsymbol{\mu}\right)^T \mathbf{D}_{\lambda_j}(\boldsymbol{\mu})\left(\mathbf{x}-\boldsymbol{\mu}\right) - L(\mathbf{x})\right\} d\mathbf{x} \end{aligned} \tag{5.10}$$

where $L(\mathbf{x})$ is given by equation (5.3). Using the transformation

$$\mathbf{y} = (\mathbf{x} - \boldsymbol{\mu}) \tag{5.11}$$

the integral in (5.10) can be evaluated exactly as

$$\text{or} \quad M_{\lambda_j}(s) = \frac{\exp\left\{s\overline{\lambda}_j + \frac{s^2}{2}\mathbf{d}_{\lambda_j}^T(\boldsymbol{\mu})\boldsymbol{\Sigma}\left[\mathbf{I} - s\boldsymbol{\Sigma}\,\mathbf{D}_{\lambda_j}(\boldsymbol{\mu})\right]^{-1}\mathbf{d}_{\lambda_j}(\boldsymbol{\mu})\right\}}{\sqrt{\left\|\mathbf{I} - s\boldsymbol{\Sigma}\,\mathbf{D}_{\lambda_j}(\boldsymbol{\mu})\right\|}} \tag{5.12}$$

To obtain the pdf of $\lambda_j(\mathbf{x})$, the inverse Laplace transform of (5.12) is required. Exact closed-form expression of the pdf can be obtained for few special cases only. Some approximate methods to obtain the pdf of $\lambda_j(\mathbf{x})$ will be discussed in Section 5.5.

If mean-centered first-order perturbation is used then $\mathbf{D}_{\lambda_j}(\boldsymbol{\mu}) = \mathbf{O}$ and from equation (5.12) we obtain

$$M_{\lambda_j}(s) \approx \exp\left\{s\overline{\lambda}_j + \frac{s^2}{2}\mathbf{d}_{\lambda_j}^T(\boldsymbol{\mu})\boldsymbol{\Sigma}\,\mathbf{d}_{\lambda_j}(\boldsymbol{\mu})\right\} \tag{5.13}$$

This implies that $\lambda_j(\mathbf{x})$ is a Gaussian random variable with mean $\overline{\lambda}_j$ and variance $\mathbf{d}_{\lambda_j}^T(\boldsymbol{\mu})\boldsymbol{\Sigma}\,\mathbf{d}_{\lambda_j}(\boldsymbol{\mu})$. However, for second-order perturbation in general the mean of the eigenvalues is not the deterministic value. The cumulants of

$\lambda_j(\mathbf{x})$ can be obtained from

$$\kappa_j^{(r)} = \frac{d^r}{ds^r} \ln M_{\lambda_j}(s)|_{s=0} \tag{5.14}$$

Here $\kappa_j^{(r)}$ is the rth order cumulant of jth eigenvalue and from equation (5.12) we have

$$\ln M_{\lambda_j}(s) = s\overline{\lambda}_j + \frac{s^2}{2}\mathbf{d}_{\lambda_j}^T(\boldsymbol{\mu})\boldsymbol{\Sigma}\left[\mathbf{I} - s\boldsymbol{\Sigma}\,\mathbf{D}_{\lambda_j}(\boldsymbol{\mu})\right]^{-1}\mathbf{d}_{\lambda_j}(\boldsymbol{\mu}) - \frac{1}{2}\ln\left\|\mathbf{I} - s\boldsymbol{\Sigma}\,\mathbf{D}_{\lambda_j}(\boldsymbol{\mu})\right\| \tag{5.15}$$

Using this expression and after some simplifications it can be shown that

$$\kappa_j^{(r)} = \overline{\lambda}_j + \frac{1}{2}\text{Trace}\left(\mathbf{D}_{\lambda_j}(\boldsymbol{\mu})\boldsymbol{\Sigma}\right) \quad \text{if} \quad r = 1, \tag{5.16}$$

$$\kappa_j^{(r)} = \frac{r!}{2}\mathbf{d}_{\lambda_j}^T(\boldsymbol{\mu})\left[\boldsymbol{\Sigma}\,\mathbf{D}_{\lambda_j}(\boldsymbol{\mu})\right]^{r-2}\boldsymbol{\Sigma}\,\mathbf{d}_{\lambda_j}(\boldsymbol{\mu}) + \frac{(r-1)!}{2}\text{Trace}\left(\left[\mathbf{D}_{\lambda_j}(\boldsymbol{\mu})\boldsymbol{\Sigma}\right]^r\right) \quad \text{if} \quad r \geq 2 \tag{5.17}$$

The mean and first few cumulants of the eigenvalues can be explicitly obtained

$$\widehat{\lambda}_j = \kappa_j^{(1)} = \overline{\lambda}_j + \frac{1}{2}\text{Trace}\left(\mathbf{D}_{\lambda_j}(\boldsymbol{\mu})\boldsymbol{\Sigma}\right) \tag{5.18}$$

$$\text{Var}\left[\lambda_j\right] = \kappa_j^{(2)} = \mathbf{d}_{\lambda_j}^T(\boldsymbol{\mu})\boldsymbol{\Sigma}\,\mathbf{d}_{\lambda_j}(\boldsymbol{\mu}) + \frac{1}{2}\text{Trace}\left(\left[\mathbf{D}_{\lambda_j}(\boldsymbol{\mu})\boldsymbol{\Sigma}\right]^2\right), \tag{5.19}$$

$$\kappa_j^{(3)} = 3\mathbf{d}_{\lambda_j}^T(\boldsymbol{\mu})\left[\boldsymbol{\Sigma}\,\mathbf{D}_{\lambda_j}(\boldsymbol{\mu})\right]\boldsymbol{\Sigma}\,\mathbf{d}_{\lambda_j}(\boldsymbol{\mu}) + \text{Trace}\left(\left[\mathbf{D}_{\lambda_j}(\boldsymbol{\mu})\boldsymbol{\Sigma}\right]^3\right), \tag{5.20}$$

$$\text{and } \kappa_j^{(4)} = 12\mathbf{d}_{\lambda_j}^T(\boldsymbol{\mu})\left[\boldsymbol{\Sigma}\,\mathbf{D}_{\lambda_j}(\boldsymbol{\mu})\right]^2\boldsymbol{\Sigma}\,\mathbf{d}_{\lambda_j}(\boldsymbol{\mu}) + 3\text{Trace}\left(\left[\mathbf{D}_{\lambda_j}(\boldsymbol{\mu})\boldsymbol{\Sigma}\right]^4\right) \tag{5.21}$$

From the cumulants, the raw moments $\mu_j^{(r)} = \text{E}\left[\lambda_j^r\right]$ and the central moments $\mu_j^{\prime(r)} = \text{E}\left[(\lambda_j - \bar{\lambda}_j)^r\right]$ can be obtained easily.

5.3 Perturbation Method Based on an Optimal Point

5.3.1 Perturbation Expansion

In the mean-centered perturbation method, $\lambda_j(\mathbf{x})$ is expanded in a Taylor series about $\mathbf{x} = \boldsymbol{\mu}$. This approach may not be suitable for all problems, especially if $\mathbf{x}$ is non-Gaussian then $p_{\mathbf{X}}(\mathbf{x})$ may not be centered around the mean. Here we are looking for a point $\mathbf{x} = \boldsymbol{\alpha}$ in the $\mathbf{x}$-space such that the Taylor series expansion of $\lambda_j(\mathbf{x})$ about this point

$$\lambda_j(\mathbf{x}) \approx \lambda_j(\boldsymbol{\alpha}) + \mathbf{d}_{\lambda_j}^T(\boldsymbol{\alpha})\,(\mathbf{x}-\boldsymbol{\alpha}) + \frac{1}{2}\,(\mathbf{x}-\boldsymbol{\alpha})^T\,\mathbf{D}_{\lambda_j}(\boldsymbol{\alpha})\,(\mathbf{x}-\boldsymbol{\alpha}) \tag{5.22}$$

is optimal in 'some sense'. The optimal point $\boldsymbol{\alpha}$ can be selected in various ways. For practical applications the mean of the eigenvalues is often the most important. For this reason, the optimal point $\boldsymbol{\alpha}$ is selected such that the mean or the first moment of each eigenvalue is calculated most accurately. The mathematical formalism presented here is not restricted to this specific criteria and can be easily modified if any moment other than the first moment is required to be obtained more accurately. Using equation (5.2) the mean of $\lambda_j(\mathbf{x})$ can be obtained as

$$\widehat{\lambda}_j = \mathrm{E}\left[\lambda_j(\mathbf{x})\right] = \int_{\mathbb{R}^m} \lambda_j(\mathbf{x}) p_{\mathbf{X}}(\mathbf{x})\,d\mathbf{x} = \int_{\mathbb{R}^m} \lambda_j(\mathbf{x}) e^{-L(\mathbf{x})}\,d\mathbf{x} \tag{5.23}$$

$$\text{or} \quad \widehat{\lambda}_j = \int_{\mathbb{R}^m} e^{-h_j(\mathbf{x})}\,d\mathbf{x} \tag{5.24}$$

$$\text{where} \quad h_j(\mathbf{x}) = L(\mathbf{x}) - \ln \lambda_j(\mathbf{x}) \tag{5.25}$$

Evaluation of the integral (5.24), either analytically or numerically, is in general difficult because (a) $\lambda_j(\mathbf{x})$ and $L(\mathbf{x})$ are complicated nonlinear functions of $\mathbf{x}$, (b) an explicit functional form $\lambda_j(\mathbf{x})$ is not easy to obtain except for

very simple problems (usually an FE run is required to obtain λ_j for every $\mathbf{x}$), and (c) the dimension of the integral m is large. For these reasons some kind of approximation is required. From equation (5.24) note that the maximum contribution to the integral comes from the neighborhood where $h_j(\mathbf{x})$ is minimum. Therefore, expand the function $h_j(\mathbf{x})$ in a Taylor series about a point where $h_j(\mathbf{x})$ has its global minimum. By doing so the error in evaluating the integral (5.24) would be minimized. Thus, the optimal point can be obtained from

$$\frac{\partial h_j(\mathbf{x})}{\partial x_k} = 0 \quad \text{or} \quad \frac{\partial L(\mathbf{x})}{\partial x_k} = \frac{1}{\lambda_j(\mathbf{x})}\frac{\partial \lambda_j(\mathbf{x})}{\partial x_k}, \quad \forall k \tag{5.26}$$

Combining the above equations for all k, at $\mathbf{x} = \boldsymbol{\alpha}$ we have

$$\mathbf{d}_{\lambda_j}(\boldsymbol{\alpha}) = \lambda_j(\boldsymbol{\alpha})\mathbf{d}_L(\boldsymbol{\alpha}) \tag{5.27}$$

Equation (5.27) implies that at the optimal point the gradient vectors of the eigenvalues and log-likelihood function are parallel. The non-linear set of equations (5.27) have to be solved numerically. Due to the explicit analytical expression of $\mathbf{d}_{\lambda_j}$ in terms of the derivative of the mass and stiffness matrices, expensive numerical differentiation of $\lambda_j(\mathbf{x})$ at each step is not needed. Moreover, for most $p_{\mathbf{X}}(\mathbf{x})$, a closed-form expression of $\mathbf{d}_L(\mathbf{x})$ is available. For example, when $\mathbf{x}$ has multivariate Gaussian distribution, $L(\mathbf{x})$ is given by equation (5.3). By differentiating this we obtain

$$\mathbf{d}_L(\mathbf{x}) = \boldsymbol{\Sigma}^{-1}(\mathbf{x} - \boldsymbol{\mu}) \tag{5.28}$$

Substituting this in equation (5.27), the optimal point $\boldsymbol{\alpha}$ can be obtained as

$$\boldsymbol{\alpha} = \boldsymbol{\mu} + \frac{1}{\lambda_j(\boldsymbol{\alpha})}\boldsymbol{\Sigma}\,\mathbf{d}_{\lambda_j}(\boldsymbol{\alpha}) \tag{5.29}$$

This equation also gives a recipe for an iterative algorithm to obtain $\boldsymbol{\alpha}$. One starts with an initial $\boldsymbol{\alpha}$ in the right-hand side and obtains an updated $\boldsymbol{\alpha}$ in the left-hand side. This procedure can be continued till the difference between the values of $\boldsymbol{\alpha}$ obtained from both sides of (5.29) is less than (l_2 vector norm can be used to measure the difference) a predefined small value. A good value to start the iteration process is $\boldsymbol{\alpha} = \boldsymbol{\mu}$, as in the case of mean-centered approach. The form of equation (5.22) is similar to that of equation (5.7). As mentioned before, when the basic random variables are non-Gaussian, determination of moments and the pdf is not straightforward. However, when $\mathbf{x}$ is Gaussian, some useful statistics of the eigenvalues can be obtained in closed-form.

5.3.2 Eigenvalue Statistics Using the Theory of Quadratic Forms

For notational convenience we rewrite the optimal perturbation expansion (5.22) as

$$\lambda_j(\mathbf{x}) \approx c_j + \mathbf{a}_j^T \mathbf{x} + \frac{1}{2}\mathbf{x}^T \mathbf{A}_j \mathbf{x} \tag{5.30}$$

where the constants $c_j \in \mathbb{R}$, $\mathbf{a}_j \in \mathbb{R}^m$ and $\mathbf{A}_j \in \mathbb{R}^{m\times m}$ are given by

$$c_j = \lambda_j(\boldsymbol{\alpha}) - \mathbf{d}_{\lambda_j}^T(\boldsymbol{\alpha})\boldsymbol{\alpha} + \frac{1}{2}\boldsymbol{\alpha}^T \mathbf{D}_{\lambda_j}(\boldsymbol{\alpha})\boldsymbol{\alpha} \tag{5.31}$$

$$\mathbf{a}_j = \mathbf{d}_{\lambda_j}(\boldsymbol{\alpha}) - \mathbf{D}_{\lambda_j}(\boldsymbol{\alpha})\boldsymbol{\alpha} \tag{5.32}$$

$$\mathbf{A}_j = \mathbf{D}_{\lambda_j}(\boldsymbol{\alpha}) \tag{5.33}$$

From equation (5.30), the closed-form expression of the moment generating function of $\lambda_j(\mathbf{x})$ can be obtained exactly in a way similar to what discussed for the case of mean-centered perturbation method. Using equation (5.3) it

can be shown that

$$M_{\lambda_j}(s) = \mathrm{E}\left[\exp\left\{s\lambda_j(\mathbf{x})\right\}\right]$$
$$= (2\pi)^{-m/2}\|\boldsymbol{\Sigma}\|^{-1/2}\int_{\mathbb{R}^m}\exp\left\{s\left(c_j + \mathbf{a}_j^T\mathbf{x} + \frac{1}{2}\mathbf{x}^T\mathbf{A}_j\mathbf{x}\right) - \frac{1}{2}\left(\mathbf{x}-\boldsymbol{\mu}\right)^T\boldsymbol{\Sigma}^{-1}\left(\mathbf{x}-\boldsymbol{\mu}\right)\right\}d\mathbf{x} \tag{5.34}$$

This m-dimensional integral can be evaluated exactly to obtain

$$M_{\lambda_j}(s) = \frac{\exp\left\{sc_j - \frac{1}{2}\boldsymbol{\mu}^T\boldsymbol{\Sigma}^{-1}\boldsymbol{\mu} + \frac{1}{2}\left(\boldsymbol{\mu}+s\boldsymbol{\Sigma}\,\mathbf{a}_j\right)^T\left[\mathbf{I}-s\boldsymbol{\Sigma}\,\mathbf{A}_j\right]^{-1}\left(\boldsymbol{\mu}+s\boldsymbol{\Sigma}\,\mathbf{a}_j\right)\right\}}{\sqrt{\|\mathbf{I}-s\boldsymbol{\Sigma}\,\mathbf{A}_j\|}} \tag{5.35}$$

From the prceeding expression, the cumulants of the eigenvalues can be evaluated using equation (5.14) as

$$\kappa_j^{(r)} = c_j + \frac{1}{2}\mathrm{Trace}\left(\mathbf{A}_j\boldsymbol{\Sigma}\right) + \frac{1}{2}\boldsymbol{\mu}^T\mathbf{A}_j\,\boldsymbol{\mu} + \mathbf{a}_j^T\boldsymbol{\mu} \quad \text{if} \quad r = 1, \tag{5.36}$$

$$\text{and} \quad \kappa_j^{(r)} = \frac{(r-1)!}{2}\mathrm{Trace}\left(\left[\mathbf{A}_j\boldsymbol{\Sigma}\right]^r\right) + \frac{r!}{2}\mathbf{a}_j^T\left[\boldsymbol{\Sigma}\,\mathbf{A}_j\right]^{r-2}\boldsymbol{\Sigma}\,\mathbf{a}_j$$
$$+ r!\,\boldsymbol{\mu}^T\left[\mathbf{A}_j\boldsymbol{\Sigma}\right]^{r-1}\mathbf{A}_j\,\boldsymbol{\mu} + r!\,\mathbf{a}_j^T\left[\boldsymbol{\Sigma}\,\mathbf{A}_j\right]^{r-1}\mathbf{A}_j\,\boldsymbol{\mu} \quad \text{if} \quad r \geq 2 \tag{5.37}$$

The mean and first few cumulants of the eigenvalues can be explicitly obtained as

$$\widehat{\lambda}_j = \kappa_j^{(1)} = c_j + \frac{1}{2}\mathrm{Trace}\left(\mathbf{A}_j\boldsymbol{\Sigma}\right) + \frac{1}{2}\boldsymbol{\mu}^T\mathbf{A}_j\,\boldsymbol{\mu} + \mathbf{a}_j^T\boldsymbol{\mu} \tag{5.38}$$

$$\mathrm{Var}\left[\lambda_j\right] = \kappa_j^{(2)} = \frac{1}{2}\mathrm{Trace}\left(\left[\mathbf{A}_j\boldsymbol{\Sigma}\right]^2\right) + \mathbf{a}_j^T\boldsymbol{\Sigma}\,\mathbf{a}_j + +2\,\boldsymbol{\mu}^T\left[\mathbf{A}_j\boldsymbol{\Sigma}\right]\mathbf{A}_j\,\boldsymbol{\mu} + 2\,\mathbf{a}_j^T\left[\boldsymbol{\Sigma}\,\mathbf{A}_j\right]\mathbf{A}_j\,\boldsymbol{\mu}, \tag{5.39}$$

$$\kappa_j^{(3)} = \mathrm{Trace}\left(\left[\mathbf{A}_j\boldsymbol{\Sigma}\right]^3\right) + 3\mathbf{a}_j^T\left[\boldsymbol{\Sigma}\,\mathbf{A}_j\right]\mathbf{a}_j + 6\,\boldsymbol{\mu}^T\left[\mathbf{A}_j\boldsymbol{\Sigma}\right]^2\mathbf{A}_j\,\boldsymbol{\mu} + 6\,\mathbf{a}_j^T\left[\boldsymbol{\Sigma}\,\mathbf{A}_j\right]^2\mathbf{A}_j\,\boldsymbol{\mu}, \tag{5.40}$$

$$\kappa_j^{(4)} = 3\mathrm{Trace}\left(\left[\mathbf{A}_j\boldsymbol{\Sigma}\right]^4\right) + 12\mathbf{a}_j^T\left[\boldsymbol{\Sigma}\,\mathbf{A}_j\right]^2\mathbf{a}_j + 24\,\boldsymbol{\mu}^T\left[\mathbf{A}_j\boldsymbol{\Sigma}\right]^3\mathbf{A}_j\,\boldsymbol{\mu} + 24\,\mathbf{a}_j^T\left[\boldsymbol{\Sigma}\,\mathbf{A}_j\right]^3\mathbf{A}_j\,\boldsymbol{\mu} \tag{5.41}$$

Since equations (5.16), (5.17) and (5.36), (5.37) give cumulants of arbitrary order, it is possible to construct the pdf of the eigenvalues from them. However, when the elements of $\mathbf{x}$ are non-Gaussian then neither the first-order perturbation nor the second-order perturbation methods are helpful because there is no general method to obtain the resulting statistics in a simple manner. In such cases the method outlined in the next section might be more useful.

5.4 Method Based on the Asymptotic Integral

5.4.1 Multidimensional Integrals in Unbounded Domains

In this section the moments of the eigenvalues are obtained based on the asymptotic approximation of the multidimensional integral. Consider a function $f(\mathbf{x}) : \mathbb{R}^m \mapsto \mathbb{R}$ which is smooth and at least twice differentiable. Suppose we want to evaluate an integral of the following form:

$$\mathcal{J} = \int_{\mathbb{R}^m} \exp\{-f(\mathbf{x})\}\, d\mathbf{x} \tag{5.42}$$

This is a m-dimensional integral over the unbounded domain $\mathbb{R}^m$. The maximum contribution to this integral comes from the neighborhood where $f(\mathbf{x})$ reaches its global minimum. Suppose that $f(\mathbf{x})$ reaches its global minimum at an *unique* point $\boldsymbol{\theta} \in \mathbb{R}^m$. Therefore, at $\mathbf{x} = \boldsymbol{\theta}$

$$\frac{\partial f(\mathbf{x})}{\partial x_k} = 0, \forall k \quad \text{or} \quad \mathbf{d}_f(\boldsymbol{\theta}) = \mathbf{0} \tag{5.43}$$

Using this, expand $f(\mathbf{x})$ in a Taylor series about $\boldsymbol{\theta}$ and rewrite equation (5.42) as

$$\begin{aligned}\mathcal{J} &= \int_{\mathbb{R}^m} \exp\left\{-\left\{f(\boldsymbol{\theta}) + \frac{1}{2}(\mathbf{x}-\boldsymbol{\theta})^T \mathbf{D}_f(\boldsymbol{\theta})(\mathbf{x}-\boldsymbol{\theta}) + \varepsilon(\mathbf{x},\boldsymbol{\theta})\right\}\right\} d\mathbf{x} \\ &= \exp\{-f(\boldsymbol{\theta})\} \int_{\mathbb{R}^m} \exp\left\{-\frac{1}{2}(\mathbf{x}-\boldsymbol{\theta})^T \mathbf{D}_f(\boldsymbol{\theta})(\mathbf{x}-\boldsymbol{\theta}) - \varepsilon(\mathbf{x},\boldsymbol{\theta})\right\} d\mathbf{x}\end{aligned} \tag{5.44}$$

where $\varepsilon(\mathbf{x},\boldsymbol{\theta})$ is the error if only the terms up to second-order were retained in the Taylor series expansion. With suitable scaling of $\mathbf{x}$ the integral in (5.42) can be transformed to the so called 'Laplace integral'. Under special conditions such integrals can be well approximated using asymptotic methods. The relevant mathematical methods and formal derivations are covered in

detail in the books by Bleistein and Handelsman (1994) and Wong (2001). Here we propose a somewhat different version of asymptotic integrals. The error $\varepsilon(\mathbf{x}, \boldsymbol{\theta})$ depends on higher order derivatives of $f(\mathbf{x})$ at $\mathbf{x} = \boldsymbol{\theta}$. If they are small compared to $f(\boldsymbol{\theta})$ and the elements of $\mathbf{D}_f(\boldsymbol{\theta})$, their contribution will be negligible to the value of the integral. Therefore, we assume $f(\boldsymbol{\theta})$ and the elements of $\mathbf{D}_f(\boldsymbol{\theta})$ are large so that

$$\left|\frac{1}{f(\boldsymbol{\theta})}\mathcal{D}^{(j)}(f(\boldsymbol{\theta}))\right| \to 0 \quad \text{and} \quad \forall k, l, \left|\frac{1}{[\mathbf{D}_f(\boldsymbol{\theta})]_{kl}}\mathcal{D}^{(j)}(f(\boldsymbol{\theta}))\right| \to 0 \quad \text{for} \quad j > 2 \tag{5.45}$$

where $\mathcal{D}^{(j)}(f(\boldsymbol{\theta}))$ is jth order derivative of $f(\mathbf{x})$ evaluated at $\mathbf{x} = \boldsymbol{\theta}$. Under such assumptions $\varepsilon(\mathbf{x}, \boldsymbol{\theta}) \to 0$. Therefore, the integral in (5.44) can be approximated as

$$\mathcal{J} \approx \exp\{-f(\boldsymbol{\theta})\} \int_{\mathbb{R}^m} \exp\left\{-\frac{1}{2}(\mathbf{x}-\boldsymbol{\theta})^T \mathbf{D}_f(\boldsymbol{\theta})(\mathbf{x}-\boldsymbol{\theta})\right\} d\mathbf{x} \tag{5.46}$$

If $\boldsymbol{\theta}$ is the global minima of $f(\mathbf{x})$ in $\mathbb{R}^m$, the symmetric Hessian matrix $\mathbf{D}_f(\boldsymbol{\theta}) \in \mathbb{R}^{m \times m}$ is also expected to be positive definite. Now use the coordinate transformation

$$\boldsymbol{\xi} = (\mathbf{x}-\boldsymbol{\theta})\mathbf{D}_f^{-1/2}(\boldsymbol{\theta}) \tag{5.47}$$

The Jacobian of this transformation is

$$\|\mathbf{J}\| = \|\mathbf{D}_f(\boldsymbol{\theta})\|^{-1/2} \tag{5.48}$$

Using equation (5.47), the integral in equation (5.46) can be evaluated as

$$\mathcal{J} \approx \exp\{-f(\boldsymbol{\theta})\} \int_{\mathbb{R}^m} \|\mathbf{D}_f(\boldsymbol{\theta})\|^{-1/2} \exp\left\{-\frac{1}{2}(\boldsymbol{\xi}^T\boldsymbol{\xi})\right\} d\boldsymbol{\xi} \tag{5.49}$$

$$\text{or} \quad \mathcal{J} \approx (2\pi)^{m/2} \exp\{-f(\boldsymbol{\theta})\} \|\mathbf{D}_f(\boldsymbol{\theta})\|^{-1/2} \tag{5.50}$$

5.4.2 Calculation of Arbitrary Moments of The Eigenvalues

An arbitrary rth order moment of the eigenvalues can be obtained from

$$\begin{aligned}\mu_j^{(r)} = \mathrm{E}\left[\lambda_j^r(\mathbf{x})\right] &= \int_{\mathbb{R}^m} \lambda_j^r(\mathbf{x}) p_{\mathbf{X}}(\mathbf{x})\, d\mathbf{x} \\ &= \int_{\mathbb{R}^m} \exp\left\{-\left(L(\mathbf{x}) - r\ln\lambda_j(\mathbf{x})\right)\right\}\, d\mathbf{x}, \quad r = 1, 2, 3\cdots\end{aligned} \tag{5.51}$$

The equation can be expressed in the form of equation (5.42) by choosing

$$f(\mathbf{x}) = L(\mathbf{x}) - r\ln\lambda_j(\mathbf{x}) \tag{5.52}$$

Differentiating the above equation with respect to x_k we obtain

$$\frac{\partial f(\mathbf{x})}{\partial x_k} = \frac{\partial L(\mathbf{x})}{\partial x_k} - \frac{r}{\lambda_j(\mathbf{x})}\frac{\partial \lambda_j(\mathbf{x})}{\partial x_k} \tag{5.53}$$

The optimal point $\boldsymbol{\theta}$ can be obtained from (5.43) by equating the above expression to zero. Therefore at $\mathbf{x} = \boldsymbol{\theta}$

$$\frac{\partial f(\mathbf{x})}{\partial x_k} = 0, \quad \forall\, k \tag{5.54}$$

$$\text{or} \quad \frac{r}{\lambda_j(\boldsymbol{\theta})}\frac{\partial \lambda_j(\boldsymbol{\theta})}{\partial x_k} = \frac{\partial L(\boldsymbol{\theta})}{\partial x_k}, \quad \forall\, k \tag{5.55}$$

$$\text{or} \quad \mathbf{d}_{\lambda_j}(\boldsymbol{\theta}) r = \lambda_j(\boldsymbol{\theta})\mathbf{d}_L(\boldsymbol{\theta}) \tag{5.56}$$

Equation (5.56) is similar to equation (5.27) and needs to solved numerically to obtain $\boldsymbol{\theta}$. The elements of the Hessian matrix $\mathbf{D}_f(\boldsymbol{\theta})$ can be obtained by differentiating equation (5.53) with respect to x_l:

$$\begin{aligned}\frac{\partial^2 f(\mathbf{x})}{\partial x_k\, \partial x_l} &= \frac{\partial^2 L(\mathbf{x})}{\partial x_k\, \partial x_l} - r\left(-\frac{1}{\lambda_j^2(\mathbf{x})}\frac{\partial \lambda_j(\mathbf{x})}{\partial x_l}\frac{\partial \lambda_j(\mathbf{x})}{\partial x_k} + \frac{1}{\lambda_j(\mathbf{x})}\frac{\partial^2 \lambda_j(\mathbf{x})}{\partial x_k\, \partial x_l}\right) \\ &= \frac{\partial^2 L(\mathbf{x})}{\partial x_k\, \partial x_l} + \frac{1}{r}\left\{\frac{r}{\lambda_j(\mathbf{x})}\frac{\partial \lambda_j(\mathbf{x})}{\partial x_k}\right\}\left\{\frac{r}{\lambda_j(\mathbf{x})}\frac{\partial \lambda_j(\mathbf{x})}{\partial x_l}\right\} - \frac{r}{\lambda_j(\mathbf{x})}\frac{\partial^2 \lambda_j(\mathbf{x})}{\partial x_k\, \partial x_l}\end{aligned} \tag{5.57}$$

At $\mathbf{x} = \boldsymbol{\theta}$ we can use equation (5.55) so that equation (5.57) reads

$$\frac{\partial^2 f(\mathbf{x})}{\partial x_k \, \partial x_l}|_{\mathbf{x}=\boldsymbol{\theta}} = \frac{\partial^2 L(\boldsymbol{\theta})}{\partial x_k \, \partial x_l} + \frac{1}{r}\frac{\partial L(\boldsymbol{\theta})}{\partial x_k}\frac{\partial L(\boldsymbol{\theta})}{\partial x_l} - \frac{r}{\lambda_j(\boldsymbol{\theta})}\frac{\partial^2 \lambda_j(\boldsymbol{\theta})}{\partial x_k \, \partial x_l} \tag{5.58}$$

Combining this equation for all k and l we have

$$\mathbf{D}_f\left(\boldsymbol{\theta}\right) = \mathbf{D}_L(\boldsymbol{\theta}) + \frac{1}{r}\mathbf{d}_L(\boldsymbol{\theta})\mathbf{d}_L(\boldsymbol{\theta})^T - \frac{r}{\lambda_j(\boldsymbol{\theta})}\mathbf{D}_{\lambda_j}(\boldsymbol{\theta}) \tag{5.59}$$

where $\mathbf{D}_{\lambda_j}(\bullet)$ is defined in equation (5.9). Using the asymptotic approximation (5.50), the rth moment of the eigenvalues can be obtained as

$$\mu_j^{(r)} \approx (2\pi)^{m/2}\lambda_j^r(\boldsymbol{\theta}) \exp\left\{-L\left(\boldsymbol{\theta}\right)\right\} \left\|\mathbf{D}_L(\boldsymbol{\theta}) + \frac{1}{r}\mathbf{d}_L(\boldsymbol{\theta})\mathbf{d}_L(\boldsymbol{\theta})^T - \frac{r}{\lambda_j(\boldsymbol{\theta})}\mathbf{D}_{\lambda_j}(\boldsymbol{\theta})\right\|^{-1/2} \tag{5.60}$$

This is perhaps the most general formula to obtain the moments of the eigenvalues of linear stochastic dynamic systems. The optimal point $\boldsymbol{\theta}$ needs to be calculated by solving non-linear set of equations equation (5.56) for each λ_j and r. Several special cases arising from equation (5.60) are of practical interest:

- *Mean of the eigenvalues:* The mean of the eigenvalues can be obtained by substituting $r = 1$ in equation (5.60), that is

$$\widehat{\lambda}_j = \mu_j^{(1)} = (2\pi)^{m/2}\lambda_j(\boldsymbol{\theta}) \exp\left\{-L\left(\boldsymbol{\theta}\right)\right\} \left\|\mathbf{D}_L(\boldsymbol{\theta}) + \mathbf{d}_L(\boldsymbol{\theta})\mathbf{d}_L(\boldsymbol{\theta})^T - \mathbf{D}_{\lambda_j}(\boldsymbol{\theta})/\lambda_j(\boldsymbol{\theta})\right\|^{-1/2} \tag{5.61}$$

- *Central moments of the eigenvalues:* Once the mean in known, the central moments can be expressed in terms of the raw moments $\mu_j^{(r)}$ using the binomial transform

$$\mu_j^{\prime(r)} = \mathrm{E}\left[\left(\lambda_j - \widehat{\lambda}_j\right)^r\right] = \sum_{k=0}^{r}\binom{r}{k}(-1)^{r-k}\mu_j^{(k)}\widehat{\lambda}_j^{r-k} \tag{5.62}$$

- *Random vector $\boldsymbol{x}$ has multivariate Gaussian distribution:* In this case $L(\mathbf{x})$ is given by equation (5.3) and by differentiating equation (5.28) we obtain

$$\text{and} \quad \mathbf{D}_L(\mathbf{x}) = \boldsymbol{\Sigma}^{-1} \tag{5.63}$$

The optimal point $\boldsymbol{\theta}$ can be obtained from equation (5.56) as

$$\boldsymbol{\theta} = \boldsymbol{\mu} + \frac{r}{\lambda_j(\boldsymbol{\theta})} \boldsymbol{\Sigma}\, \mathbf{d}_{\lambda_j}(\boldsymbol{\theta}) \tag{5.64}$$

Using equation (5.28) and equation (5.63), the Hessian matrix can be derived from equation (5.59) as

$$\begin{aligned} \mathbf{D}_f(\boldsymbol{\theta}) &= \boldsymbol{\Sigma}^{-1} + \frac{1}{r}\boldsymbol{\Sigma}^{-1}(\boldsymbol{\theta}-\boldsymbol{\mu})(\boldsymbol{\theta}-\boldsymbol{\mu})^T \boldsymbol{\Sigma}^{-1} - \frac{r}{\lambda_j(\boldsymbol{\theta})}\mathbf{D}_{\lambda_j}(\boldsymbol{\theta}) \\ &= \boldsymbol{\Sigma}^{-1}\left(\mathbf{I} + \frac{1}{r}(\boldsymbol{\theta}-\boldsymbol{\mu})(\boldsymbol{\theta}-\boldsymbol{\mu})^T \boldsymbol{\Sigma}^{-1}\right) - \frac{r}{\lambda_j(\boldsymbol{\theta})}\mathbf{D}_{\lambda_j}(\boldsymbol{\theta}) \end{aligned} \tag{5.65}$$

Therefore, the rth moment of the eigenvalues can be obtained from equation (5.60) as

$$\mu_j^{(r)} \approx \lambda_j^r(\boldsymbol{\theta}) \exp\left\{-\frac{1}{2}(\boldsymbol{\theta}-\boldsymbol{\mu})^T \boldsymbol{\Sigma}^{-1}(\boldsymbol{\theta}-\boldsymbol{\mu})\right\} \|\boldsymbol{\Sigma}\|^{-1/2} \|\mathbf{D}_f(\boldsymbol{\theta})\|^{-1/2} \tag{5.66}$$

The probability density function of the eigenvalues is considered in the next section.

5.5 Probability Density Function of the Eigenvalues

5.5.1 Maximum Entropy Probability Density Function

Once the cumulants/moments of the eigenvalues are known, the pdf of the eigenvalues can be obtained using Maximum Entropy Method (MEM). Because Eqs. (5.16), (5.17), (5.36), (5.37) and (5.60) can be used to calculate any arbitrary order cumulant and moment, the pdf can be obtained accurately by taking higher order terms.

Since $\mathbf{M}$ and $\mathbf{K}$ are symmetric and positive definite random matrices, all the eigenvalues are real and positive. Suppose the pdf of λ_j is given by $p_{\lambda_j}(u)$ where $u \in \mathbb{R}$ is positive, that is $u \in [0, \infty]$. Considering that only first n moments are used, the pdf of each eigenvalue must satisfy the following constraints:

$$\int_0^\infty p_{\lambda_j}(u)du = 1 \tag{5.67}$$

$$\text{and} \quad \int_0^\infty u^r p_{\lambda_j}(u)du = \mu_j^{(r)}, \quad r = 1, 2, 3, \cdots, n \tag{5.68}$$

Using Shannon's measure of entropy

$$\mathcal{S} = -\int_0^\infty p_{\lambda_j}(u) \ln p_{\lambda_j}(u)du \tag{5.69}$$

we construct the Lagrangian

$$\mathcal{L} = -\int_0^\infty p_{\lambda_j}(u) \ln p_{\lambda_j}(u)du - (\rho_0 - 1)\left[\int_0^\infty p_{\lambda_j}(u)du - 1\right] - \sum_{r=1}^{n} \rho_r \left[\int_0^\infty u^r p_{\lambda_j}(u)du - \mu_j^{(r)}\right] \tag{5.70}$$

where $\rho_r, r = 0, 1, 2, \cdots, n$ are Lagrange multipliers. The function $p_{\lambda_j}(u)$ which maximizes $\mathcal{L}$ can be obtained using the calculus of variations. Using the Euler-

Lagrange equation the solution is given by

$$p_{\lambda_j}(u) = \exp\left\{-\rho_0 - \sum_{i=1}^{n} \rho_i u^i\right\} = \exp\{-\rho_0\} \exp\left\{-\sum_{i=1}^{n} \rho_i u^i\right\}, \quad u \geq 0 \tag{5.71}$$

The Lagrange multipliers can be obtained from the constraint equations (5.67) and (5.68) as

$$\exp\{\rho_0\} = \int_0^\infty \exp\left\{-\sum_{i=1}^{n} \rho_i u^i\right\} du \tag{5.72}$$

$$\text{and} \quad \exp\{\rho_0\}\, \mu_j^{(r)} = \int_0^\infty u^r \exp\left\{-\sum_{i=1}^{n} \rho_i u^i\right\} du, \quad \text{for} \quad r = 0, 1, 2, \cdots n \tag{5.73}$$

Closed-form expressions for ρ_r are in general not possible for all n. If we take $n = 2$, then the resulting pdf can be expressed by a truncated Gaussian density function

$$p_{\lambda_j}(u) = \frac{1}{\sqrt{2\pi}\sigma_j\, \Phi\left(\widehat{\lambda}_j/\sigma_j\right)} \exp\left\{-\frac{\left(u - \widehat{\lambda}_j\right)^2}{2\sigma_j^2}\right\}, \quad u \geq 0 \tag{5.74}$$

where σ_j is given by

$$\sigma_j^2 = \mu_j^{(2)} - \widehat{\lambda}_j^2 \tag{5.75}$$

The approach presented above can also be used in conjunction with the perturbation methods by transforming the cumulants obtained from Eqs. (5.16), (5.17), (5.36) and (5.37) to moments. The truncated Gaussian density function derived here ensures that the probability of any eigenvalues becoming negative is zero.

5.5.2 Approximation by χ^2 Probability Density Function

We use an approximation analogous to Pearson's (Pearson, 1959) three moment central χ^2 approximation to the distribution of a noncentral χ^2 . The pdf of the eigenvalues are approximated as

$$p_{\lambda_j}(u) \approx \eta_j + \gamma_j \chi^2_{\nu_j}(u) \tag{5.76}$$

where $\chi^2_{\nu_j}(u)$ is a central χ^2 density function with ν_j degrees-of-freedom. The constants η_j, γ_j, and ν_j are obtained such that the first three moments of λ_j are equal to that of the approximated χ^2 pdf. The moment generating function of the approximated χ^2 pdf is given by

$$\mathrm{E}\left[\exp\left\{-s\left(\eta_j + \gamma_j \chi^2_{\nu_j}\right)\right\}\right] = \exp\left\{-s\eta_j\right\}\left(1 + 2s\gamma_j\right)^{-\nu_j/2} \tag{5.77}$$

Equating the first three moments we have

$$\eta_j + \nu_j\gamma_j = \mu_j^{(1)}, \tag{5.78}$$

$$\eta_j{}^2 + 2\eta_j\nu_j\gamma_j + \nu_j{}^2\gamma_j{}^2 + 2\nu_j\gamma_j{}^2 = \mu_j^{(2)} \tag{5.79}$$

and $$\eta_j{}^3 + 3\eta_j{}^2\nu_j\gamma_j + 3\eta_j\nu_j{}^2\gamma_j{}^2 + 6\eta_j\nu_j\gamma_j{}^2 + \nu_j{}^3\gamma_j{}^3 + 6\nu_j{}^2\gamma_j{}^3 + 8\nu_j\gamma_j{}^3 = \mu_j^{(3)} \tag{5.80}$$

This set of coupled non-linear equations can be solved exactly in closed-form to obtain η_j, γ_j, and ν_j:

$$\eta_j = \frac{\mu_j^{(1)^2}\mu_j^{(2)} - 2\,\mu_j^{(2)^2} + \mu_j^{(1)}\mu_j^{(3)}}{2\,\mu_j^{(1)^3} - 3\,\mu_j^{(1)}\mu_j^{(2)} + \mu_j^{(3)}} \tag{5.81}$$

$$\gamma_j = \frac{2\,\mu_j^{(1)^3} - 3\,\mu_j^{(1)}\mu_j^{(2)} + \mu_j^{(3)}}{4\left(\mu_j^{(2)} - \mu_j^{(1)^2}\right)}, \tag{5.82}$$

$$\text{and } \nu_j = 8\,\frac{\left(\mu_j^{(2)} - \mu_j^{(1)^2}\right)^3}{\left(2\,\mu_j^{(1)^3} - 3\,\mu_j^{(1)}\mu_j^{(2)} + \mu_3'\right)^2} \tag{5.83}$$

Moments of $\lambda_j(\mathbf{x})$ obtained in equation (5.60), can be used directly in the right-hand side of these equations. Alternatively, this approach can also be used in conjunction with the perturbation methods by transforming the cumulants obtained from Eqs. (5.16), (5.17), (5.36) and (5.37) to moments. Using the transformation in equation (5.76) the approximate probability density function of $\lambda_j(\mathbf{x})$ is given by

$$p_{\lambda_j}(u) \approx \frac{1}{\gamma_j} p_{\chi^2_{\nu_j}}\left(\frac{u-\eta_j}{\gamma_j}\right) = \frac{(u-\eta_j)^{\nu_j/2-1}\exp\left\{-(u-\eta_j)/2\gamma_j\right\}}{(2\gamma_j)^{\nu_j/2}\Gamma(\nu_j/2)} \tag{5.84}$$

The two approximated pdf proposed here have simple forms but it should be noted that they are not exhaustive. Given the moments/cumulants, different probability density functions can be fitted using different methods. Application of the approximate pdfs derived here is illustrated in the next section.

5.6 Numerical Examples

5.6.1 A two DOF system

System model and computational methodology

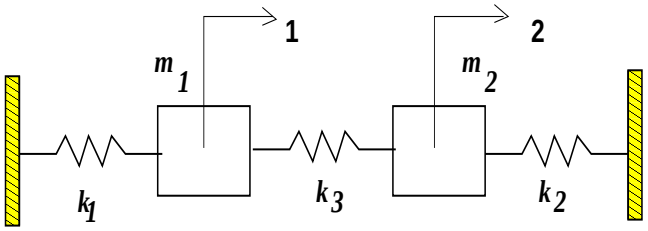

Figure 5.1: The undamped two degree-of-system system, $m_1 = 1$ Kg, $m_2 = 1.5$ Kg, $\bar{k}_1 = 1000$ N/m, $\bar{k}_2 = 1100$ N/m and $k_3 = 100$ N/m.

A simple two-degree-of-freedom undamped system has been considered to illustrate a possible application of the expressions developed so far. The main purpose of this example is to understand how the proposed methods compare with the existing methods. Figure 5.1 shows the example, together with the numerical values of the masses and spring stiffnesses. The system matrices for the example are given by

$$\mathbf{M} = \begin{bmatrix} m_1 & 0 \\ 0 & m_1 \end{bmatrix} \quad \text{and} \quad \mathbf{K} = \begin{bmatrix} k_1 + k_3 & -k_3 \\ -k_3 & k_2 + k_3 \end{bmatrix} \tag{5.85}$$

It is assumed that only the stiffness parameters k_1 and k_2 are uncertain so that $k_i = \bar{k}_i(1 + \epsilon_i x_i)$, $i = 1, 2$ and $\bar{k}_i$ denote the deterministic values of the spring constants. Here $\mathbf{x} = \{x_1, x_2\}^T \in \mathbb{R}^2$ is a vector of standard Gaussian random variables, that is $\boldsymbol{\mu} = \mathbf{0}$ and $\boldsymbol{\Sigma} = \mathbf{I}$. The numerical values of the 'strength parameters' are considered as $\epsilon_1 = \epsilon_2 = 0.25$. The strength parameters are

selected so that the system matrices are almost surely positive definite. Noting that $\mathbf{M}$ is independent of $\mathbf{x}$ and $\mathbf{K}$ is a linear function of $\mathbf{x}$, the derivative of the system matrices with respect to the random vector $\mathbf{x}$ can be obtained as

$$\frac{\partial \mathbf{K}}{\partial x_1} = \epsilon_1 \begin{bmatrix} \bar{k}_1 & 0 \\ 0 & 0 \end{bmatrix}, \quad \frac{\partial \mathbf{K}}{\partial x_2} = \epsilon_2 \begin{bmatrix} 0 & 0 \\ 0 & \bar{k}_2 \end{bmatrix}, \tag{5.86}$$

$$\frac{\partial \mathbf{M}}{\partial x_i} = \mathbf{O} \quad \text{and} \quad \frac{\partial^2 \mathbf{K}}{\partial x_i \, \partial x_j} = \mathbf{O} \tag{5.87}$$

We calculate the raw moments and the probability density functions of the two eigenvalues of the system. Recall that the eigenvalues obtained from equation (5.1) are square of the natural frequencies ($\lambda_j = \omega_j^2$). Following six methods are used to obtain the moments and the pdfs:

1. *Mean-centered first-order perturbation:* This case arises when $\mathbf{D}_{\lambda_j}(\boldsymbol{\mu})$ in the Taylor series expansion (5.7) is assumed to be a null matrix so that only the first-order terms are retained. This is the simplest approximation, and as mentioned earlier, results in Gaussian distribution of the eigenvalues. Recalling that for this problem $\boldsymbol{\mu} = \mathbf{0}$ and $\boldsymbol{\Sigma} = \mathbf{I}$, the resulting statistics for this special case can be obtained from Eqs. (5.18) and (5.19) as

$$\widehat{\lambda}_j = \overline{\lambda}_j \tag{5.88}$$

$$\text{and} \quad \text{Var}\left[\lambda_j\right] = \mathbf{d}_{\lambda_j}^T(\mathbf{0}) \mathbf{d}_{\lambda_j}(\mathbf{0}) \tag{5.89}$$

The gradient vector $\mathbf{d}_{\lambda_j}(\mathbf{0})$ can be obtained from equation (B.2) using the system derivative matrices (5.86) and (5.87).

2. *Mean-centered second-order perturbation:* In this case all the terms in equation (5.7) are retained. This approximation results in a quadratic form in Gaussian random variables. The resulting statistics can be obtained from Eqs. (5.16) and (5.17) by substituting $\boldsymbol{\mu} = \mathbf{0}$ and $\boldsymbol{\Sigma} = \mathbf{I}$. The elements of the Hessian matrix $\mathbf{D}_{\lambda_j}(\mathbf{0})$ can be obtained from equation (B.4) and using the system derivative matrices (5.86) and (5.87).

3. *Optimal point first-order perturbation:* This case arises when $\mathbf{D}_{\lambda_j}(\boldsymbol{\alpha})$ in the Taylor series expansion (5.22) is assumed to be a null matrix so that only the first-order terms are retained. Like its mean-centered counterpart, this approach also results in a Gaussian distribution of the eigenvalues. From equation (5.30) we have

$$c_j = \lambda_j(\boldsymbol{\alpha}) - \mathbf{d}_{\lambda_j}^T(\boldsymbol{\alpha})\boldsymbol{\alpha}, \quad \mathbf{a}_j = \mathbf{d}_{\lambda_j}(\boldsymbol{\alpha}) \quad \text{and} \quad \mathbf{A}_j = \mathbf{O} \tag{5.90}$$

The equation to obtain the optimal point $\boldsymbol{\alpha}$ can be given from equation (5.29) as

$$\boldsymbol{\alpha} = \mathbf{d}_{\lambda_j}(\boldsymbol{\alpha})/\lambda_j(\boldsymbol{\alpha}) \quad \text{or} \quad \mathbf{d}_{\lambda_j}(\boldsymbol{\alpha}) = \lambda_j(\boldsymbol{\alpha})\boldsymbol{\alpha} \tag{5.91}$$

Using these equations, the mean and the variance can be obtained as special cases of Eqs. (5.38) and (5.39)

$$\widehat{\lambda}_j = \lambda_j(\boldsymbol{\alpha}) - \mathbf{d}_{\lambda_j}^T(\boldsymbol{\alpha})\boldsymbol{\alpha} = \lambda_j(\boldsymbol{\alpha}) - \lambda_j(\boldsymbol{\alpha})\boldsymbol{\alpha}^T\boldsymbol{\alpha} \tag{5.92}$$

$$\text{or} \quad \widehat{\lambda}_j = \lambda_j(\boldsymbol{\alpha})\left(1 - |\boldsymbol{\alpha}|^2\right) \tag{5.93}$$

$$\text{and} \quad \text{Var}\left[\lambda_j\right] = \mathbf{d}_{\lambda_j}^T(\boldsymbol{\alpha})\mathbf{d}_{\lambda_j}(\boldsymbol{\alpha}) = \lambda_j^2(\boldsymbol{\alpha})|\boldsymbol{\alpha}|^2 \tag{5.94}$$

4. *Optimal point second-order perturbation:* In this case all the terms in

equation (5.22) are retained. Like the mean-centered approach, this approximation also results in a quadratic form in Gaussian random variables, but with different coefficients. The resulting statistics can be obtained from Eqs. (5.36) and (5.37).

5. *Method based on the asymptotic integral:* In this case the moments can be obtained using equation (5.60). For the standardized Gaussian random vector substituting $\boldsymbol{\mu} = \mathbf{0}$ and $\boldsymbol{\Sigma} = \mathbf{I}$ in equation (5.66) the moment formula can be simplified to

$$\mu_j^{(r)} \approx \lambda_j^r(\boldsymbol{\theta}) \exp\left\{-\frac{1}{2}|\boldsymbol{\theta}|^2\right\} \left\|\mathbf{I} + \frac{1}{r}\boldsymbol{\theta}\boldsymbol{\theta}^T/r - \frac{r}{\lambda_j(\boldsymbol{\theta})}\mathbf{D}_{\lambda_j}(\boldsymbol{\theta})\right\|^{-1/2}, \tag{5.95}$$

and $$\boldsymbol{\theta} = r\mathbf{d}_{\lambda_j}(\boldsymbol{\theta})/\lambda_j(\boldsymbol{\theta}), \quad r = 1, 2, 3, \cdots \tag{5.96}$$

The vector $\boldsymbol{\theta}$ needs to be calculated for each r and j from equation (5.96) using the iterative approach discussed before. The moments obtained from equation (5.95) can be used to obtain the pdf using the approach given in Section 5.5.

6. *Monte Carlo Simulation:* The samples of two independent Gaussian random variables x_1 and x_2 are generated and the eigenvalues are computed directly from (5.1). A total of 15000 samples are used to obtain the statistical moments and pdf of both the eigenvalues. Results obtained from the Monte Carlo simulation is assumed to be the benchmark for the purpose of comparing the five analytical methods described above.

Numerical results

Figure 5.2 shows the percentage error for the first four raw moments of the first eigenvalue. The percentage error for an arbitrary kth moment of an eigenvalue

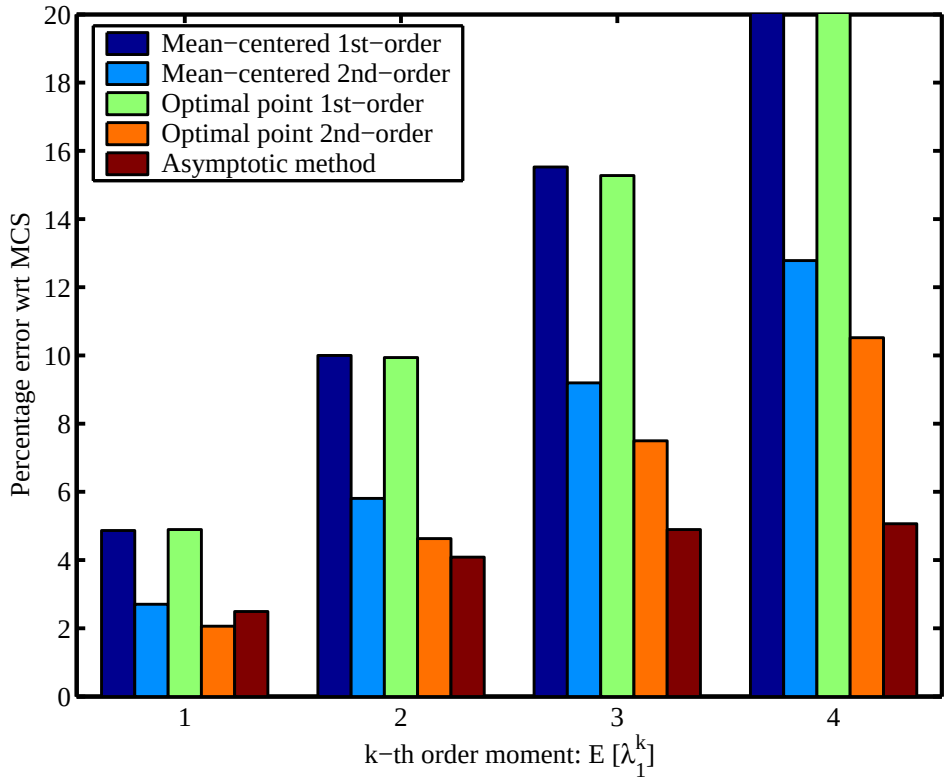

Figure 5.2: Percentage error for the first eigenvalue.

obtained using any one of the five analytical methods is given by

$$\text{Error}_{i\text{th method}} = \frac{\left|\{\mu_j^{(r)}\}_{i\text{th method}} - \{\mu_j^{(r)}\}_{\text{MCS}}\right|}{\{\mu_j^{(r)}\}_{\text{MCS}}} \times 100, \quad i = 1, \cdots 5 \qquad (5.97)$$

Percentage error for the first four raw moments of the second eigenvalue is shown in figure 5.3. For both eigenvalues error corresponding to the mean-centered first-order perturbation method is more than the other four methods. Error corresponding to the optimal point first-order perturbation method fol-

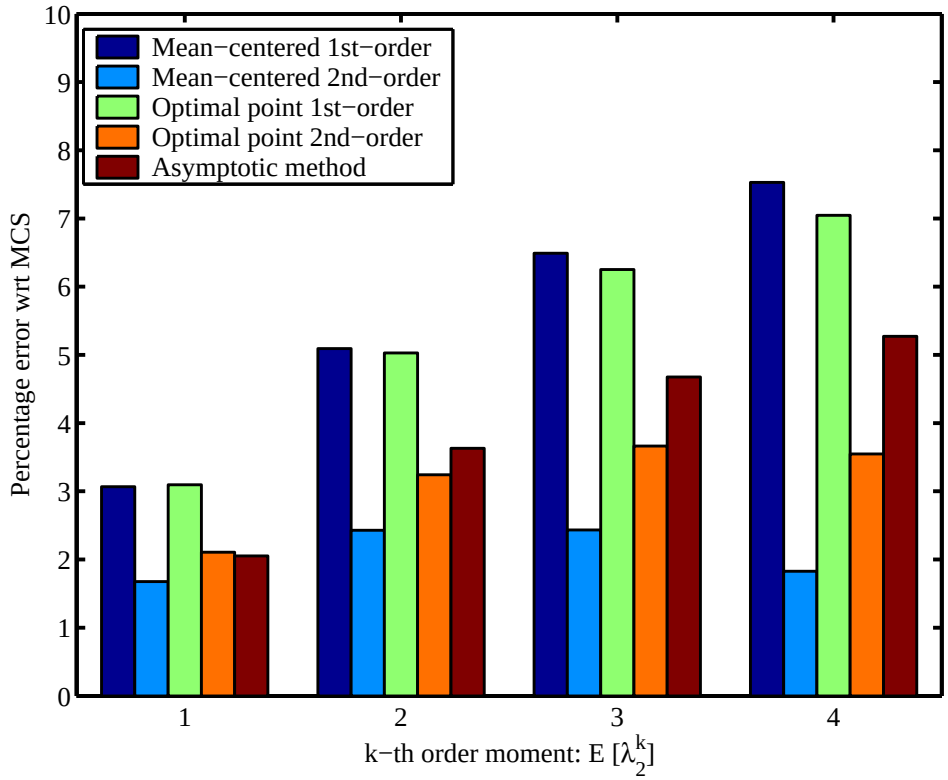

Figure 5.3: Percentage error for the second eigenvalue.

lows next. Moments obtained from mean-centered and optimal point second-order perturbation methods are more accurate compared to their corresponding first-order counterparts. In general the moments obtained from the asymptotic formula (5.60) turns out to be quite accurate. Absolute error for the second eigenvalue is less compared to the first eigenvalue. For the first eigenvalue, the moments obtained from the asymptotic formula turns out to be the most accurate, while for the second eigenvalue, mean-centered second-order perturbation method yields most accurate results.

Now consider the probability density function of the eigenvalues. Figures 5.4 and 5.5 respectively show the pdf of the first and the second eigenvalue

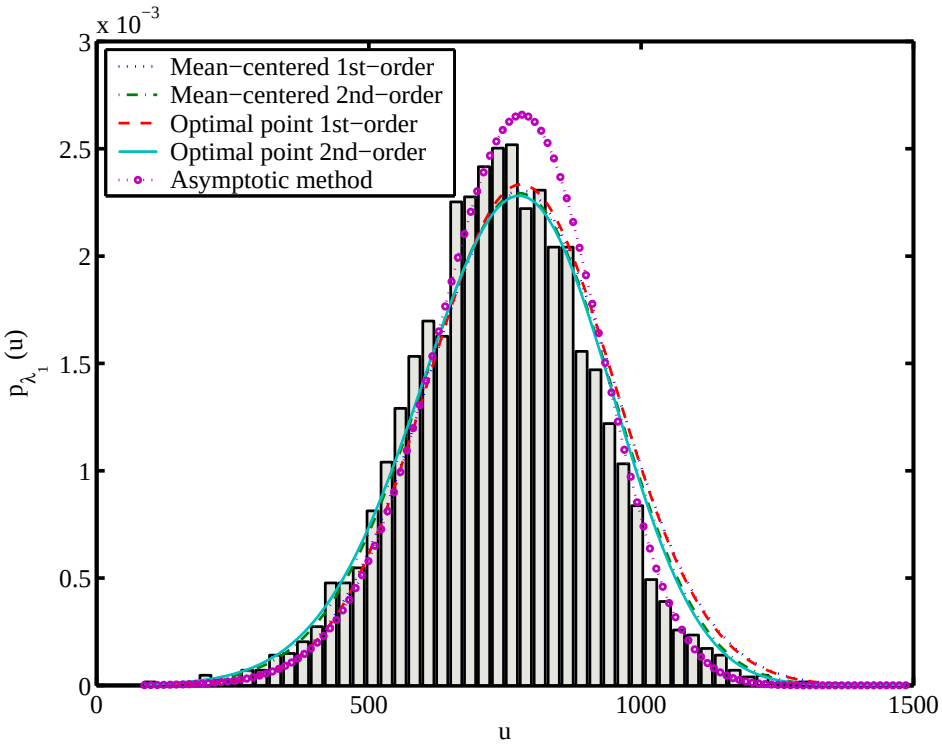

Figure 5.4: Probability density function of the first eigenvalue.

obtained from the five methods described earlier. The pdf corresponding to first five methods are obtained using the χ^2 distribution in equation (5.84). The constants appearing in this equation are calculated from the moments using Eqs. (5.81)–(5.83). In the same plots, normalized histograms of the eigenvalues obtained from the Monte Carlo simulation are also plotted. For the first eigenvalue, pdf from the second-order perturbation methods are accurate in the lower and in the upper tail. For the second eigenvalue, pdf from the asymptotic moments is accurate over the whole curve.

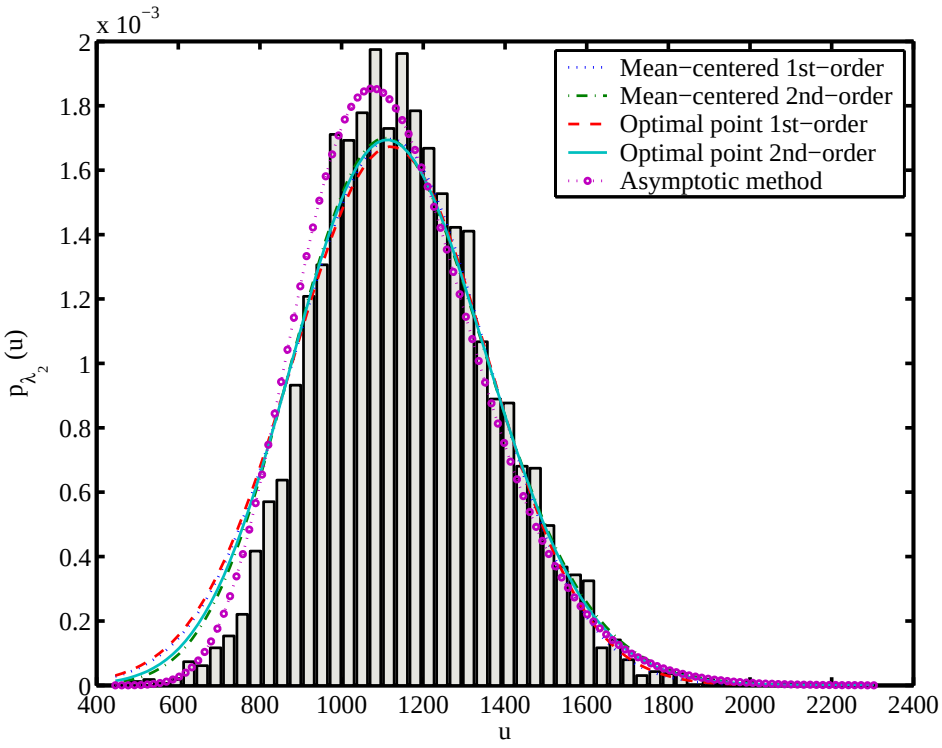

Figure 5.5: Probability density function of the second eigenvalue.

5.6.2 A Three Dof System with Closely Spaced Eigenvalues

System model and computational methodology

A three-degree-of-freedom undamped spring-mass system, taken from Friswell (1996), is shown in figure 5.6. The main purpose of this example is to understand how the proposed methods work when some of the system eigenvalues are closely spaced. This is an interesting case because it is well known that closely spaced eigenvalues are parameter sensitive. We will investigate how the parameter uncertainty effects the eigenvalue distribution in such cases. This study has particular relevance with dynamics of nominally symmetric rotating machineries, for example, turbine blades with random imperfections. The

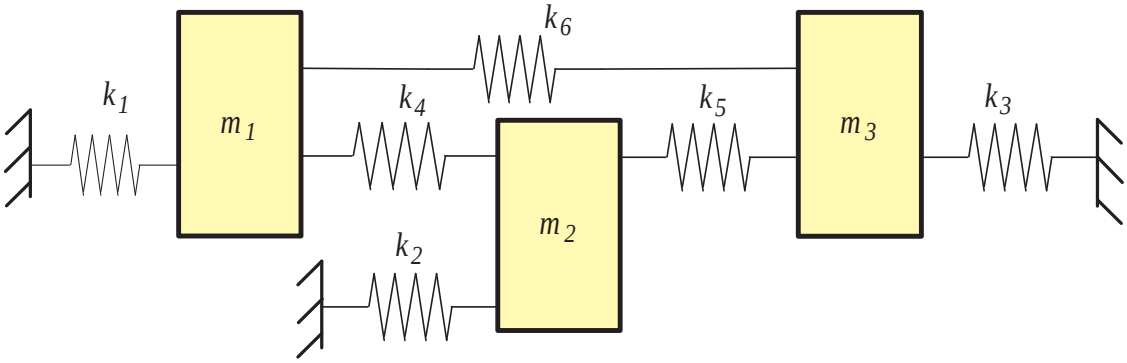

Figure 5.6: The three degree-of-freedom random system.

mass and stiffness matrices of the example system are given by

$$\mathbf{M} = \begin{bmatrix} m_1 & 0 & 0 \\ 0 & m_2 & 0 \\ 0 & 0 & m_3 \end{bmatrix} \quad \text{and} \quad \mathbf{K} = \begin{bmatrix} k_1 + k_4 + k_6 & -k_4 & -k_6 \\ -k_4 & k_4 + k_5 + k_6 & -k_5 \\ -k_6 & -k_5 & k_5 + k_3 + k_6 \end{bmatrix} \tag{5.98}$$

It is assumed that all mass and stiffness constants are random. The randomness in these parameters are assumed to be of the following form:

$$m_i = \overline{m}_i \left(1 + \epsilon_m x_i\right), \quad i = 1, 2, 3 \tag{5.99}$$

$$k_i = \overline{k}_i \left(1 + \epsilon_k x_{i+3}\right), \quad i = 1, \cdots, 6 \tag{5.100}$$

Here $\mathbf{x} = \{x_1, \cdots, x_9\}^T \in \mathbb{R}^9$ is the vector of random variables. It is assumed that all random variables are Gaussian and uncorrelated with zero mean and unit standard deviation, that is $\boldsymbol{\mu} = \mathbf{0}$ and $\boldsymbol{\Sigma} = \mathbf{I}$. Therefore, the mean values of m_i and k_i are given by $\overline{m}_i$ and $\overline{k}_i$. The numerical values of both the 'strength parameters' ϵ_m and ϵ_k are fixed at 0.15. In order to obtain statistics of the eigenvalues using the methods proposed here the gradient vector and the Hessian matrix of the eigenvalues are required. As shown in Section B,

this in turn requires the derivative of the system matrices with respect to the entries of $\mathbf{x}$. For most practical problems, which usually involve Finite Element modeling, these derivatives need to be determined numerically. However, for this simple example the derivatives can be obtained in closed-form. For the mass matrix we have

$$\frac{\partial \mathbf{M}}{\partial x_1} = \begin{bmatrix} \overline{m}_1\epsilon_m & 0 & 0 \\ 0 & 0 & 0 \\ 0 & 0 & 0 \end{bmatrix}, \quad \frac{\partial \mathbf{M}}{\partial x_2} = \begin{bmatrix} 0 & 0 & 0 \\ 0 & \overline{m}_2\epsilon_m & 0 \\ 0 & 0 & 0 \end{bmatrix}, \quad \frac{\partial \mathbf{M}}{\partial x_3} = \begin{bmatrix} 0 & 0 & 0 \\ 0 & 0 & 0 \\ 0 & 0 & \overline{m}_3\epsilon_m \end{bmatrix} \tag{5.101}$$

All other $\dfrac{\partial \mathbf{M}}{\partial x_i}$ are null matrices. For the derivative of the stiffness matrix

$$\frac{\partial \mathbf{K}}{\partial x_4} = \begin{bmatrix} \overline{k}_1\epsilon_k & 0 & 0 \\ 0 & 0 & 0 \\ 0 & 0 & 0 \end{bmatrix}, \quad \frac{\partial \mathbf{K}}{\partial x_5} = \begin{bmatrix} 0 & 0 & 0 \\ 0 & \overline{k}_2\epsilon_k & 0 \\ 0 & 0 & 0 \end{bmatrix}, \quad \frac{\partial \mathbf{M}}{\partial x_6} = \begin{bmatrix} 0 & 0 & 0 \\ 0 & 0 & 0 \\ 0 & 0 & \overline{k}_3\epsilon_k \end{bmatrix}$$

$$\frac{\partial \mathbf{K}}{\partial x_7} = \begin{bmatrix} \overline{k}_4\epsilon_k & -\overline{k}_4\epsilon_k & 0 \\ -\overline{k}_4\epsilon_k & \overline{k}_4\epsilon_k & 0 \\ 0 & 0 & 0 \end{bmatrix}, \quad \frac{\partial \mathbf{K}}{\partial x_8} = \begin{bmatrix} 0 & 0 & 0 \\ 0 & \overline{k}_5\epsilon_k & -\overline{k}_5\epsilon_k \\ 0 & -\overline{k}_5\epsilon_k & \overline{k}_5\epsilon_k \end{bmatrix}, \quad \frac{\partial \mathbf{M}}{\partial x_9} = \begin{bmatrix} \overline{k}_6\epsilon_k & 0 & -\overline{k}_6\epsilon_k \\ 0 & 0 & 0 \\ -\overline{k}_6\epsilon_k & 0 & \overline{k}_6\epsilon_k \end{bmatrix} \tag{5.102}$$

and all other $\dfrac{\partial \mathbf{K}}{\partial x_i}$ are null matrices. Also note that all of the first-order derivative matrices are independent of $\mathbf{x}$. For this reason, all the higher order derivatives of the $\mathbf{M}(\mathbf{x})$ and $\mathbf{K}(\mathbf{x})$ matrices are null matrices.

We calculate the moments and the probability density functions of the three eigenvalues of the system. The following two sets of physically meaningful parameter values are considered:

- *Case 1: All eigenvalues are well separated*

  For this case $\overline{m}_i = 1.0$ kg for $i = 1, 2, 3$; $\overline{k}_i = 1.0$ N/m for $i = 1, \cdots, 5$ and $k_6 = 3.0$ N/m.

- *Case 2: Two eigenvalues are close*

  All parameter values are the same except $k_6 = 1.275$ N/m.

The moments of the eigenvalues for the above two cases are calculated from Eqs. (5.95) and (5.96). The moments are then used to obtain σ_j from equation (5.75) and the constants in Eqs. (5.81)–(5.83). Using these constants the truncated Gaussian pdf and the χ^2 pdf of the eigenvalues are obtained from Eqs. (5.74) and (5.84) respectively. These results are compared with Monte Carlo simulation. The samples of the nine independent Gaussian random variables $x_i, i = 1, \cdots, 9$ are generated and the eigenvalues are computed directly from equation (5.1). A total of 15000 samples are used to obtain the statistical moments and histograms of the pdf of the eigenvalues. The results obtained from Monte Carlo simulation are assumed to be the benchmark for the purpose of comparing the analytical methods. For the purpose of determining the accuracy, we again calculate the percentage error associated with an arbitrary rth moment using equation (5.97). The results for the two cases are presented and discussed in the next subsection.

Numerical results

Case 1: All eigenvalues are well separated

When all of the eigenvalues are well separated their derivatives with respect to the system parameters generally behave well. For the given parameter values the eigenvalues of the corresponding deterministic system is given by

$$\overline{\lambda}_1 = 1, \quad \overline{\lambda}_2 = 4, \quad \text{and} \quad \overline{\lambda}_3 = 8 \tag{5.103}$$

The random 'scatter' of the eigenvalues is shown in figure 5.7 for 1000 samples from the Monte Carlo simulation. It can be seen that the highest eigenvalue

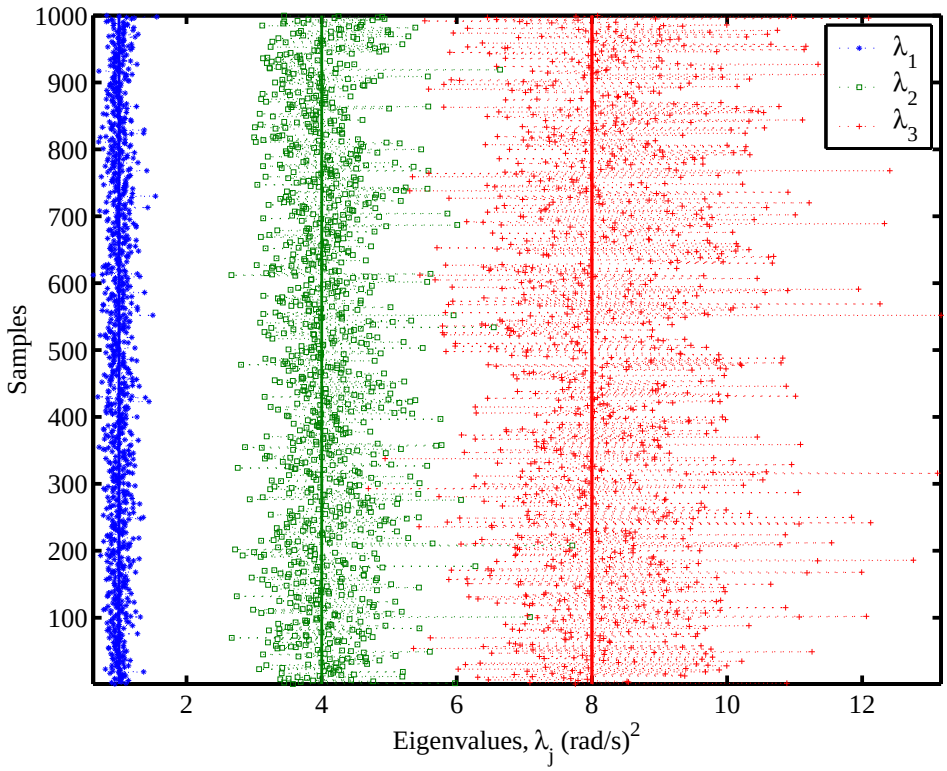

Figure 5.7: Statistical scatter in the eigenvalues; Case 1.

has the maximum scatter and because the eigenvalues are well separated, there is very little statistical overlap between them. Figure 5.8 shows the percentage

error for the first four moments of the eigenvalues. These errors are reasonably

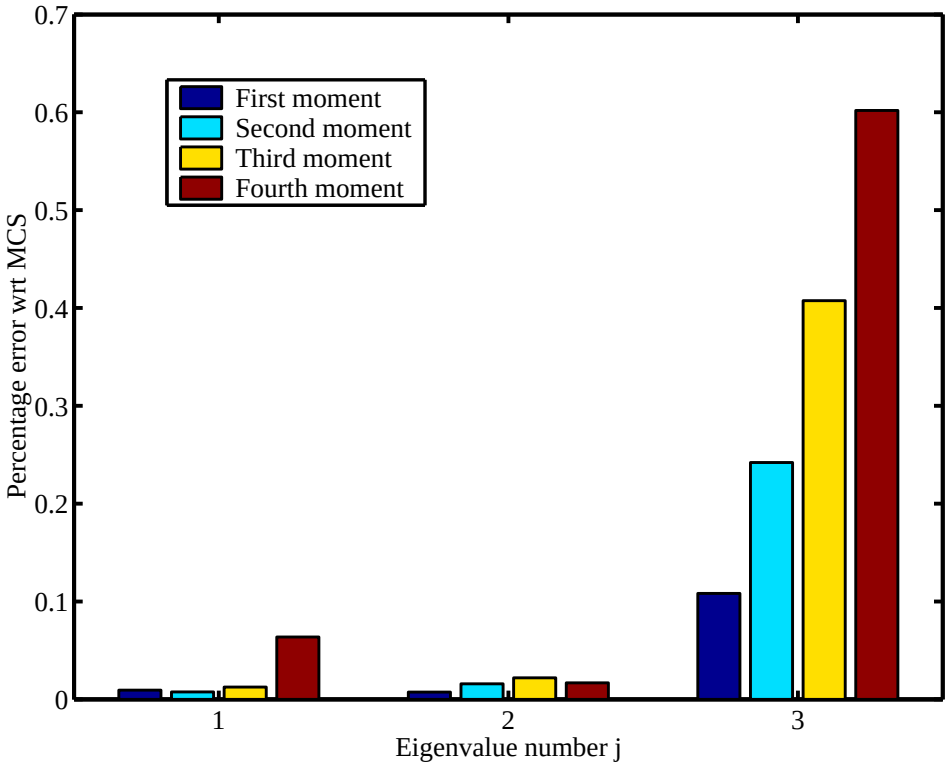

Figure 5.8: Percentage error for first four moments of the eigenvalues; Case 1.

small considering that the strength of randomness for all nine random variables are 15%. Error associated with higher eigenvalues are higher and also for a fixed eigenvalue, the higher order moments have more errors.

Now consider the probability density function of the eigenvalues. The pdf of the first eigenvalue obtained from the two methods are shown in figure 5.9. On the same plot, normalized histograms of the eigenvalue obtained from the Monte Carlo simulation are also shown. Both approximate methods match well with the Monte Carlo simulation result. This is expected since the first three moments are obtained accurately (less than 0.2% error as seen in fig-

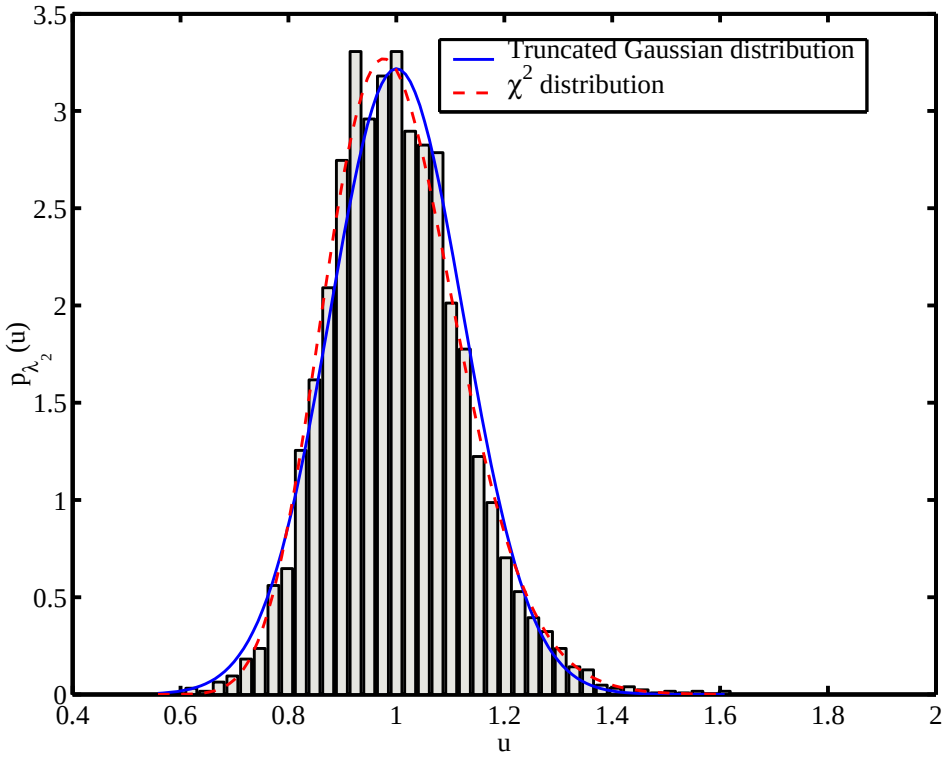

Figure 5.9: Probability density function of the first eigenvalue; Case 1.

ure 5.8). The probability density functions of the second and third eigenvalues are shown in figure 5.10. The region of statistical overlap is indeed small and can be verified from the plot of the actual samples in figure 5.7. Again, both approximate methods match well with the Monte Carlo simulation result.

Case 2: Two eigenvalues are close

When some eigenvalues are closely spaced, their derivatives with respect to the system parameters may not behave well (Friswell, 1996). Indeed, if repeated eigenvalues exist, the formulation proposed here breaks down. The purpose of studying this case is to investigate how the proposed methods work when there are closely spaced eigenvalues so that there is a significant statistical

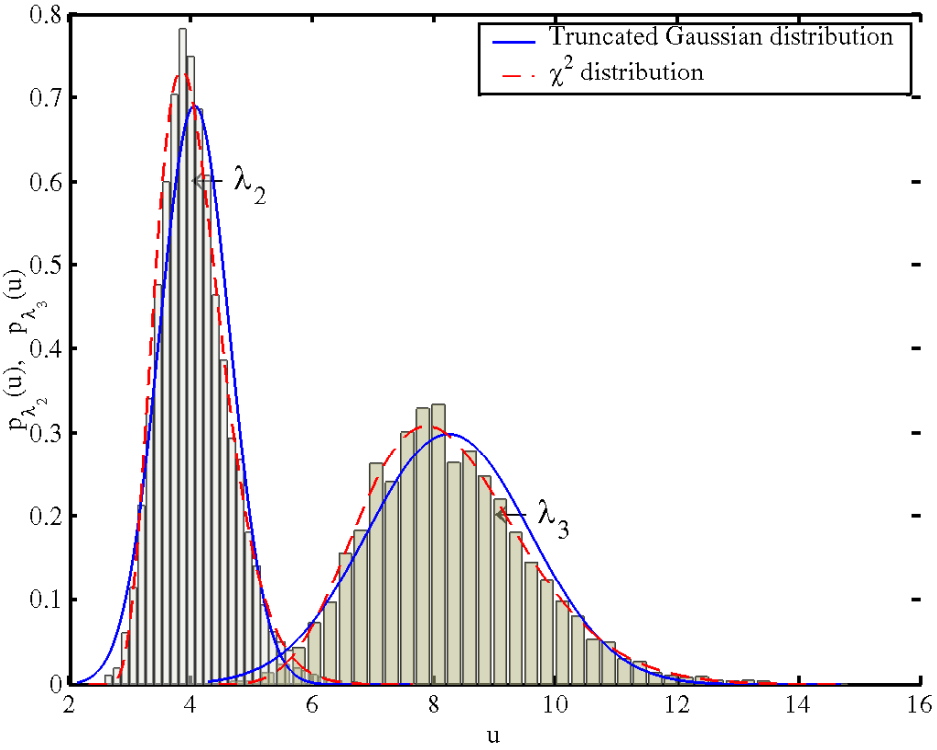

Figure 5.10: Probability density functions of the second and third eigenvalues; Case 1.

overlap between them. For the given parameter values the eigenvalues of the corresponding deterministic system are calculated as

$$\overline{\lambda}_1 = 1, \quad \overline{\lambda}_2 = 4, \quad \text{and} \quad \overline{\lambda}_3 = 4.55 \tag{5.104}$$

Clearly $\overline{\lambda}_2$ and $\overline{\lambda}_3$ are close to each other. The random scatter of the eigenvalues is shown in figure 5.11 for 1000 samples from the Monte Carlo simulation. It can be seen that the third eigenvalue has the maximum scatter and because the second and the third eigenvalues are close there is significant statistical overlap between them. Figure 5.12 shows the percentage error for the first four moments of the eigenvalues. The general trend of these errors are similar to the previous case except that the magnitudes of the errors corresponding to

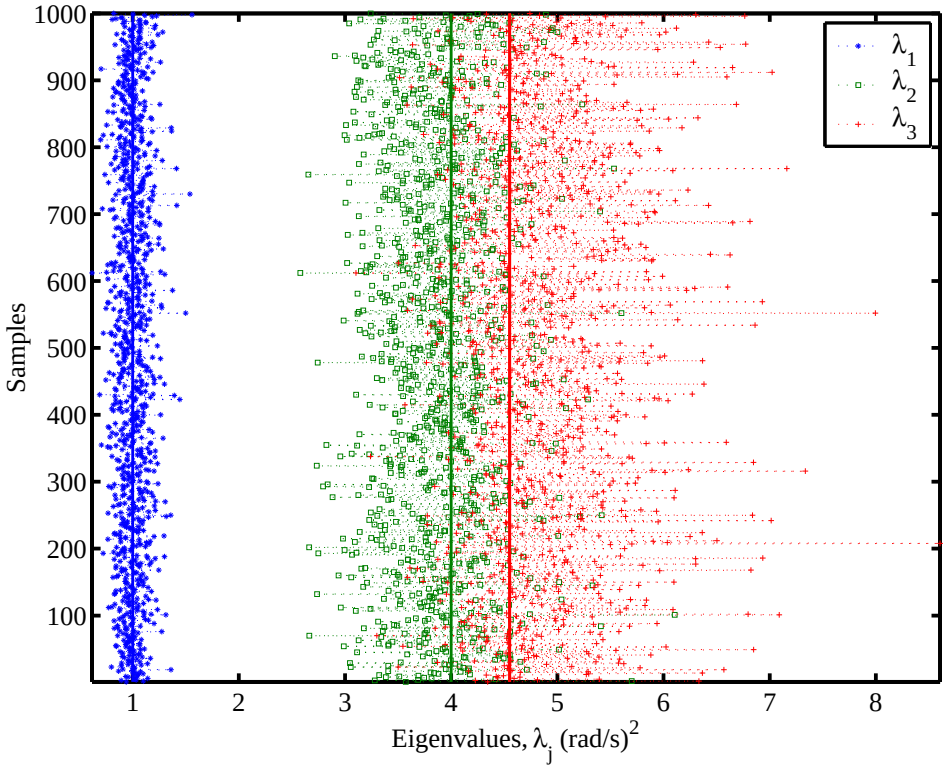

Figure 5.11: Statistical scatter in the eigenvalues; Case 2.

second and third eigenvalues are higher. This is expected because these two eigenvalues are close to each other.

The probability density function of the first eigenvalue obtained from the two methods are shown in figure 5.13. On the same plot, normalized histograms of the eigenvalue obtained from Monte Carlo simulation are also shown. As in the previous case, both approximate methods match well with the Monte Carlo simulation result. This is expected since the first three moments are obtained accurately for this case also. The probability density functions of the second and third eigenvalues are shown in figure 5.14. There is a significant region of statistical overlap which can also be verified from the plot of the

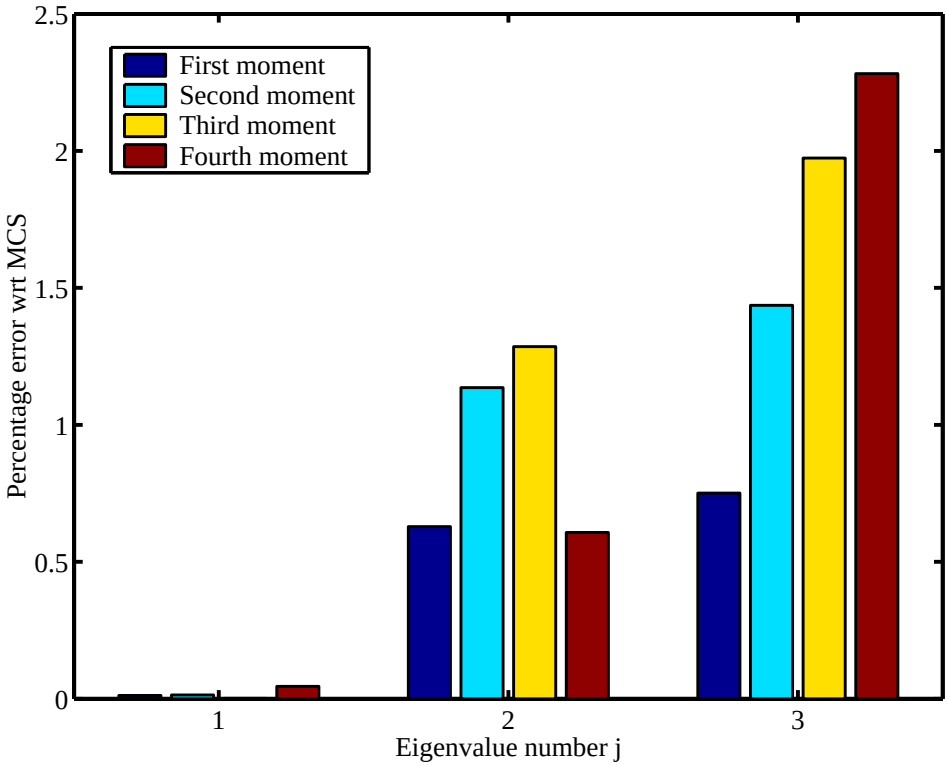

Figure 5.12: Percentage error for first four moments of the eigenvalues; Case 2.

actual samples in figure 5.11. In this case the truncated Gaussian density function performs better than the χ^2 density function. However, none of the approximate methods match the Monte Carlo simulation result as well as in the previous case.

5.7 Conclusions

The statistics of the eigenvalues of discrete linear dynamic systems with parameter uncertainties have been discussed in this lecture. It is assumed that the mass and stiffness matrices are smooth and at least twice differentiable functions of a set of random variables. The random variables are in general considered to be non-Gaussian. The usual assumption of small randomness

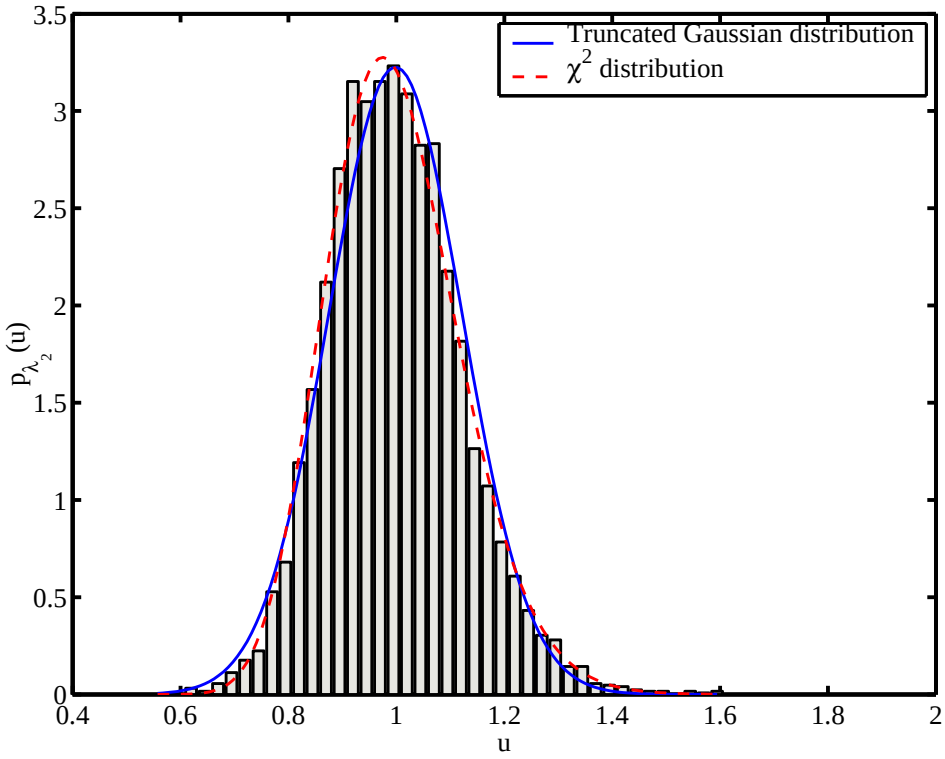

Figure 5.13: Probability density function of the first eigenvalue; Case 2.

employed in most mean-centered based perturbation analysis is not employed here. Two methods, namely (a) optimal point expansion method, and (b) asymptotic moment method, have been outlined. The optimal point is obtained so that the mean of the eigenvalues are estimated most accurately. Both methods are based on an unconstrained optimization problem. Moments and cumulants of arbitrary orders are derived for both the approaches. Two simple approximations for the probability density function of the eigenvalues are derived. One is in terms of a truncated Gaussian random variable obtained using the maximum entropy principle. The other is a χ^2 random variable approximation based on matching the first three moments of the eigenvalues.

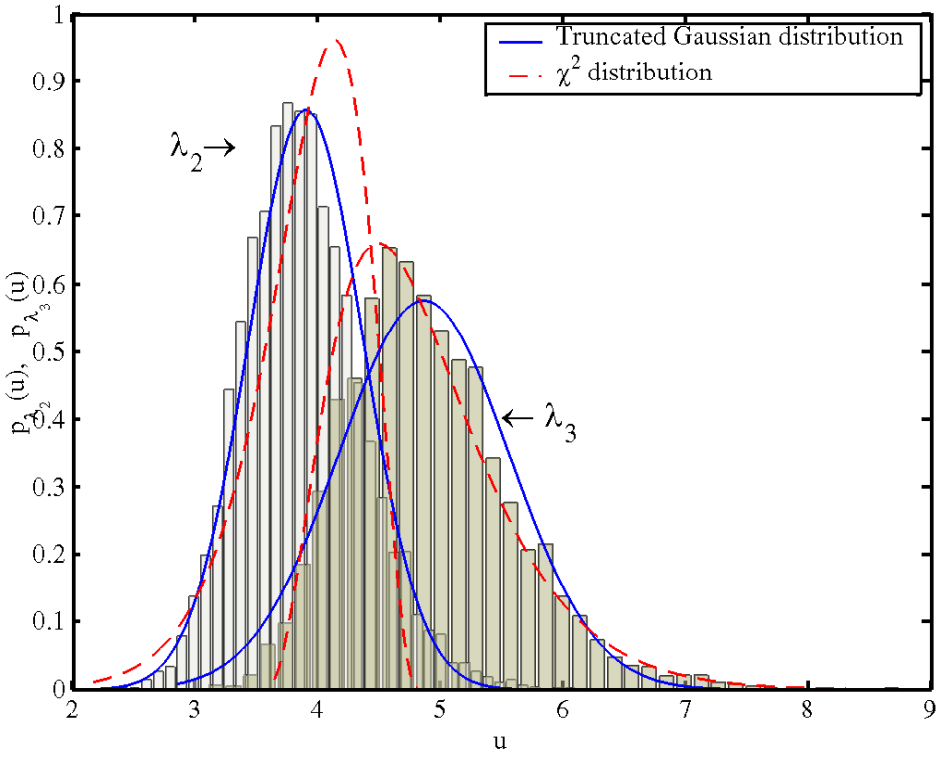

Figure 5.14: Probability density functions of the second and third eigenvalues; Case 2.

Both formulations yield closed-form expressions of the pdf which can be computed easily. Proposed formulae are applied to two problems. The moments and the pdf match encouragingly well with the corresponding Monte Carlo simulation results. However, when some eigenvalues are closely spaced, the proposed methods do not produce very accurate results. Further research is required to deal with systems with closely spaced or repeated eigenvalues.

References

S. Adhikari. Dynamics of non-viscously damped linear systems. *ASCE Journal of Engineering Mechanics*, 128(3):328–339, March 2002.

S. Adhikari. Energy Dissipation in Vibrating Structures. Master's thesis, Cambridge University Engineering Department, Cambridge, UK, May 1998. First Year Report.

S. Adhikari. *Damping Models for Structural Vibration*. PhD thesis, Cambridge University Engineering Department, Cambridge, UK, September 2000.

R. J. Allemang and D. L. Brown. A correlation coefficient for modal vector analysis. In *Proceedings of the 1st International Modal Analysis Conference (IMAC)*, pages 110–116, Orlando, FL, 1982.

K. F. Alvin, L. D. Peterson, and K. C. Park. Extraction of normal modes and full modal damping from complex modal parameters. *AIAA Journal*, 35(7): 1187–1194, July 1997.

R. L. Bagley and P. J. Torvik. Fractional calculus–a different approach to the analysis of viscoelastically damped structures. *AIAA Journal*, 21(5): 741–748, May 1983.

M. Baruch. Identification of the damping matrix. Technical Report TAE No.803, Technion, Israel, Faculty of Aerospace Engineering, Israel Institute of Technology, Haifa, May 1997.

H. Benaroya. Random eigenvalues, algebraic methods and structural dynamic models. *Applied Mathematics and Computation*, 52:37–66, 1992.

H. Benaroya and M. Rehak. Finite element methods in probabilistic structural analysis: a selective review. *Applied Mechanics Reviews, ASME*, 41(5):201–213, 1988.

M. A. Biot. Variational principles in irreversible thermodynamics with application to viscoelasticity. *Physical Review*, 97(6):1463–1469, 1955.

M. A. Biot. Linear thermodynamics and the mechanics of solids. In *Proceedings of the Third U. S. National Congress on Applied Mechanics*, pages 1–18, New York, 1958. ASME.

Norman Bleistein and Richard A. Handelsman. *Asymptotic Expansions of Integrals*. Holt, Rinehart and Winston, New York, USA, 1994.

W. E. Boyce. *Random Eigenvalue Problems*. Probabilistic methods in applied mathematics. Academic Press, New York, 1968.

K. J. Buhariwala. Dynamic response of viscoelastic fibre reinforced composite materials. Master's thesis, University of Toronto, Institute for Aerospace Studies, 1982.

T. K. Caughey and M. E. J. O'Kelly. Classical normal modes in damped linear dynamic systems. *Transactions of ASME, Journal of Applied Mechanics*, 32: 583–588, September 1965.

S. Y. Chen, M. S. Ju, and Y. G. Tsuei. Extraction of normal modes for highly coupled incomplete systems with general damping. *Mechanical Systems and Signal Processing*, 10(1):93–106, 1996.

J. D. Collins and W. T. Thomson. The eigenvalue problem for structural systems with statistical properties. *AIAA Journal*, 7(4):642–648, April 1969.

D. J. Ewins. *Modal Testing: Theory and Practice*. Research Studies Press, Baldock, England, second edition, 2000.

R. L. Fox and M. P. Kapoor. Rates of change of eigenvalues and eigenvectors. *AIAA Journal*, 6(12):2426–2429, December 1968.

M. I. Friswell. The derivatives of repeated eigenvalues and their associated eigenvectors. *ASME Journal of Vibration and Acoustics*, 18:390–397, July 1996.

M. I. Friswell and J. E. Mottershead. *Finite Element Model Updating in Structural Dynamics*. Kluwer Academic Publishers, The Netherlands, 1995.

M. Géradin and D. Rixen. *Mechanical Vibrations*. John Wiely & Sons, New York, NY, second edition, 1997. Translation of: Théorie des Vibrations.

R. Ghanem and P.D. Spanos. *Stochastic Finite Elements: A Spectral Approach*. Springer-Verlag, New York, USA, 1991.

D. F. Golla and P. C. Hughes. Dynamics of viscoelastic structures - a time domain finite element formulation. *Transactions of ASME, Journal of Applied Mechanics*, 52:897–906, December 1985.

G. C. Hart. Eigenvalue uncertainties in stressed structure. *Journal of Engineering Mechanics, ASCE*, 99(EM3):481–494, June 1973.

T. K. Hasselman and G. C. Hart. Modal analysis of random structural system. *Journal of Engineering Mechanics, ASCE*, 98(EM3):561–579, June 1972.

T. K. Hasselsman. A method of constructing a full modal damping matrix from experimental measurements. *AIAA Journal*, 10(4):526–527, 1972.

R. A. Ibrahim. Structural dynamics with parameter uncertainties. *Applied Mechanics Reviews, ASME*, 40(3):309–328, 1987.

S. R. Ibrahim. Dynamic modeling of structures from measured complex modes. *AIAA Journal*, 21(6):898–901, June 1983.

M. Kleiber and T. D. Hien. *The Stochastic Finite Element Method*. John Wiley, Chichester, 1992.

G. A. Lesieutre and D. L. Mingori. Finite element modeling of frequency-dependent material properties using augmented thermodynamic fields. *AIAA Journal of Guidance, Control and Dynamics*, 13:1040–1050, 1990.

R. H. Lyon and R. G. Dejong. *Theory and Application of Statistical Energy Analysis*. Butterworth-Heinmann, Boston, second edition, 1995.

N. M. M. Maia and J. M. M. Silva, editors. *Theoretical and Experimental Modal Analysis*. Engineering Dynamics Series. Research Studies Press, Taunton, England, 1997. Series Editor, J. B. Robetrs.

C. S. Manohar and S. Gupta. Modeling and evaluation of structural reliability: Current status and future directions. In K. S. Jagadish and R. N. Iyengar, editors, *Research reviews in structural engineering, Golden Jubilee Publications of Department of Civil Engineering, Indian Institute of Science, Bangalore*. University Press, 2003.

C. S. Manohar and R. A. Ibrahim. Progress in structural dynamics with stochastic parameter variations: 1987 to 1998. *Applied Mechanics Reviews, ASME*, 52(5):177–197, May 1999.

C. S. Manohar and A. J. Keane. Statistics of energy flow in one dimentional subsystems. *Philosophical Transactions of Royal Society of London*, A346: 525–542, 1994.

D. J. McTavish and P. C. Hughes. Modeling of linear viscoelastic space structures. *Transactions of ASME, Journal of Vibration and Acoustics*, 115: 103–110, January 1993.

C. Minas and D. J. Inman. Identification of a nonproportional damping matrix from incomplete modal information. *Transactions of ASME, Journal of Vibration and Acoustics*, 113:219–224, April 1991.

J. E. Mottershead. Theory for the estimation of structural vibration parameters from incomplete data. *AIAA Journal*, 28(3):559–561, 1990.

E. S. Pearson. Note on an approximation to the distribution of non-central χ^2. *Biometrica*, 46:364, 1959.

R. H. Plaut and K. Huseyin. Derivative of eigenvalues and eigenvectors in non-self adjoint systems. *AIAA Journal*, 11(2):250–251, February 1973.

S. Anantha Ramu and R. Ganesan. A galerkin finite element technique for stochastic field problems. *Computer Methods in Applied Mechanics andEngineering*, 105:315–331, 1993.

Lord Rayleigh. *Theory of Sound (two volumes).* Dover Publications, New York, 1945 re-issue, second edition, 1877.

T. S. Sankar, S. A. Ramu, and R. Ganesan. Stochastic finite element analysis for high speed rotors. *Journal of Vibration and Accoustic, ASME*, 115:59–64, 1993.

J. Vom Scheidt and Walter Purkert. *Random Eigenvalue Problems.* North Holland, New York, 1983.

J. M. Montalvao E Silva and Nuno M. M. Maia, editors. *Modal Analysis and Testing: Proceedings of the NATO Advanced Study Institute*, NATO Science Series: E: Applied Science, Sesimbra, Portugal, 3-15 May 1998.

R. Wong. *Asymptotic Approximations of Integrals.* Society of Industrial and Applied Mathematics, Philadelphia, PA, USA, 2001. First published by Academic Press Inc. in 1989.

J. Woodhouse. Linear damping models for structural vibration. *Journal of Sound and Vibration*, 215(3):547–569, 1998.

B. Yang and X. Wu. Modal expansion of structural systems with time delays. *AIAA Journal*, 36(12):2218–2224, December 1998.

A Derivation of the Residues in the Transfer Function of Non-viscously Damped Dynamic Systems

The eigenvectors of the dynamic stiffness matrix play an important role in determining the residues of the transfer function matrix. For any given $s \in \mathbb{C}$, the eigenvalue problem associated with the dynamic stiffness matrix can be expressed by

$$\mathbf{D}(s)\boldsymbol{\phi}_k(s) = \nu_k(s)\boldsymbol{\phi}_k(s), \quad \forall\, k = 1, \cdots, N. \tag{A.1}$$

In the preceding equation the eigenvalues $\nu_k(s) \in \mathbb{C}$ are the roots of the characteristic equation

$$\det\left[\mathbf{D}(s) - \nu(s)\mathbf{I}_N\right] = 0 \tag{A.2}$$

and $\boldsymbol{\phi}_k(s) \in \mathbb{C}^N$ is the k-th eigenvector of $\mathbf{D}(s)$. The symbols $\nu_k(s)$ and $\boldsymbol{\phi}_k(s)$ indicate functional dependence of these quantities on the complex parameter s. Such a continuous dependence is expected whenever $\mathbf{D}(s)$ is a sufficiently smooth matrix function of s. It should be noted that because $\mathbf{D}(s)$ is an $N \times N$ complex matrix for a fixed s, the number of eigenvalues (and consequently the eigenvectors) must be N. Further, it can be shown that, for distinct eigenvalues, $\boldsymbol{\phi}_k(s)$ also satisfy an orthogonality relationship although $\mathbf{z}_k$ do not enjoy any such simple relationship. We normalize $\boldsymbol{\phi}_k(s)$ such that

$$\boldsymbol{\phi}_j^T(s)\boldsymbol{\phi}_k(s) = \delta_{kj}, \quad \forall\, k, j = 1, \cdots, N \tag{A.3}$$

In view of the above relationship, from equation (A.1) we have

$$\boldsymbol{\phi}_j^T(s)\mathbf{D}(s)\boldsymbol{\phi}_k(s) = \nu_k(s)\delta_{kj}, \quad \forall\, k, j = 1, \cdots, N \tag{A.4}$$

or in the matrix form

$$\mathbf{\Phi}^T(s)\mathbf{D}(s)\mathbf{\Phi}(s) = \boldsymbol{\nu}(s). \tag{A.5}$$

Here

$$\mathbf{\Phi}(s) = [\boldsymbol{\phi}_1(s), \boldsymbol{\phi}_2(s), \cdots, \boldsymbol{\phi}_N(s)] \in \mathbb{C}^{N\times N}, \tag{A.6}$$

$$\text{and} \quad \boldsymbol{\nu}(s) = \text{diag}\,[\nu_1(s), \nu_2(s), \cdots, \nu_N(s)] \in \mathbb{C}^{N\times N}. \tag{A.7}$$

It is possible to establish the relationships between the original eigenvalue problem of the system defined by equation (1.45) and that by equation (A.1). Consider the case when the parameter s approaches any one of the system eigenvalues, say s_j. Since *all* the $\nu_k(s)$ are assumed to be distinct, for nontrivial eigenvectors, comparing equations (1.45) and (A.1) we can conclude that one and only one of the $\nu_k(s)$ must be zero when $s \to s_j$ (see Yang and Wu, 1998). Suppose that the r-th eigenvalue of the eigenvalue problem (A.1) is zero when $s \to s_j$. It is also clear that the eigenvector in (A.1) corresponding to the r-th eigenvalue also approaches the eigenvector in (1.45) as $s \to s_j$. Thus, when $s = s_j$ one has

$$\nu_r(s_j) = 0 \quad \text{and} \quad \nu_k(s_j) \neq 0, \forall k = 1, \cdots, N; \neq r \tag{A.8}$$

and also

$$\boldsymbol{\phi}_r(s_j) = \mathbf{z}_j. \tag{A.9}$$

These equations completely relate the eigensolutions of (1.45) with (A.1). Now, these relationships will be utilized to obtain the residues of the transfer function matrix.

From equation (A.5) one has

$$\mathbf{D}^{-1}(s) = \mathbf{\Phi}(s)\boldsymbol{\nu}^{-1}(s)\mathbf{\Phi}^T(s). \tag{A.10}$$

Using the expression of the transfer function in equation (1.63) and noting that $\boldsymbol{\nu}(s)$ is a diagonal matrix, we may expand the right-hand side of the above equation to obtain

$$\mathbf{H}(s) = \mathbf{D}^{-1}(s) = \sum_{k=1}^{N} \frac{\boldsymbol{\phi}_k(s)\boldsymbol{\phi}_k^T(s)}{\nu_k(s)}. \tag{A.11}$$

Separation of the r-th term in the above sum yields

$$\mathbf{H}(s) = \frac{\boldsymbol{\phi}_r(s)\boldsymbol{\phi}_r^T(s)}{\nu_r(s)} + \left[\sum_{\substack{k=1\\k\neq r}}^{N} \frac{\boldsymbol{\phi}_k(s)\boldsymbol{\phi}_k^T(s)}{\nu_k(s)}\right]. \tag{A.12}$$

Clearly, when $s \to s_j$, the second term of the right-hand side of equation (A.12) is analytic because according to equation (A.8) $\nu_k(s_j) \neq 0, \forall k = 1, \cdots, N; \neq r$. Now, from equation (1.66) the residue at $s = s_j$ may be obtained as

$$\begin{aligned}
\mathbf{R}_j &\stackrel{\text{def}}{=} \lim_{s\to s_j}(s - s_j)\left\{\frac{\boldsymbol{\phi}_r(s)\boldsymbol{\phi}_r^T(s)}{\nu_r(s)} + \left[\sum_{\substack{k=1\\k\neq r}}^{N} \frac{\boldsymbol{\phi}_k(s)\boldsymbol{\phi}_k^T(s)}{\nu_k(s)}\right]\right\} \\
&= \lim_{s\to s_j}(s - s_j)\frac{\boldsymbol{\phi}_r(s)\boldsymbol{\phi}_r^T(s)}{\nu_r(s)} \\
&= \frac{\boldsymbol{\phi}_r(s)\boldsymbol{\phi}_r^T(s)|_{s=s_j}}{\frac{\partial \nu_r(s)}{\partial s}|_{s=s_j}} + \lim_{s\to s_j}\frac{(s - s_j)\frac{\partial}{\partial s}\left[\boldsymbol{\phi}_k(s)\boldsymbol{\phi}_k^T(s)\right]}{\frac{\partial \nu_r(s)}{\partial s}} \quad \text{(using l'Hôspital's rule)} \\
&= \frac{\mathbf{z}_j\mathbf{z}_j^T}{\frac{\partial \nu_r(s)}{\partial s}|_{s=s_j}} \qquad \text{(by equation (A.9))}.
\end{aligned} \tag{A.13}$$

The denominator in the above expression for the residues, $\frac{\partial \nu_r(s)}{\partial s}|_{s=s_j}$, is still unknown. Now, consider the r-th eigenvalue problem associated with the dynamic stiffness matrix. Differentiation of equation (A.1) for $k = r$ with respect to s yields

$$\frac{\partial \mathbf{D}(s)}{\partial s}\boldsymbol{\phi}_r(s) + \mathbf{D}(s)\frac{\partial \boldsymbol{\phi}_r(s)}{\partial s} = \frac{\partial \nu_r(s)}{\partial s}\boldsymbol{\phi}_r(s) + \nu_r(s)\frac{\partial \boldsymbol{\phi}_r(s)}{\partial s}. \tag{A.14}$$

Premultiplying the above equation by $\boldsymbol{\phi}_r^T(s)$ and rearranging one obtains

$$\boldsymbol{\phi}_r^T(s)\frac{\partial \mathbf{D}(s)}{\partial s}\boldsymbol{\phi}_r(s) + \left[\boldsymbol{\phi}_r^T(s)\mathbf{D}(s) - \boldsymbol{\phi}_r^T(s)\nu_r(s)\right]\frac{\partial \boldsymbol{\phi}_r(s)}{\partial s} = \boldsymbol{\phi}_r^T(s)\frac{\partial \nu_r(s)}{\partial s}\boldsymbol{\phi}_r(s). \tag{A.15}$$

Taking transpose of equation (A.1) it follows that the second term of the left-hand side of the above equation is zero. Using the normalizing condition in (A.3) and letting $s \to s_j$, from equation (A.15) we have

$$\frac{\partial \nu_r(s)}{\partial s}|_{s=s_j} = \mathbf{z}_j^T\frac{\partial \mathbf{D}(s)}{\partial s}|_{s=s_j}\mathbf{z}_j = \mathbf{z}_j^T\frac{\partial \mathbf{D}(s_j)}{\partial s_j}\mathbf{z}_j. \tag{A.16}$$

The term $\dfrac{\partial \mathbf{D}(s_j)}{\partial s_j}$ can be obtained by differentiating equation (1.61) as

$$\frac{\partial \mathbf{D}(s_j)}{\partial s_j} = 2s_j\mathbf{M} + \mathbf{G}(s_j) + s_j\frac{\partial \mathbf{G}(s_j)}{\partial s_j}. \tag{A.17}$$

Using (A.13) and (A.16) one finally obtains the residue as

$$\mathbf{R}_j = \frac{\mathbf{z}_j\mathbf{z}_j^T}{\mathbf{z}_j^T\frac{\partial \mathbf{D}(s_j)}{\partial s_j}\mathbf{z}_j}. \tag{A.18}$$

The above equation completely relates the transfer function residues to the eigenvalues and eigenvectors of the system.

B Gradient vector and Hessian matrix of the eigenvalues

The eigenvectors of symmetric linear systems are orthogonal with respect to the mass and stiffness matrices. Normalize the eigenvectors so that they are unity mass normalized, that is,

$$\boldsymbol{\phi}_j^T \mathbf{M} \boldsymbol{\phi}_j = 1 \tag{B.1}$$

Using this and differentiating equation (5.1) with respect to x_k, following Fox and Kapoor (1968) it can be shown that for any $\mathbf{x}$

$$\frac{\partial \lambda_j(\mathbf{x})}{\partial x_k} = \boldsymbol{\phi}_j(\mathbf{x})^T \boldsymbol{\mathcal{G}}_{jk}(\mathbf{x}) \boldsymbol{\phi}_j(\mathbf{x}) \tag{B.2}$$

$$\text{where} \quad \boldsymbol{\mathcal{G}}_{jk}(\mathbf{x}) = \left[\frac{\partial \mathbf{K}(\mathbf{x})}{\partial x_k} - \lambda_j(\mathbf{x}) \frac{\partial \mathbf{M}(\mathbf{x})}{\partial x_k} \right] \tag{B.3}$$

Differentiating equation (5.1) with respect to x_k and x_l Plaut and Huseyin (1973) have shown that, providing the eigenvalues are distinct,

$$\begin{aligned} \frac{\partial^2 \lambda_j(\mathbf{x})}{\partial x_k \, \partial x_l} = {} & \boldsymbol{\phi}_j(\mathbf{x})^T \left[\frac{\partial^2 \mathbf{K}(\mathbf{x})}{\partial x_k \, \partial x_l} - \lambda_j(\mathbf{x}) \frac{\partial^2 \mathbf{M}(\mathbf{x})}{\partial x_k \, \partial x_l} \right] \boldsymbol{\phi}_j(\mathbf{x}) \\ & - \left(\boldsymbol{\phi}_j(\mathbf{x})^T \frac{\partial \mathbf{M}(\mathbf{x})}{\partial x_k} \boldsymbol{\phi}_j(\mathbf{x}) \right) \left(\boldsymbol{\phi}_j(\mathbf{x})^T \boldsymbol{\mathcal{G}}_{jl}(\mathbf{x}) \boldsymbol{\phi}_j(\mathbf{x}) \right) \\ & - \left(\boldsymbol{\phi}_j(\mathbf{x})^T \frac{\partial \mathbf{M}(\mathbf{x})}{\partial x_l} \boldsymbol{\phi}_j(\mathbf{x}) \right) \left(\boldsymbol{\phi}_j(\mathbf{x})^T \boldsymbol{\mathcal{G}}_{jk}(\mathbf{x}) \boldsymbol{\phi}_j(\mathbf{x}) \right) \\ & + 2 \sum_{r=1}^{N} \frac{\left(\boldsymbol{\phi}_r(\mathbf{x})^T \boldsymbol{\mathcal{G}}_{jk}(\mathbf{x}) \boldsymbol{\phi}_j(\mathbf{x}) \right) \left(\boldsymbol{\phi}_r(\mathbf{x})^T \boldsymbol{\mathcal{G}}_{jl}(\mathbf{x}) \boldsymbol{\phi}_j(\mathbf{x}) \right)}{\lambda_j(\mathbf{x}) - \lambda_r(\mathbf{x})} \end{aligned} \tag{B.4}$$

Equations (B.2) and (B.4) completely define the elements of the gradient vector and Hessian matrix of the eigenvalues.